https://doi.org/10.1070/RCR4924

# Detonation nanodiamonds: new aspects in the theory and practice of synthesis, properties and applications

**Valery Yu. Dolmatov,[a]* Alexander N. Ozerin,[b] Inna I. Kulakova,[c] Oleksandr O. Bochechka,[d] Natalia M. Lapchuk,[e] Vesa Myllymäki,[f] Asko Vehanen[f]**

*[a] Federal State Unitary Enterprise, Special Design and Technology Bureau 'Technolog', Sovetsky prosp. 33a, 192076 Saint Petersburg, Russian Federation*
*[b] N.S.Enikolopov Institute of Synthetic Polymer Materials, Russian Academy of Sciences, ul. Profsoyuznaya 70, 117393 Moscow, Russian Federation*
*[c] Department of Chemistry, Lomonosov Moscow State University, Leninskie Gory 1, stroenie 3, 119991 Moscow, Russian Federation*
*[d] V.N.Bakul Institute for Superhard Materials of the National Academy of Sciences of Ukraine, ul. Avtozavodskaya 2, 04074 Kiev, Ukraine*
*[e] Faculty of Physics, Belarusian State University, ul. Bobruiskaya 5, 220030 Minsk, Belarus*
*[f] Carbodeon Ltd. Oy, Pakkalankuja 5, 01510 Vantaa, Finland*

The review describes the current state of research concerning detonation nanodiamonds, including production, methods of studying the properties and applications. The main achievements in the theory and practice of synthesis of detonation nanodiamonds over the past 15 years are addressed systematically; the influence of control factors on this process, performed using single or mixed explosives, are discussed. A new highly economical and environmentally friendly method for chemical purification of nanodiamonds is described. The operational characteristics of new materials based on nanodiamonds are presented. The application prospects of nanodiamonds in traditional and new fields are demonstrated.
The bibliography includes 214 references.

**V.Yu.Dolmatov**. Doctor of Technical Sciences, Head of the Research Laboratory of the SCTB Technolog.
E-mail: diamondcentre@mail.ru
*Current research interests*: theoretical and applied principles of synthesis and chemical purification of detonation nanodiamonds, development of new methods for producing modified and doped nanodiamonds, surface chemistry of nanomaterials, development of techniques for using nanodiamonds in various fields of technology.
**A.N.Ozerin**. Doctor of Chemical Sciences, Scientific Supervisor of ISPM RAS.
E-mail: ozerin@ispm.ru
*Current research interests*: high-molecular-weight compounds; physics and mechanics of polymers and polymer composite materials; chemistry of macromolecular compounds; technology for processing polymers and polymer composites; condensed matter physics; chemical physics; X-ray diffraction analysis of polymers; computer simulation.
**I.I.Kulakova**. PhD in Chemistry, Leading Researcher at the Division of Petroleum Chemistry and Organic Catalysis, Department of Chemistry, MSU.
E-mail: inna-kulakova@yandex.ru
*Current research interests*: heterogeneous catalysis, surface chemistry of solids, chemical modification of detonation nanodiamonds, application of modified nanodiamonds in catalysis and biomedicine.
**O.O.Bochechka**. Doctor of Technical Sciences, Deputy Director for Research, ISM NAS of Ukraine.
E-mail: bochechka@ism.kiev.ua
*Current research interests*: high-pressure and high-temperature interaction of diamond (carbon) powders with gases ($O_2$, CO, $CO_2$) and metal melts (Ni, Co, Cu); sintering of nanopowders: diamonds, SiC, *etc*.
**N.M.Lapchuk**. PhD in Physics and Mathematics, Associate Professor, Department of Physics of Semiconductors and Nanoelectronics, Faculty of Physics, BSU.
E-mail: lapchuk@bsu.by
*Current research interests*: electron paramagnetic resonance of carbon-containing materials: natural and synthetic diamonds, pyrolytic graphite, polymers, brown and hard coals, crude oil and oil refining products; radiation resistance of silicon and carbon-containing materials.
**V.Myllymäki**. PhD in Chemistry, Chief Executive Officer, Carbodeon Ltd. Oy.
E-mail: vesa.myllymaki@carbodeon.com
*Current research interests*: synthesis of detonation nanodiamonds, modification of their surface, development of their applications in electroplating, polymer chemistry and other fields of technology.
**A.Vehanen**. Doctor of Technology, Director of Carbodeon Ltd. Oy.
E-mail: asko.vehanen@carbodeon.com
*Current research interests*: synthesis of detonation nanodiamonds, modification of their surface, development of their applications in electroplating, polymer chemistry and other fields of technology.

Translation: Z.P.Svitanko

**Received 10 October 2019**

© 2020 Uspekhi Khimii, ZIOC RAS, Russian Academy of Sciences and IOP Publishing Limited

## Contents

1. Introduction 1430
2. Detonation synthesis of nanodiamonds 1430
2.1. Possible mechanism of the synthesis of nanodiamonds 1430
2.2. Regularities of the detonation synthesis of nanodiamonds 1432
2.3. Diamond detonation blend 1434
2.3.1. Particle morphology of the diamond blend 1435
2.3.2. Isolation of detonation nanodiamonds from the diamond detonation blend 1435
3. Properties of detonation nanodiamonds 1436
3.1. Structure and composition of primary particles 1436
3.2. Stability of suspensions of detonation nanodiamonds 1438
3.3. Optical properties of detonation nanodiamonds 1438
3.3.1. IR spectra 1438
3.3.2. Raman spectra and photoluminescence 1439
3.4. Characteristic features of paramagnetism of doped detonation nanodiamonds 1440
3.4.1. Characteristic features of paramagnetism of DNDs doped with boron and phosphorus atoms during the synthesis 1440
3.4.2. Dispersion of magnetic susceptibility 1441
3.4.3. Characteristic features of formation of highly conductive structures in DND powders under conditions of electron paramagnetic resonance 1442
3.4.4. Thermal stability of detonation nanodiamonds 1442
3.5. Methods for chemical modification of the surface of detonation nanodiamonds 1443
4. Applications of detonation nanodiamonds 1444
4.1. Fluorinated nanodiamonds as unique neutron reflectors 1444
4.2. DND – CNT hybrid material 1444
4.3. Electrochemical metal – diamond coatings 1445
4.3.1. Chromium – diamond coatings 1445
4.3.2. Nickel – diamond coatings 1445
4.3.3. Electrochemical diamond-containing anodized aluminium oxide coatings 1446
4.3.4. Silver – diamond coatings 1447
4.3.5. Gold – diamond coatings 1447
4.3.6. Zinc – diamond coatings 1448
4.4. Bulk metal – nanodiamond composites 1448
4.5. Composite materials based on polymers 1448
4.5.1. Elastomer – diamond composite materials 1449
4.5.2. Polymer – diamond composites based on thermoplastics 1450
4.5.3. Tribology of polymer composites 1451
4.5.4. Polymer – DND composites for special applications 1451
4.6. Antifriction oil compositions with detonation nanodiamonds 1452
4.7. Catalysts based on detonation nanodiamonds 1453
4.8. Polycrystalline materials made of nanodiamonds 1453
4.9. Modified detonation nanodiamonds for biomedical applications 1454
4.9.1. Nanodiamonds as fluorescent labels 1455
4.9.2. Nanodiamonds for drug delivery 1455
4.9.3. Imaging of nanodiamonds 1456
4.9.4. Specific *in vivo* activity of DND – glycine conjugate 1457
5. Conclusion 1457

List of abbreviations:

ATR — attenuated total reflection,
BAS — biologically active substance,
BTF — benzotrifuroxan, benzotris(1,2,5-oxadiazole 1,4,7-trioxide),
CEC — composite electrochemical coatings,
CNT — carbon nanotubes,
CRZ — chemical reaction zone,
DB — diamond detonation blend,
DGEBA — diglycidyl ether of bisphenol A,
DND — detonation nanodiamond,
DP — detonation products,
DS — drug substance,
FL — fluorescence,
HPA — high-pressure apparatus,
NV — nitrogen vacancy,
OB — oxygen balance,
OPBI — highly heat-resistant poly[2,2′-(*p*-oxydiphenylene)-5,5′-bibenzimidazole],
PA6 — polyamide 6 (kapron),
PDMS — polydimethylsiloxane,
PPase — pyrophosphatase,
PVA — polyvinyl alcohol,
RDX — hexogen (cyclotrimethylenetrinitramine),
TATB — 1,3,5-triamino-2,4,6-trinitrobenzene,
TETA — triethylenetetramine,
TH — a charge of TNT (trotyl) and RDX (hexogen),
TNT — 2,4,6- trinitrotoluene (trotyl),
UHMWPE — ultrahigh molecular weight polyethylene,
UPTFE — ultradispersed polytetrafluoroethylene,
VTMOS — vinyltrimethoxysilane.

## 1. Introduction

More than 50 years have passed since the discovery of detonation nanodiamonds (DNDs), 4 – 6 nm carbon particles. The last decade witnessed a revival of the interest in DNDs. The range of raw materials for the synthesis of nanodiamonds is being expanded: new explosives extracted from ammunition are now used. Modified and doped DNDs were obtained, a new environmentally safe and economically feasible processes for their chemical purification appeared. This led to a significant change in the properties of DNDs (for example, high conductivity [1] arising upon doping) and increased the potential for their use in micro- and nanoelectronics. Studying the properties of DNDs and DND-based materials expanded their applications in traditional and new fields.

Not all important DND characteristics correspond to analogous values of large crystallites: the heat conductivity of the DND powder is two orders of magnitude lower than that of a bulk crystal; the radiation resistance of the crystallite can be high only when there are no metal or nonmetal impurities on the surface or in the pores of the DND powder; chemical inertness of the DND core is only implied, since the functional groups present on the nanocrystal surface make it, conversely, fairly chemically reactive. Doping of DND crystallites with heteroatoms (nitrogen, silicon, phosphorus, boron) results in the change in optical, magnetic and thermophysical properties. Currently, nitrogen doping of DND crystallites to give nitrogen vacancy (NV) centres is considered to be most promising. These nanocrystals can be regarded as elements of a quantum computer. The generation of NV centres in DND crystallites can give an impetus for the development of nanodiamond spintronics.

The studies of properties of pristine and modified DNDs are being expanded, and the number of relevant publications increases every year.[2–4] The interest is evidently focused on practical application of DNDs in various fields of science, technology, medicine and biology.

Detonation nanodiamonds can serve as examples of diversity and inexhaustibility of the properties of the nanoworld. They belong to the family of nanocarbons, which includes fullerenes, carbon nanotubes, graphene, globular nanocarbon, onions and other structures, and are among the few products that are commercially manufactured. Traditionally, DNDs are produced in industry starting from mixtures of 2,4,6-trinitrotoluene (TNT) and RDX (cyclotrimethylenetrinitramine) in which the component ratio is 50 : 50 or 60 : 40. Other aromatic nitro derivatives, for example, tetryl (*N*-methyl-*N*-2,4,6-tetranitroaniline), have also been proposed for this purpose. The DND production at the Plant 'Plastmass' (Kopeisk, Russia) is wholly based on the use of tetryl.

The originality of the method of DND synthesis consists in the fact that the 'surplus' carbon atoms in the molecules of explosives serve as the source of carbon, that is, the starting compounds have a negative oxygen balance (OB).† In other words, they contain less oxygen than it is necessary for oxidation of all combustible components. The use of DNDs in various industry branches is driven by the need to crucially improve the performance characteristics of composite materials. With the existing level of development of the synthesis and understanding of application prospects of DNDs, they are now considered among the most advantageous carbon nanomaterials for nanotechnologies.

The purpose of the present review is to systematize the available data on DNDs, taking into account their unique properties, new production processes and applications in various fields of science and technology. This is not an exhaustive description, in view of the limited size of the review, but an account specially addressing the above aspects.

## 2. Detonation synthesis of nanodiamonds

### 2.1. Possible mechanism of the synthesis of nanodiamonds

The views on the mechanism of the detonation synthesis of DNDs that prevailed a decade ago are described in detail.[5–7] This description is fragmentary and often contradictory. In view of the enormous temperature (3000 – 4300 K) and pressure (20 – 30 GPa), thousands of chemical reactions involved and, what is most important, short time of the detonation transformation of explosives (0.1 – 0.3 μs), currently there is no evidence-based proof for the processes that take place in the space from the detonation wave front to the Chapman – Jouguet plane,‡ *i.e.*, in the chemical reaction zone§ (CRZ). Therefore, it is also difficult to conceive the chemical and physical processes that originate upon expansion of the gaseous detonation products (DP)¶ and involve condensed carbon. It is believed that at least 80% of the explosion energy is released in the CRZ, while correspondingly ~20% of the energy is released behind the Chapman – Jouguet plane.

In many studies (*e.g.*, Refs 8 – 12), it is assumed that the major process of formation of DND crystallites starts after the detonation wave front has propagated up to the Chapman – Jouguet plane and ends much further from this plane upon DP expansion. The growth of DNDs is terminated not only because of decrease in the pressure and temperature, but rather due to a decrease in the concentration of carbon radicals.

Meanwhile, there are different points of view on the DND formation process. The use of small-angle X-ray scattering made it possible [13,14] to study the evolution of carbon particle size at the onset of explosive detonation front. Immediately behind the detonation front, the authors detected condensed carbon nanoparticles with a density exceeding the density of plasma in the CRZ and determined the size of these particles to be up to 2 nm. As the process goes on, the diameter of dense nanocarbon particles ($d$) increases to reach, within ~4.5 μs, different values depending on the type of the initial explosive. For explosives such as 1,3,5-triamino-2,4,6-trinitrobenzene (TATB), a mixture of TNT and RDX (TH), and benzotrifuroxan (BTF), the $d$ values were as follows

† Oxygen balance is the mass of oxygen that remains after oxidation of all carbon contained in the explosive molecule to give carbon dioxide and oxidation of all hydrogen to give water divided by the mass of the taken explosive, expressed in percentage. Nitrogen is assumed to remain in the free state.

‡ The plane in which the energy release stops and the substance flux velocity is equal to the local sound velocity.

§ The chemical reaction zone is the area located immediately behind the detonation front of the explosive (hundreds of micrometres) separating the initial explosives from gaseous explosion products. In this zone, heat evolution takes place, its temperature is ~3000 – 4500 K, the pressure is ~18 – 35 GPa and the substance density is ~2.3 g cm$^{-3}$.

¶ Gaseous and solid products formed upon detonation of the explosive.

| Explosive | TATB | TH 50 : 50 | BTF |
|---|---|---|---|
| $d$/nm | ~2.8 | ~6 – 7 | ~7.2 |

In the authors' opinion, in the case of TATB, these particles represent graphite-like carbon rather than DND nanocrystallites. It is noteworthy that small-angle X-ray scattering procedures make it possible to determine only the particle size, while other methods are needed to prove their graphite or diamond structure.

Explosives used for the production of DNDs have a relatively high negative oxygen balance; therefore, a high concentration of non-oxidized carbon is formed in the CRZ during the explosion. Note that thousands of radical reactions take place in the CRZ and the composition of plasma constantly changes. The $P$,$T$ conditions in the plasma containing condensed carbon correspond to the stability area of the diamond phase, which gives rise to DND pre-structure, which can hardly be converted to a non-diamond carbon state. The complete dissociation of the starting explosive into atoms during explosion, assumed by many researchers (*e.g.*, Refs 15 – 17), seems unlikely. Indeed, complete dissociation into atoms of, for example, TNT requires an energy of ~24 000 kJ kg$^{-1}$; meanwhile the heat of explosion is ~4300 kJ kg$^{-1}$, *i.e.*, it is ~5 times lower.[18] The RDX dissociation requires ~19 000 kJ kg$^{-1}$, while the heat of its explosion is only ~5700 kJ kg$^{-1}$ (~3 times lower). In the case of potent BTF explosive, ~25 000 kJ kg$^{-1}$ are needed for dissociation into atoms, whereas the heat of explosive destruction does not exceed ~5900 kJ kg$^{-1}$ (~24% of the required value). Thus, complete dissociation of explosives, including carbon, is impossible. The condensation of carbon atoms into some amorphous carbon phase in combination with liquid-drop coalescence is also of little probability.[19] The formation of DNDs from a highly supersaturated carbon vapour is extremely doubtful.[16, 17]

The degradation of explosives is a complex multistage process comprising both consecutive and parallel reactions. Upon detonation, there is no enough time for chemical equilibrium of the products to be established, since the reactions do not proceed to completion and give certain amounts of intermediates. Varying the initial density of the charge results in changed composition of detonation products. The experiments that determine the composition of cold detonation products do not provide information about their composition in the Chapman – Jouguet plane, because the composition changes upon expansion and cooling. It was shown[20] that at temperature >800 K, all nitro compounds decompose by a radical mechanism. Furthermore, according to a theoretical study,[21] the RDX degradation mechanism dominating in the gas phase is a radical mechanism in which radical anions decompose *via* elimination of the $NO_2^-$ anion.[22]

Linstrom[23] studied the electrospray ionization mass spectra of RDX and identified two peaks at $m/z$ 30 and 46 corresponding to nitrogen mono- and dioxide. Presumably, there are several mechanisms of formation of nanodiamond crystallites.[18] The parent fragment that forms the base for future nanocrystallites is the $C_2^{\bullet}$ dimer radical, and one of the mechanisms may follow energetically the most favourable pathway, which includes the formation of cyclohexane followed by its conversion to ionized adamantane. For example, degradation of RDX gives, most likely, $CH_2^{\bullet\bullet}$, $C_2^{\bullet}$, CO, $H^{\bullet}$, $N_2$, CN, $N_x$ and O. The presence of hydrogen radical allows closing the chain of reactions. In this case, the growth of nanocrystallites is due to the attack of the nanodiamond particle surface by the $C_2^{\bullet}$ radical, *i.e.*, it occurs by a diffusion mechanism.[10] The arrangement of carbon atoms in the adamantane molecule largely resembles that in the diamond crystal lattice. According to Dolmatov *et al.*,[18] hydrogen-containing explosives, for example TNT, provide the growth of the DND particle not only *via* the attack by $C_2^{\bullet}$, but also *via* the competitive attack by methyl radicals. Therefore, the yield of DNDs is ~1.5 times higher from TNT-containing mixtures than from 1,3,5-trinitrobenzene.

The appearance of DND particles is facilitated by not only physical process parameters (pressure and temperature), but to a considerable extent by chemical reactions

**Table 1**. Characteristics of the views on DND formation.

| No. | Main results | Ref. | Comments of authors of this review |
|---|---|---|---|
| 1 | The formation of DND crystallites starts in the chemical reaction zone and ends in the beginning of the isoentropic (Taylor) expansion of detonation products | 8 – 12 | Basically correct, but no detailed elaboration |
| 2 | Using small-angle X-ray scattering, the evolution of carbon nanoparticle size was followed starting from the time of passing of the detonation wave front | 13, 14 | Only carbon is detected, while its allotropes are unknown. The time of existence of the chemical reaction zone is 0.1 – 0.3 μs, while the time of particle growth is 10 – 30 times longer. These data are very important |
| 3 | Complete dissociation of explosive molecules into atoms. Homogenization of 'free' carbon atoms and the subsequent condensation to amorphous phase in combination with liquid-drop coalescence or carbon coagulation and crystallization | 15 – 17 | This seems unlikely. Complete bond rupture in the explosive molecule requires 4 – 5.5 times more energy than the energy released upon detonation |
| 4 | The DND pre-structure is formed throughout the chemical reaction zone from $C_2$ radicals. Nanodiamond may appear through the following sequence of transformations: cyclohexane → adamantane → diamond. The process ends as the detonation products start to expand. The DND growth stops due to accumulation of structural defects of the crystallite, termination of $sp^2$ to $sp^3$ transition of carbon atoms and exhaustion of carbon radicals (recombination) | 18 | This is quite probable |

caused by the fundamental properties of carbon both in and behind the CRZ. As soon as the $C_2^{\bullet}$ free radicals have been exhausted and defects in the structure of the growing nanoparticle (behind the Chapman – Jouguet plane) have been accumulated, the crystallite growth is terminated. According to Dolmatov *et al.*,[18] this mechanism of DND formation may be universal, with the $C_2^{\bullet}$ radical being the initial species.

The views on the possible mechanism of DND formation are summarized in Table 1. More detailed description of the mechanism of formation of DND crystallites would be possible only after new instrumental methods for analysis of fast processes are developed.

### 2.2. Regularities of the detonation synthesis of nanodiamonds

A number of regular patterns reflecting the influence of operating parameters on the yields of DNDs and diamond detonation blend (DB) after explosion are now established.[6, 7, 24 – 26] These parameters include

— contents of charge components and specific power;
— effect of additives on the explosive charge;
— oxygen balance of the charge;
— density and dimensions of the charge;
— heat capacity and composition of the gas atmosphere in the explosion chamber;
— optimal ratio of the chamber volume and the mass of the explosive charge.

There are three options for firing the charge for the production of DNDs:

— in the atmosphere of inert gas (nitrogen, argon, $CO_2$, *etc.*) or in the gaseous products of the explosion;
— in water armour of the charge;
— in ice armour of the charge.

The first option leads to low yields of diamond-containing products ($<4$ mass % for DNDs) and the greatest incombustible impurity content (up to 30 mass %) in the DB due to the strong action of the detonation wave on the wall of the explosion chamber with the simultaneous corrosive action of acidic gases.

When a water shell is used (second option), the yields of DB and DNDs (4.5 mass % – 6 mass % for DNDs) are higher. Water efficiently lowers the temperature of expansion of detonation products, thus preventing conversion of DNDs to a non-diamond carbon (graphite, onion carbon, graphene, soot). The amount of incombustible residue in the DB is 9 mass % – 10 mass %, while that in DNDs is 0.5 mass % – 0.9 mass %. Firing the explosive charge in a shell reduces the discharge rate of detonation products, thus bringing their composition closer to the equilibrium one with carbon oxidation to $CO_2$. Furthermore, a water shell increases the time during which the pressure remains within the diamond stability region.

The third option provides the highest yield of DB and DNDs ($\sim$6 mass %), but pieces of ice strike against the steel wall of the explosion chamber, which reduces its service life, and the content of incombustible impurities in DB reaches 9 mass % – 13 mass %, while in the purified nanodiamonds it is 1.2 mass % – 1.5 mass %. The water or ice shell of the explosive charge retards the expansion of the detonation products, thus providing for more complete chemical reactions in the CRZ and behind the Chapman – Jouguet plane; it also efficiently withdraws excess heat released upon decomposition of the explosives and preserves crystallites.[6, 7, 13, 14]

While selecting the composition of an explosive charge, one should also consider economic factors,[13] that is, it is better to use commercially available inexpensive explosives. The list of these explosives is moderate, first of all, these are TNT and RDX. Whereas the use of these single explosives results in very low yields of DNDs (0.7 mass % – 0.9 mass % and 0.3 mass % – 1.0 mass %, respectively), the use of their mixture (TH) ($\sim$50 : 50) results in DND yields of up to 8.2 mass %, with other factors being optimized. Among single explosives, only tetryl provides a DND yield of $>7.0$ mass %. The commercial manufacture of tetryl has been terminated, but its inventories are very large.[27] The same yield is provided by using binary[28] and ternary[29] mixtures based on tetryl.

Despite the possibility of optimizing the key parameters that affect the synthesis of nanodiamonds, it is still impossible to express the elucidated dependences as simple formulae. Petrov[30] investigated the effect of the addition of solid organic compounds, including both inactive compounds (naphthalene, wax, *etc.*) and rather powerful explo-

**Table 2**. Yields of DB and DNDs from RDX of the addition of organic compounds (including explosives).[30]

| No. | Compound added | | Explosive charge density /g cm$^{-3}$ | OB (%) | Yield (mass %) | | DND specific surface area /m$^2$ g$^{-1}$ |
|---|---|---|---|---|---|---|---|
| | name | amount (mass %) | | | DB | DND | |
| 1 | Paraffin | 20 | 1.45 | −86.5 | 14.6 | 1.83 | 479 |
| 2 | Naphthalene | 15 | – | −63.3 | 11.4 | 1.20 | – |
| 3 | 2,4,6-Trinitromesitylene | 40 | 1.61 | −54.4 | 13.36 | 6.15 | 272 |
| 4 | 2,4,6-Trinitrotoluene | 60 | 1.65 | −53.0 | 10.6 | 8.4 | 310 |
| 5 | 2,4,6-Trinitroxylene | 40 | 1.64 | −48.7 | 11.2 | 5.12 | 232.7 |
| 6 | Tetryl | 100 | 1.61 | −47.4 | 9.10 | 4.10 | 427.5 |
| 7 | 2,4-Dinitrazapentane | 60 | 1.56 | −43.7 | 7.3 | 1.9 | 427.5 |
| 8 | 1,3,5-Trinitrobenzene | 60 | 1.69 | −42.4 | 8.45 | 5.48 | 312.1 |
| 9 | 2,4,6-Trinitrophenol | 50 | 1.67 | −40.5 | 7.20 | 4.06 | 261.6 |
| 10 | 2,4,6-Trinitrocresol | 40 | 1.69 | −38.0 | 7.37 | 4.72 | 240.0 |
| 11 | 2,2′,4,4′,6,6′-Hexanitrodiphenylamine | 50 | 1.67 | −37.2 | 6.86 | 5.22 | – |
| 12 | Tetryl | 50 | 1.63 | −34.5 | 3.41 | 2.47 | – |
| 13 | 2,3,4,6-Tetranitroaniline | 70 | 1.60 | −29.0 | 4.07 | 2.42 | 123.6 |
| 14 | 1,3,5-Trinitrobenzene | 20 | 1.71 | −28.5 | 4.74 | 2.90 | 210.5 |
| 15 | 2,4,6-Trinitroresorcinol | 40 | 1.69 | −27.3 | 5.53 | 3.21 | 244.8 |

**Table 3**. Yields of DB and DNDs from mixtures of RDX and trinitrotoluene.

| No. | Explosive charge | | | | OB (%) | DB yield (mass %) | DND content in DB (mass %) | DND yield (mass %) | Content of incombustible components in DND (mass %) | Ref. |
|---|---|---|---|---|---|---|---|---|---|---|
| | fabrication and detonation conditions | composition (mass %) | | density /g cm$^{-3}$ | | | | | | |
| | | TNT | TH | | | | | | | |
| 1 | Casting, gas phase ($N_2$) | 100 | 0 | 1.59 | −74.0 | 18.0 | 15.0 | 2.7 | – | 31, 32 |
| 2 | Casting, gas phase | 60 | 40 | 1.67 | −53.0 | 13.6 | – | 5.16 | – | 31 |
| 3 | Compaction, gas phase ($N_2$) | 0 | 100 | 1.61 | −21.6 | 7.0 | 8.6 | 0.6 | – | 30 |
| 4 | Casting, gas phase | 50 | 50 | 1.64 | −47.8 | 9.8 | 43.0 | 4.2 | 0.9 | 33 |
| 5 | Compaction, water | 50 | 50 | 1.62 | −47.8 | 12.6 | 45.9 | 5.8 | 0.77 | 33 |
| 6 | Compaction, aqueous solution of urotropin | 50 | 50 | 1.63 | −47.8 | 9.4 | 64.7 | 6.1 | 0.20 | 33 |
| 7 | Casting, aqueous solution of urotropin | 50 | 50 | 1.62 | −47.8 | 9.1 | 65.0 | 5.9 | 0.7 | 33 |

sives (TNT, trinitrobenzene, *etc.*), to RDX on the yields of DB and DNDs. The explosive charges were obtained by pressing and fired without a shell. The results of experiments of other authors with TNT, RDX and their mixtures have been reported.[31–33] The available data[30–33] were analyzed by Dolmatov[24] and are summarized in Tables 2 and 3.

From the standpoint of cost of detonation synthesis and decreasing burden on the chemical purification stage, the optimal DND yield is 5.0 mass %–8.0 mass % based on explosives with an oxygen balance from −35% to −55% and charges with a density of 1.60–1.70 g cm$^{-3}$ (Ref. 34).

According to Dolmatov *et al.*,[35] specific power and the related yield of DNDs are universal characteristics of explosives. The time of energy release upon explosion can be assumed to be equal to the time it takes for the compound or detonation products to move from the detonation wave front to the Chapman–Jouguet plane (*i.e.*, from the beginning to the end of the chemical reaction zone). This time may be tenths or hundredths of a microsecond. For many practical calculations, the exact time of existence of the chemical reaction zone has a crucial importance; it can serve to determine the real power of an explosive, which is different for different types of explosives or their mixtures. All other conditions being equal, this parameter strongly affects the DND yield. The explosive power is expressed as the quantity of heat released upon explosion of unit weight of the explosive per unit time (1 μs).

The heats of explosion of various types of explosives or their mixtures were determined many times, and the results did not differ much; the time of existence of the chemical reaction zone was determined rather accurately.[36–38] The non-monotonic dependence of the DND yield on the specific power of explosive is depicted in Fig. 1. If the optimum yield of DNDs is taken to be ⩾ 5 mass %, it is necessary to use explosives with a power in the range of 30–60 kJ kg$^{-1}$ μs$^{-1}$. The best result was obtained by using TH (60 : 40) fired in a water shell. The other suitable charges are tetryl, TH (50 : 50), TH (40 : 60), TH (36 : 64)[35] and binary[28] and ternary[29] charges based on tetryl.

The DND yield also depends non-monotonically on the DP pressure in the Chapman–Jouguet plane (Fig. 2), which makes it possible to choose the optimal composition of the explosive. The DP pressure should be in the range from 21 to 28.5 GPa.

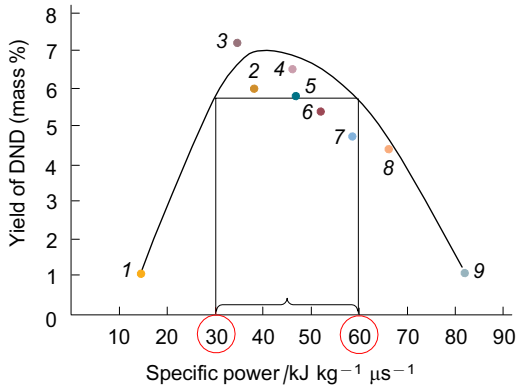



**Figure 1.** Dependence of the DND yield on the specific power of the explosive.[35]

| Item | Explosive | Yield (mass %) | Item | Explosive | Yield (mass %) |
|---|---|---|---|---|---|
| *1* | TNT | 1.06 | *6* | TH (36 : 64) | 5.4 |
| *2* | TH (50 : 50) | 6 | *7* | TH (70 : 30) | 4.7 |
| *3* | TH (60 : 40) | 7.2 | *8* | TH (30 : 70) | 4.4 |
| *4* | Tetryl | 6.5 | *9* | RDX | 1.1 |
| *5* | TH (40 : 60) | 5.8 | | | |

The authors are grateful to Springer and *Journal of Superhard Materials* for the permission to reproduce this Figure.

Thus, one can conclude that for producing DNDs in a stable yield of ⩾5 mass %, the explosive (or explosive composition) should have the following characteristics:

— oxygen balance from −35% to −55%;

— charge density > 1.6 g cm$^{-3}$;

— explosive specific power from 30 000 to 60 000 kJ kg$^{-1}$ μs$^{-1}$;

— pressure of detonation products in the Chapman–Jouguet plane from 21 to 28 GPa.

Dolmatov[24] described the synthesis of DNDs from a 50 : 50 TG mixture with an oxygen balance of 47.8%. Thus, 47.8 mass % of carbon can theoretically remain in this composition after explosion in the condensed state. However, the yield of free carbon (DB) based on the initial explosive mass is only 12.65 mass %, with only ~50 mass % being the DNDs. As noted above, the DB and DND yields are strongly affected by the gas medium of the explosion chamber (the reducing nature of gases is preferable).[25, 39]

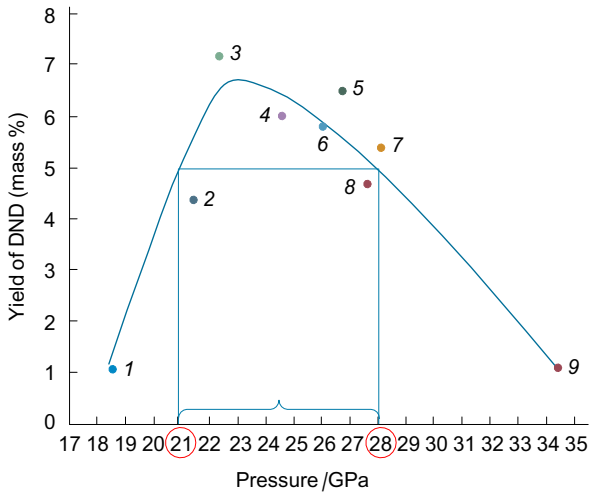



**Figure 2.** Dependence of the DND yield on the pressure at the Chapman – Jouguet plane.[35]

| Item | Explosive | Yield (mass %) | Item | Explosive | Yield (mass %) |
|---|---|---|---|---|---|
| *1* | TNT | 1 | *6* | TH (40 : 60) | 5.8 |
| *2* | TH (30 : 70) | 4.4 | *7* | TH (36 : 64) | 5.4 |
| *3* | TH (50 : 50) | 7.2 | *8* | TH (70 : 30) | 4.7 |
| *4* | TH (60 : 40) | 6 | *9* | RDX | 1.1 |
| *5* | Tetryl | 6.5 | | | |

The authors are grateful to Springer and *Journal of Superhard Materials* for the permission to reproduce this Figure.

The experience with commercial production of the diamond detonation blend and nanodiamonds with the established optimal process parameters using 50 : 50 TH and a shell of an urotropin solution in distilled water showed that it is possible to attain a DB yield of up to 12 mass %, with up to 68 mass % nanodiamonds being contained in the blend (the yield of nanodiamonds from 50 : 50 TH is up to 8.2 mass %). The highest yield of nanodiamonds was 8.25 mass %.

The incombustible impurities in purified DNDs, especially iron, chromium, manganese, lead and mercury, have an adverse effect on the properties of diamond-containing composites. In some cases, the purity of nanodiamonds becomes the crucial factor for their possible applications (*e.g.*, as slow neutron reflectors, parts of semiconductor devices, luminophore dopants). As a rule, after the chemical purification of nanodiamonds, the content of incombustible impurities decreases 5 – 8-fold; therefore, it is very important to examine the possibility to reduce their amount during the synthesis by doping the water shell of the TH charge with various compounds (preferably, the yield of nanodiamonds should simultaneously increase).[18]

The effect of these dopants on the amount and composition of incombustible impurities and the yield of nanodiamonds has been studied.[39] The compounds added to the water shell included boric acid, Trilon B, aminotetrazole, hydrazine, ammonia, urotropin and urea. The addition of these compounds generates a reducing atmosphere during and after detonation. This atmosphere has a beneficial effect on the yield of the blend and nanodiamonds, since it prevents the oxidation of condensed carbon *via* attack by carbon dioxide and water at the high temperatures of post-detonation processes. Compounds that were used as aqueous solutions in the shell were chosen for the following reasons:

— the harsh gases no longer attack condensed carbon, but easily react with reducing agents; the yield of condensed carbon thus increases;

— during chemical purification of DNDs, boric acid can react with metal oxides and thus convert them to compounds readily soluble in acids;

— Trilon B is known to be a good complexing agent towards many metals and metal salts;

— the use of aminotetrazole is driven by the possibility to increase the concentration of nitrogen in the nanodiamond crystallites.

The highest yields of nanodiamonds (6.9 mass %) and the diamond blend (13.4 mass %) were attained when the charge was armoured with an aqueous solution of urotropin. The use of an aqueous solution of hydrazine and urea to armour the charge results in a virtually identical yield of nanodiamonds ($\sim$6.29 mass % and $\sim$6.9 mass %, respectively). The use of Trilon B and aminotetrazole proved to be least efficient. The presence of urotropin minimized the amount of impurities in the blend; it was 1.96 mass %, while the highest amount of impurities (7 mass % – 9 mass %) was observed in the case of Trilon B. The introduction of dopants into the water shell cannot influence the synthesis of nanodiamonds, but in this case, the nanodiamonds that have already formed can be preserved, *i.e.*, their yield increases and the amount of incombustible impurities decreases, as has been demonstrated by Dolmatov.[39] Unexpectedly, it was shown that urotropin behaves as a chelator at high temperatures, while Trilon B, on the contrary, does not exhibit this type of behaviour, possibly due to a very short time of reaction with metal oxides at high temperatures. When aqueous solutions of the above compounds were used as shells for explosive charges, the impurity content in nanodiamonds decreased, on average, 3-fold compared to the use of distilled water.

In addition to the optimized conditions of the DND synthesis reported in the publication cited above,[34] these results demonstrate that for increasing the DND yield, the following is necessary:

— addition of a reducing agent (urotropin, Trilon B, hydrazine, urea) to the charge shell consisting of water or an aqueous solution;[39] it is better to use a cylindrical charge (technologically the simplest shape) with an aspect ratio $\geqslant$2;[6, 7]

— the heat capacity of the non-oxidative gas medium in the explosion chamber should be as high as possible; the use of $CO_2$ would be best of all, but in reality, gaseous products of previous detonations of explosive charges are used.[6, 7]

An optimal combination of the above conditions would result in an economically plausible DND yield of $>$5 mass %.

### 2.3. Diamond detonation blend

A DB nanoparticle has a complex and unusual structure consisting of three major parts: a classic diamond core (cubic system, $sp^3$-hybridized carbon atoms), transient structures composed of both $sp^3$- and $sp^2$-hybridized carbon atoms and a distorted graphene shell of $sp^2$-hybridized carbon atoms. Most of non-diamond carbon allotropes occur on the surface of the diamond-like core and form a common hybrid structure with the core, fragments of which are connected not only by physical interactions, but also by

chemical bonds. The isolation of pure diamond-like structures with reproducible characteristics is impossible without chemical treatment with energy release sufficient to rupture strong carbon – carbon bonds. Despite the fact that X-ray diffraction methods show DND particles in DB as separate objects, they do not form a clearly defined separate phase component.

#### 2.3.1. Particle morphology of the diamond blend

A study of Voznyakovskii *et al.*[40] is devoted to the morphology of DB particles. The small-angle X-ray scattering method was used. The authors proposed the following model for the structure of DB particles: a highly oblate ellipsoid of revolution with a 40 – 50 nm diameter and 2 – 3 nm thickness. According to X-ray diffraction data, the size of subparticles of DND aggregates is 2 – 7 nm. Considering the ratio of the mass fractions of amorphous and crystalline phases, the major part of amorphous carbon is presumably concentrated along the equator of the particle (Fig. 3). The presented model is phenomenological and does not contradict the theoretical models of DND particle morphology known from the literature. The proposed model also adequately explains the reinforcement effect upon the use of DB in polymer materials science. This effect is related to the adsorption activity of DB particles caused by DND particles incorporated in them.

#### 2.3.2. Isolation of detonation nanodiamonds from the diamond detonation blend

Chemical purification is the most expensive and intricate stage in the DND production. The purification methods used determine the consumer properties of nanodiamonds, while the difficulty of implementing these methods dictates the final product cost and applicability. The DND production process includes two key stages: detonation synthesis and chemical purification (often consisting of several steps). The prime cost of chemical purification is $\sim 2/3$ of the prime cost of the nanodiamond synthesis. During the chemical purification, the textural characteristics of DB do not change monotonically, but change stepwise, which distinguishes the diamond blend from other carbon materials.[41]

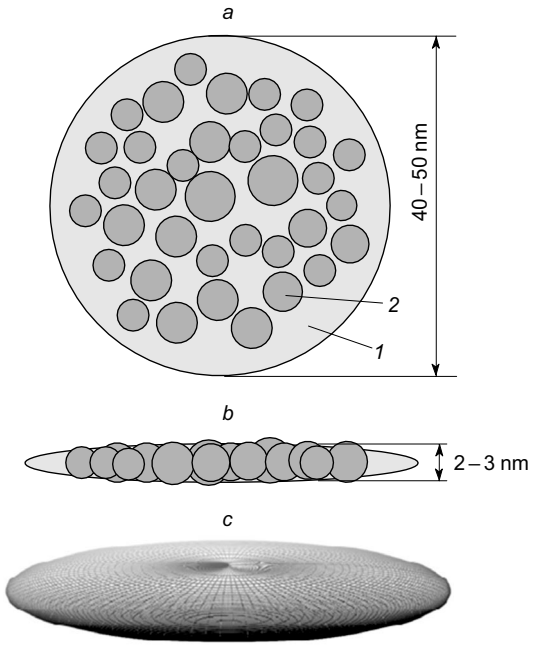



**Figure 3.** Model of the DB particle as an oblate ellipsoid of revolution.[40] (*a*) top view, (*b*) side view, (*c*) 3D model; (*1*) amorphous carbon, (*2*) incorporated DND particles.
The authors are grateful to Springer and *Journal of Superhard Materials* for the permission to reproduce this Figure.

Most of the proposed purification procedures are suitable only as laboratory methods. Some designs can be rationally implemented only in a large-scale plant, which may have a lot of specialized equipment blocks.[5]

The liquid-phase purification methods combining oxidation and acid dissolution of metals are preferable. Many designs for these methods have been proposed; several groups of such processes are considered below.

The use of only nitric acid for oxidation of aqueous solutions necessitates conducting the process at elevated pressure to ensure that it occurs in the liquid phase. A one-stage thermooxidative treatment with nitric acid at elevated pressure has been proposed.[42] According to a patent,[43] the diamond blend is subjected to a two-stage treatment with aqueous nitric acid, first, with 50% – 99% $HNO_3$ at 80 – 180 °C and then with 10% – 40% $HNO_3$ at 220 – 280 °C. The main drawback of these processes is the use of relatively concentrated nitric acid, which is taken in a large excess necessary to achieve high oxidation rates and the required degree of removal of non-diamond carbon from the DB.

However, nitric acid is not only consumed for the target oxidation of non-diamond carbon, but a considerable part of the acid undergoes thermal decomposition to nitrogen oxides. The presence of a large amount of highly reactive nitrogen dioxide accounts for the high corrosive activity of the medium. This reduces the service life of equipment, and the corrosion products make a considerable contribution to the ash content of the final product. The liquid DND suspension formed after the oxidative thermal treatment has a very high residual concentration of nitric acid (20% – 30%), which has to be separated and recycled back to the process. The recycling of a part of waste nitric acid is technically implementable, but special distillation and fractionation units are required to remove soluble salts and preconcentrate aqueous solutions of nitric acid for reuse. As a result, the major material and labour resources are spent for maintaining the acid circulation, the volume of which is more than an order of magnitude higher than the volume of the processed target product.

The authors of a patent[44] used oxidative thermal treatment of DB in the form of suspension containing a solid phase at a concentration of $\leqslant 5\%$ with an aqueous solution of ammonium nitrate in acidic medium (pH < 1). The required acidity of the medium was generated by adding a small amount of nitric acid up to its concentration in water of 5 mass % – 10 mass % (Table 4). Ammonium nitrate was taken in an excess with respect to the carbon material (10 – 15 parts of ammonium nitrate per part of the carbon material). The reaction was conducted at 200 – 260 °C until gas evolution ceased, which indicated that the oxidation was over and ammonium nitrate decomposed. Nitric acid contained in the aqueous solution did not considerably affect the degree of oxidation, because of its low amount, but ensured the high acidity of the medium. This considerably decreased the temperature of the onset of decomposition of ammonium nitrate, and the target oxidation process could be conducted at the above-indicated temperature of 200 – 260 °C. This ensured decomposition of ammonium

**Table 4**. Features of chemical purification methods of diamond blend.

| No. | Method | Features | Ref. |
|---|---|---|---|
| 1 | Treatment of DB with 2% – 40% $HNO_3$ with compressed air oxygen (200 – 280 °C, 5 – 15 MPa) | Large amounts of nitrogen oxides, large excess of $HNO_3$, enhanced corrosion of the equipment | 42 |
| 2 | Two-stage treatment of DB with aqueous $HNO_3$: first, 50% – 99% $HNO_3$ at 80 – 180 °C, then 10% – 40% $HNO_3$ at 220 – 280 °C | Large amounts of nitrogen oxides, large excess of $HNO_3$, enhanced corrosion of the equipment | 43 |
| 3 | One-stage treatment of DB with 5% – 10% $HNO_3$ with $NH_4NO_3$ at 200 – 260 °C | Only neutral nitrogen is released; virtually no corrosion of the equipment | 44 |

nitrate by a mechanism in which nitrogen is formed as the only gaseous product, while the released oxygen is spent for the oxidation of the carbon component.

Owing to the presence of some nitric acid in the reaction mixture, metallic impurities remain in the dissolved state and are converted, upon oxidation, to readily soluble metal nitrates. Oxidation is performed with excess oxidant (ammonium nitrate); this allows efficient removal of all non-diamond carbon components of the DB. The excess of ammonium nitrate, which remains after the oxidation of non-diamond carbon, completely decomposes in this system to non-toxic products (water, nitrogen and oxygen), which ensures completion of the oxidation of carbon components and the absence of nitrites and nitrogen oxides in the dissolved products.

This purification procedure affords a suspension of high-purity nanodispersed diamonds as a hydrosol in a dilute (1% – 5%) aqueous solution of nitric acid. Water-soluble impurities are washed away with deionized water by standard procedures. A benefit of this method is the absence of toxic nitrogen oxides in reaction products, which eliminates the need of using expensive systems for absorption and regeneration of nitric acid. The oxidation at this temperature in titanium autoclaves virtually excludes corrosion of the vessel and contamination of the target product by titanium dioxide. Owing to low content of nitric acid in the spent reaction mixture, it is possible to do without acid circulation.

Volkov[45] studied the composition of impurities for 22 samples of purified nanodiamonds from various manufacturers by atomic emission spectroscopy. Despite relatively efficient, in some cases, chemical purification, more than 70 elements were detected in the nanodiamonds. The limit of detection of alkali metals (Cs and Rb) was 100 ppm, while the limits of detection of other ($>50$) elements was 1 ppm. The relative standard deviation for reproducibility of the results in the 1 – 10 000 ppm range was 0.05 – 0.1.

The contents of elements in the DND samples were highly different (Table 5). Small amounts of Fe, Ti, Al, Cr, Si, Ca and Cu were found. Among these elements, Fe, Cr, Cu and Al are most unfavourable. Iron is the most injurious impurity for the subsequent application of nanodiamonds. The highest iron content (0.5 mass % – 0.9 mass %) was found for DND samples manufactured by the Science and Production CJSC Sinta (see Table 5). The highest copper content was inherent in samples of the Federal Science and Production Centre OJSC Altai (up to 1.5 mass %) and the Real Dzerzhinsk (0.05 mass % – 0.10 mass %), while the lowest copper content was present in samples of the Special Design and Technology Bureau (SCTB) Technolog (0.003 mass % – 0.004 mass %). The aluminium contents were as follows: 0.07 mass % to 0.15 mass % (Nanocarbon Research Institute Co. Ltd, Japan); 0.1 mass % (Nano-Group Co.); 0.07 mass % (Federal Science and Production Centre OJSC Altai); and 0.002 mass % (SCTB Technolog). Mercury, chromium and lead are the most toxic elements. In the nanodiamond samples supplied by the OJSC Altai, the contents of these elements and incombustible impurities were higher than in samples of other manufacturers. The highest amount of chromium was found in DNDs manufactured by the CJSC Sinta (0.16 mass %). The samples of the SCTB Technolog contained almost no lead (at the sensitivity level of the instrument).

## 3. Properties of detonation nanodiamonds

### 3.1. Structure and composition of primary particles

As a rule, the average size of diamond nanoparticles that have time to form during the detonation process is 4 – 6 nm. Fast change in the $P,T$ conditions of DND formation and

**Table 5**. Content of mercury, iron and incombustible impurities in DND samples produced by various manufacturers.[45]

| No. | Manufacturer | Contents | | |
|---|---|---|---|---|
| | | mercury ($10^{-8} \times$ mass %) | iron (mass %) | incombustible impurities (except for oxygen in oxides) (mass %) |
| 1 | Real Dzerzhinsk, Russian Federation | 0.021 – 0.075 | 0.5 – 0.6 | 0.1 – 1.31 |
| 2 | CJSC Sinta, Belarus' | 0.023 – 0.46 | 0.5 – 0.9 | 0.33 – 1.97 |
| 3 | NanoGroup Co., Czechia | 0.025 | 0.4 | 1.92 |
| 4 | ALIT, Ukraine | 0.028 | – | 1.63 |
| 5 | PlasmaChem GmbH, Germany | 0.028 – 1.6 | 0.3 | 0.32 – 1.93 |
| 6 | Nanocarbon Research Institute Co. Ltd, Japan | 0.035 | – | 0.62 – 1.21 |
| 7 | SCTB Technolog, Russian Federation | 0.082 – 0.195 | 0.12 – 0.18 | 0.43 – 0.55 |
| 8 | OJSC Altai, Russian Federation | 37 – 717 | 0.3 – 0.65 | 0.94 – 2.69 |

short times (0.1 – 0.3 μs) of plasma existence in the CRZ and post-detonation processes give rise to unique properties of the resulting particles. The structure of DNDs has a considerable number of defects both on the surface and inside the crystallites. The heteroatoms (oxygen, hydrogen, nitrogen), which are present in the explosive, occur not only in the surface functional groups, but also inside the crystallites. Nitrogen exists in the crystallite also as an NV centre; most of nitrogen and hydrogen are dissolved in the diamond as it is formed. This is evidenced by the fact that analysis of the gas phase obtained upon mechanical crushing of DNDs *in vacuo* revealed considerable amounts of nitrogen and hydrogen molecules.† After chemical purification, DND is a grey-coloured aggregated powder in which aggregates of nanocrystallites are highly different in size and strength.[1, 3, 7, 46] The powder contains quite a lot of oxygen, hydrogen and nitrogen atoms, which are mainly chemically bound to the particle surface or physically retained on the surface.[47]

The quantity of heteroatoms in the nanodiamond crystallites depends on many parameters of the synthesis, first of all, on the composition of explosive. The content of surface impurities is also affected by the chemical purification procedure. Nanodiamond contains carbon atoms (90% – 97%) mainly, in the diamond form, surface oxygen atoms (3 mass % – 4.5 mass %) incorporated in functional groups, hydrogen atoms (0.6 mass % – 2.2 mass %) both in functional groups and in the dissolved state, nitrogen atoms (1.8 mass % – 2.8 mass %) mainly dissolved in the crystallites and incombustible impurities (0.04 mass % – 6.0 mass %). The incombustible impurities are mainly composed of iron, calcium, titanium, copper, chromium and silicon oxides. The titanium, silicon and lead impurities are most difficult to remove.[46 – 50]

The primary nanodiamond particles have a complex structure.[47, 49 – 51] According to Kulakova,[47] they can be likened to bulky molecules in which carbon occurs as a rigid diamond core surrounded by a shell of $sp^2$- and $sp^3$-hybridized carbon atoms. This shell is coated mainly by oxygenated functional groups. The structure of the DND crystallites depends on many conditions of synthesis and chemical purification and can markedly vary among nanodiamonds manufactured by different companies.[5, 47, 49 – 52]

According to transmission electron microscopy data, the primary DND particles have a spherical shape with a size of 4 – 6 nm and a narrow size distribution. This conclusion was confirmed by Kulakova *et al.*,[51] who used small-angle X-ray scattering. Electron diffraction study for the DNDs manufactured by the SHTB Technolog after various types of chemical treatment showed a typical diamond diffraction. For a primary diamond particle of ~5 nm size, the inner diameter of the diamond phase was found to be ~3 nm and the thickness of the disrupted carbon shell was ~1 nm. Transition from the diamond core to the carbon shell was gradual, as no sharp change in the crystal potential was noted. The structure and the size of the diamond core were virtually unaffected by treatment of DNDs with chemicals such as chlorine, hydrogen, fluorine or alkyl halides. No non-diamond carbon was found in this study in either initial or modified DND particles.

† Private communication of A.L.Vereshchagin, Doctor of Chemical Sciences, Head of the Department of General Chemistry and Expert Evaluation of Commodities, Biysk Technological Institute.

The oxygen and hydrogen atoms are incorporated in functional groups on the DND surface. The DND crystallites contain much nitrogen, the content of which decreases only slightly after high-temperature treatment.[1] Some of nitrogen atoms occur in DNDs as nitrogen-containing surface functional groups, since DNDs have been purified with nitric acid. Indeed, Korol'kov [53] found nitrate groups in the initial DNDs and showed that after reductive treatment, there were no such groups on the DND surface. However, the total nitrogen content of DNDs remained rather high after both air and hydrogen treatment. Hence, nitrogen is also present within the DND particle. Meanwhile, the question arises whether it is located in the disrupted carbon shell or in the diamond core. It was shown [51] that oxidation of DND particles (almost up to complete oxidation of the sample) is accompanied by the parallel release of carbon dioxide and nitrogen. This unambiguously indicates that nitrogen that is not incorporated in functional groups is uniformly distributed throughout the DND bulk.

The micrographs of DND samples obtained using either a 50 : 50 TH mixture or anhydrous BTF are presented in Fig. 4.[54] Whereas the crystallites obtained from the former hydrogen-containing explosives had an average size of ~5 nm, in the case of BTF, the size of the sintered spherical crystalline DND particles was ~100 nm.

The spherical particle is formed as a result of simultaneous action of very high temperature (~4700 K) and pressure (36 GPa) behind the detonation wave and the Chapman – Jouguet plane.

A calculation of the distribution of carbon atoms in DNDs [55] showed that factors restricting the growth (⩽8 nm) of the diamond core include disruption of the long-range order and accumulation of structural defects in the crystal lattice during the carbon nanoparticle growth during post-detonation processes. Comparison of carbon atom distributions in the detonation nanodiamond and in the defect-free diamond showed a change in the coordination number in the outer coordination sphere of the nanodiamond. In the coordination spheres, some atoms are missing (lattice defects), which changes the structure and morphology of the DND surface. Defective structures are more reactive and are more readily oxidized during the chemical purification.

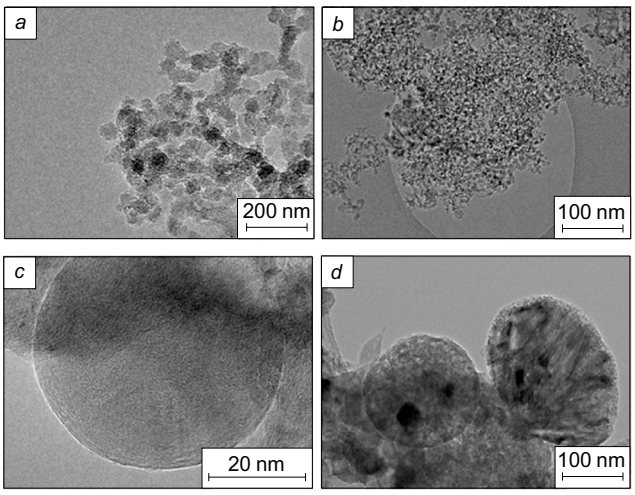



**Figure 4.** Micrographs of DNDs obtained from 50 : 50 TH (*a*, *b*) and BTF (*c*, *d*).[54]

The surface of DND particles bears various functional groups (mainly, oxygenated groups, such as carboxyl, ester, ether, lactone, *etc.*), the nature and the ratio of which are determined by details of DND production, isolation and purification.[3, 7, 49, 56, 57] This circumstance often complicates their practical use. Therefore, methods for the physicochemical treatment of the nanodiamond particle become significant. This treatment makes it possible to modify the nanoparticle surface and may give rise to either a monofunctional surface coating or a surface layer of inorganic or organic compounds, *i.e.*, it opens a way for a targeted change in the physicochemical properties of nanodiamonds, which in turns allows the use of modified particles as new promising products. This material combines the properties of the diamond core and grafted compounds on the crystallite surface.

### 3.2. Stability of suspensions of detonation nanodiamonds

Strong aggregation of nanoparticles complicates the production of composites. The smaller the aggregates (in the limiting cases, these are 4 – 10 nm particles), the more difficult it is to destroy them; but in this case, they are more uniformly distributed throughout the matrix and interact more efficiently with the matrix. The detonation nanodiamonds isolated from DB or subjected to modification after purification are most suitable as aqueous suspensions for processes that use aqueous media (*e.g.*, galvanic processes; preparation of some polymer – diamond composites). In these suspensions, Dents are most disaggregated. It was shown [58, 59] that the faces of nanodiamond particles possess on electrostatic potential of different signs. This is the reason for their active aggregation and this promotes effective immobilization of various molecules on the surface. The electrostatic potential of nanocrystals can vary depending on the method of surface treatment, the shape and the ratio of (111) and (100) surfaces. According to Barnard,[58] for a truncated octahedral diamond nanocrystallite, a high positive potential is inherent in the (100)/(111) edge and the (100) face. A high negative potential is found for the graphitized (111) face. Therefore, such nanocrystallites form strong aggregates.

The results of stability studies of DND suspensions [60] confirmed that at room temperature in water, a ζ-potential of 30 mV is sufficient to ensure coagulation stability, and the sign of the surface charge is insignificant. The physical causes for the appearance of excess charge on the surface of colloidal particles and the accompanying formation of an electric double layer can be different, *e.g.*, selective adsorption of ions from solution or reactions of surface chemical groups with water.

The dependence of the ζ-potential on the pH of a suspension of DNDs produced by dry synthesis, isolated from the detonation carbon by chromic acid mixture oxidation, is depicted in Fig. 5. Curve *1* shows the change in the ζ-potential sign. For this sample of nanodiamond suspension, the stability regions are located at pH < 5 and pH > 10. A similar dependence is typical of suspensions of all DNDs isolated from the detonation products by the liquid-phase method. The complex shape of the dependence is attributable to the presence of several types of functional groups.

The attempts to significantly reduce the size of DND aggregates in aqueous suspensions by high-power ultrasonic treatment or by adding surfactants did not meet with success. The purpose of disaggregation of strong DND

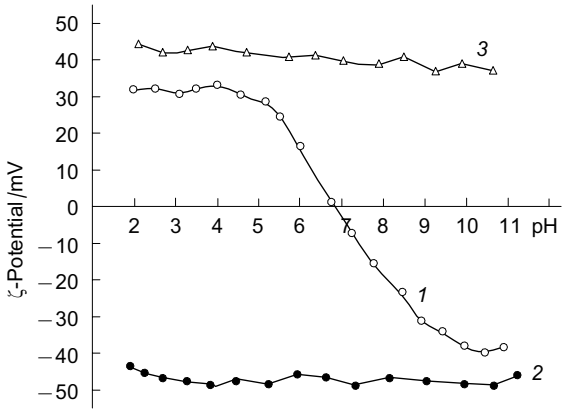



**Figure 5.** Dependences of the ζ-potential of DND particles on the suspension pH.[3] (*1*) commercial DNDs produced by dry synthesis; (*2*) disaggregated DNDs obtained by the process of oxidation; (*3*) disaggregated nanodiamond obtained by the process of reduction.

structures was to prepare native diamond nanoparticles of 4 – 6 nm size. The primary particle aggregates were found, and it was agreed that the size of such aggregates would not exceed 100 nm. Secondary aggregates with a size from 100 to 2000 nm decrease upon ultrasonic treatment. Pentecost *et al.*[61] described a peculiar DND disaggregation technique by grinding in the medium of salt or sugar, which did not introduce any impurities that would require the subsequent chemical purification. In this case, repeated aggregation did not take place even after the suspension was dried and then dispersed in water. The characteristic particle size of the suspension was in the 5 – 20 nm range.

Oxygen treatment of purified DNDs at temperatures of ~450 °C followed by centrifugation results in complete DND disaggregation and gives a suspension of primary DND particles with a size distribution maximum at 4 nm.[62] The annealing in hydrogen at 500 °C also facilitates the isolation of a suspension of 4 nm nanoparticles from dispersed DND solutions upon subsequent centrifugation of the product.

The DND functionalization endows the nanodiamonds with hydrophilicity or hydrophobicity. The suitable functional groups include oxygen-containing halide, hydride and methyl groups.[63, 64]

It was shown [65] that the stability of aqueous suspensions is affected by cationic surfactants, the suspension stability being determined by the adsorption capacity of the surfactant (ζ-potential) and the hydrophilicity of the nanodiamond surface. The coagulation stability of DNDs in water is provided by a ζ-potential of 30 mV. The adsorption activity of surfactants considerably depends on the length of the hydrocarbon chain in their molecules; the longer the chain the higher the hydrophobicity and the lower the adsorption capacity of the surfactant. The initial DNDs were exposed to air oxygen in a furnace for 120 min at a temperature of 420 °C.

### 3.3. Optical properties of detonation nanodiamonds

#### 3.3.1. IR spectra

Infrared spectroscopy is an important method for determination of the physicochemical properties of solids.[63, 66 – 68] Small-sized diamond particles have a large specific surface area, and various surface groups have their own character-

istic absorption bands in the IR range. The intensity of the intrinsic absorption of the diamond phase in the 400 – 4000 $cm^{-1}$ range is low; therefore, the IR spectroscopy is quite applicable for identifying functional groups on the DND surface.

Dolmatov *et al.*[66] and Buchatskaya *et al.*[67] studied diamonds of different origin (natural DNDs and DNDs produced by static and dynamic synthesis) subjected to various types of chemical purification. The purpose of these studies was to identify the differences between the IR spectra of these different sorts of diamonds and the influence of the chemical purification procedure on the type of functional groups.

The IR spectra of the diamonds exhibit absorption bands of the hydroxyl groups of both adsorbed water molecules (3244 – 3418 $cm^{-1}$) and particles attached to the surface (1635 – 1609 and 3935 – 3850 $cm^{-1}$). The absorption bands at 2800 – 2930 $cm^{-1}$ are due to C—H vibrations. It was found that, irrespective of the diamond origin, purification with sulfuric acid results in the appearance of the S—S and C—S modes in the IR spectra, while after nitric acid treatment, the IR spectra exhibit C—N modes. Absorption bands for impurity nitrogen centres in the 1558 – 1566 $cm^{-1}$ range were found for natural diamonds (1558 $cm^{-1}$) and diamond micro-powders obtained by dynamic synthesis (1566 $cm^{-1}$). Thus, IR spectra provide information on not only the presence of various functional groups on the diamond surface, but also the appearance of S- and N-containing groups depending on the purification method. Kulakova[47] demonstrated that the functional composition of the DND surface changes on exposure to gases.

The IR spectrum of pristine nanodiamonds shows a distinct band with a maximum at 3405 $cm^{-1}$, which can be assigned to hydrogen vibrations of adsorbed water and surface OH groups. In the 3000 – 2800 $cm^{-1}$ range, weak C—H stretching bands are detected. The surface C=O group gives rise to an absorption band at 1737 $cm^{-1}$. The OH bending vibrations are responsible for the band at 1617 $cm^{-1}$. The 1345 – 1122 $cm^{-1}$ absorption band can be attributed to the diamond lattice vibrations. On treatment of DNDs with air oxygen at 400°C, the absorption band at 1737 $cm^{-1}$, caused by carbonyl vibrations, shifts to 1791 $cm^{-1}$, which is most likely indicative of further oxidation of the DND surface and formation of a C—O—C bond located near C=O groups.

Treatment of DNDs with hydrogen leads to complete disappearance of C=O groups and, hence, the IR absorption band of these groups also disappears; however, new absorption bands appear at 2941 and 2877 $cm^{-1}$, indicating the formation of C—H bonds on the diamond ($sp^3$-hybridized) carbon. The absorption band at 2941 $cm^{-1}$ can be assigned to the hydrogen atom attached to carbon located on the octahedral face, while the 2877 $cm^{-1}$ band is attributable to the bond between hydrogen and carbon atoms located on the cubic face of the nanodiamond.[53]

#### 3.3.2. Raman spectra and photoluminescence

The popularity of Raman spectroscopy is due to the fact that each carbon allotrope can be easily recognized in the Raman spectrum. This method is used to determine the degree of perfection of the crystal structure, phase purity and crystallite size.[69] Owing to a high luminescence quantum yield and absolute photostability of some impurity centres, nanodiamond has been acknowledged as one of the most promising materials for the design of single-photon emitters and photoluminescent biomarkers.

The Raman spectrum of thoroughly purified nanodiamond has at least four components.[69] The dominant maximum in the range of 1000 – 2000 $cm^{-1}$ is composed of four major components (peaks). The peak centred at 1326 $cm^{-1}$ corresponds to the diamond phase; the other components occur at 1250, 1630 – 1640 and 1730 $cm^{-1}$. As the size of nanodiamond crystallites decreases, additional peaks may appear in the Raman spectra, which are associated with a considerable increase in the surface area to volume ratio of the nanodiamond. Simultaneously, the position and shape of the major diamond maximum change.[69] This effect of crystallite size on the Raman spectrum has been called phonon localization. For diamonds, phonon localization becomes noticeable when the crystallite size is $< 30$ nm.[68]

In the Raman spectra of DNDs, the major band usually looks like a characteristic narrow line at 1330 $cm^{-1}$ (Ref. 68). All nanodiamond samples give rise to the same band at the same wavelength of 1325 $cm^{-1}$, which corresponds to carbon atoms of the diamond lattice ($sp^3$-hybridization); the minor shift accompanied by broadening towards lower frequency is caused by the nano-scale of DNDs.

The peak corresponding to $sp^2$-hybridized carbon atoms in graphene and in graphite-containing materials is usually located in the frequency range of 1560 – 1580 $cm^{-1}$. In the Raman spectra of DNDs, this peak was found at 1632, 1610 and 1604 $cm^{-1}$ for native, oxidized and reduced samples, respectively. The most pronounced shift to higher frequency was found for native nanodiamond, the surface of which contained the greatest number of C=O groups. The reduced DNDs with no carbonyl groups found on the surface showed the smallest shift to a higher frequency. According to published data,[69] the products containing C=O groups exhibit Raman bands in the 1600 – 1700 $cm^{-1}$ range.

It follows from the above that the surfaces of test samples bear functional groups containing $sp^2$-hybridized carbon atoms bound to oxygen. These carbon atoms are manifested in this range of the Raman spectra, along with the C=C double bond, which is similar to the bond in graphite, but is somewhat distorted.

Kulakova[47] confirmed the structure of the DND particle as having a diamond core corresponding to the cubic system, surrounded by $sp^2$- and $sp^3$-hybridized carbon atoms.

For a long period of time, only a broad photoluminescence (PL) band has been recorded for DNDs in the wavelength range of 400 – 700 nm with the intensity maximum depending on the excitation wavelength. The origin of PL is presumably related to structural defects on the surface of DND crystallites. Presumably, there are no optically active defects (first of all, involving nitrogen) in the crystallite bulk (or their concentration is very low). Switching to studying luminescence of single DND particles irradiated with electrons opened up the possibility to considerably suppress the luminescence background caused by surface defects, while the use of continuous-wave laser excitation[70] allowed for detecting the bright photoluminescence of the NV centres in separate crystallites or in moderate-size aggregates of nanodiamonds.

Studies of the photoemission properties of DNDs in combination with Raman spectroscopy were used to estimate the size of diamond nanocrystallites that exhibited

intense photoluminescence associated with NV centres. The Raman spectra measured for the points of bright luminescence showed the absence of a shift of the diamond line relative to the wavelength of 1332.5 $cm^{-1}$; according to the phonon localization model, this implies that the intense local luminescence of NV centres is related to >20 nm crystallites. Using highly sensitive photoluminescence detection systems, it was possible to detect single NV centres in separate non-irradiated DND crystallites with 5 nm size. It was found that PL of a crystallite of this size blinks at a definite frequency.[71] In the sintered DND clusters, the concentration of NV centres is $10^{20}-10^{21}$ $cm^{-3}$. The luminescence of these samples retained high intensity for 2 h.

Zhornik *et al.*[62] succeeded in obtaining DNDs with an abnormally high concentration of the NV centres. For this purpose, they sintered the pristine DND crystallites (4–5 nm) at 1500°C and 6 GPa for 20 s. Structural studies of the obtained sample showed that sintering was accompanied by self-assembly of diamond nanocrystallites into oriented aggregates with a size of ~1–10 μm.

According to estimates carried out by electron paramagnetic resonance (EPR) spectroscopy, the concentration of NV centres in sintered DND clusters was $10^{20}-10^{21}$ $cm^{-3}$ (Ref. 62). The liquid-phase oxidation of DNDs with a $H_2SO_4-HNO_3$ acid mixture (4:1) was accompanied by the appearance of luminescence properties of DND–COOH, which was reflected as a very high intensity and unusual shape of the Raman spectra. The luminescence of DND–COOH was manifested over a relatively broad wavelength range (450–650 nm), had a maximum at 510 nm and persisted over a relatively long period of time. Therefore, studies of one sample can be carried out for long.

It was also shown that chemical modification of DNDs with nitrogen-containing compounds (diamines and glycine) gives rise to luminescence in a narrower range (450–550 nm) with a maximum at 510 nm; in this case, too, photobleaching does not take place. In the authors' opinion, this is an advantage of chemically modified DNDs over less stable luminescent probes, which are normally used in biological investigations. This fact, together with non-toxicity, makes modified nanodiamonds applicable for the imaging of intracellular processes.

### 3.4. Characteristic features of paramagnetism of doped detonation nanodiamonds

EPR spectroscopy is a potent non-destructive method for studying nanostructured materials, which is suitable for investigation of the spatial arrangement of point defects in the crystal structure and the electronic and magnetic properties of nanoparticles in composite,[72,73] crystalline[74,75] and polycrystalline[76–78] materials. The paramagnetic properties of nanodiamonds are caused, first of all, by the unpaired electron located on the cleaved chemical bond and by impurity defects, *e.g.*, P1 and NV centres. This makes EPR spectroscopy a unique tool for characterizing a nanodiamond particle as a separate object.[79] The nanodiamond structure is such that most of unpaired electrons are located under the shell, including the incomplete surface of the proper diamond nanocrystallite. During purification of raw nanodiamonds, it is impossible to completely remove the stubborn metallic and magnetic impurities, which can be efficiently detected by EPR spectroscopy.[80] This method makes it possible to detect a minimum number of paramagnetic centres if more than $10^{11}$ spins per gram are present in a substance. For a typical sample, the minimum detectable concentration of paramagnetic centres is $10^{-9}$ mol $L^{-1}$ (Ref. 81).

Detonation nanodiamonds have a high concentration of paramagnetic centres ($\sim 2\times10^{19}$ spins per gram), and this opens up the opportunity for using scientific results in spintronics.‡ Furthermore, considering the prospects for the use of nanodiamonds as sources of single photons, optical biomarkers and ultrasensitive magnetometers,[82–85] it is relevant to study the influence of acceptor and donor impurity atoms in the diamond core on the DND properties.[86]

A characteristic feature of nanodiamonds found in meteorites is an abnormally high content of impurity nitrogen, which can reach 20 000 ppm (2.0 mass %).[87–89] A silicon structural impurity was identified in the crystal lattice of nanodiamond grains isolated from meteorites of various chemical classes. Therefore, a relevant task is to establish the influence of the targeted doping of nanodiamond crystals (in particular, with boron and phosphorus) on their paramagnetic and optical properties.

#### 3.4.1. Characteristic features of paramagnetism of DNDs doped with boron and phosphorus atoms during the synthesis

A number of nanodiamond samples, both undoped (DND20) and doped with phosphorus (DND32) and boron (DND36) during the synthesis, manufactured by the SCTB Technolog were studied by EPR spectroscopy.

The EPR spectra were measured by sweeping a 300 mT magnetic field; therefore, it is possible to compare the spectra using the given reference line. Unlike the pristine DND sample, the doped DND samples showed a hyperfine structure in the EPR spectra (Fig. 6). In the magnetic field region of ~190 mT, the signal of the reference sample (ruby) is present.[39,90]

The EPR spectra recorded directly in the resonance enhancement region (magnetic field sweep of 10 mT) showed[90] that introduction of dopant atoms into nanodiamonds affects the EPR spectral parameters, in particular, the line width ($\Delta B$) changed compared with the line width of the pristine sample. Indeed, in the case of DND20, the EPR line width was 0.89 mT, while for the phosphorus-doped DND32 and boron-doped DND36 samples, the line widths decreased to 0.73 and 0.75 mT, respectively.

After doping, the concentration of detected paramagnetic centres in the samples decreased: by 10% in DND32 (phosphorus) and by 5% in DND36 (boron). The changes in the dispersion of magnetic susceptibility in the resonance enhancement region were also different for the prostine and doped DND samples.

Thus, the EPR study showed the possibility of doping diamond nanocrystallites with boron and phosphorus during the synthesis.[90] The change in the parameters of the EPR spectra of DND powders modified by these dopant atoms indicates, first, the possibility of targeted modification of the nanodiamond lattice with a desired dopant and, second, good prospects of using EPR spectroscopy for diagnosis of the quality of nanodiamond feedstock and the degree of diamond purification from undesired impurities at any stage after the synthesis.[91–93]

‡ In spintronic devices, as opposed to conventional electronic devices, the energy or information is transported by spin current rather than electrical current.[82,83]

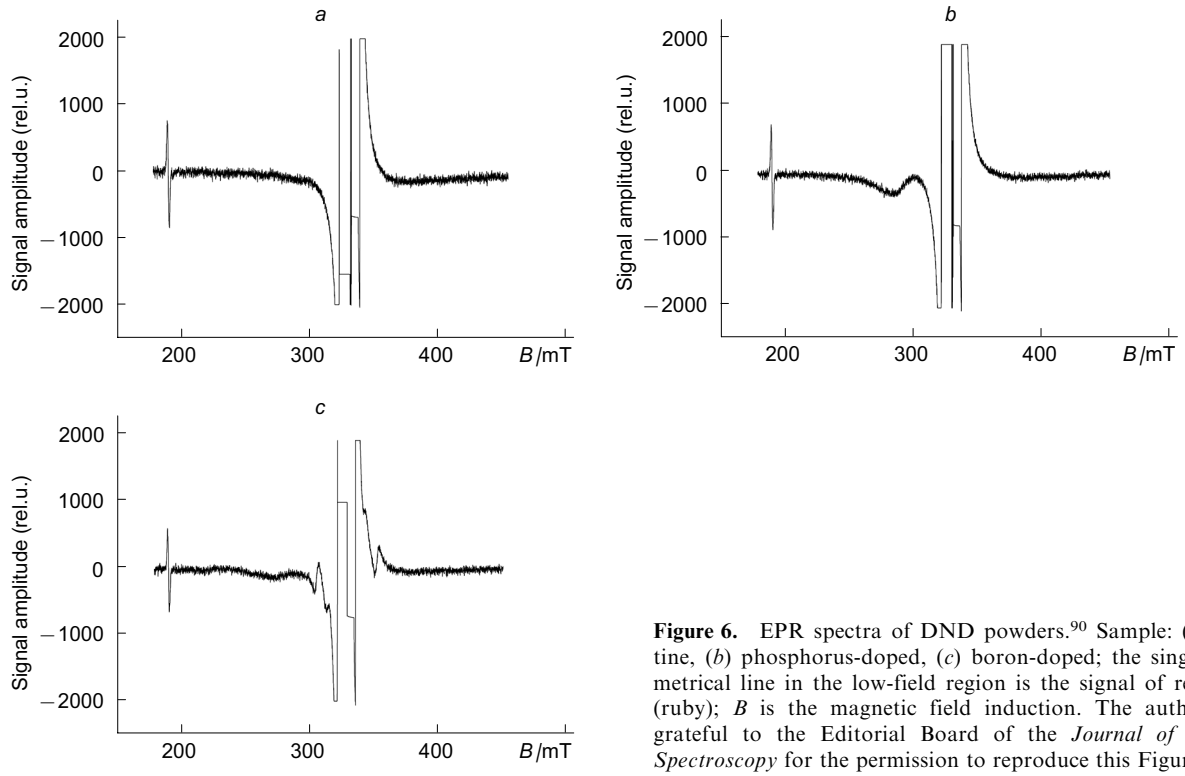



**Figure 6.** EPR spectra of DND powders.[90] Sample: (*a*) pristine, (*b*) phosphorus-doped, (*c*) boron-doped; the single symmetrical line in the low-field region is the signal of reference (ruby); $B$ is the magnetic field induction. The authors are grateful to the Editorial Board of the *Journal of Applied Spectroscopy* for the permission to reproduce this Figure.

### 3.4.2. Dispersion of magnetic susceptibility

EPR spectroscopy studies of DND samples revealed, for the first time, the unique difference between DND and any other bulk diamond. Recording the EPR spectra of DND samples, unlike the spectra of diamonds of different origin, during resonant absorption, showed[90] a non-monotonic change in the cavity frequency, which was used to calculate the magnetic susceptibility dispersion $X_1$ (Fig. 7).

The dispersion of magnetic susceptibility of the sample is manifested as a change in the cavity frequency. This parameter proved to be very sensitive to DND modification by dopant atoms.

A magnetic susceptibility dispersion was observed previously in neutron-irradiated CVD[§]-diamonds; this characteristic of the diamond proved to be highly sensitive to neutron fluence. The dispersion in the diamonds was not observed at neutron fluences of $< 5 \times 10^{20}$ cm$^{-2}$. This was noted by Poklonskaya,[94] who was the first to calculate the magnetic susceptibility dispersion for neutron-irradiated CVD diamond. A comparison of the data obtained for DND samples and CVD diamond samples irradiated with neutrons with the fluence of $5 \times 10^{20}$ cm$^{-2}$ provides the following conclusions:

— appearance of the dispersion in these samples is a consequence of particularly the uniform nanostructuring of the diamonds, since paramagnetic centres in them occur in identical environment of a structured system of atoms;

— for CVD diamond samples, neutron fluence of $5 \times 10^{20}$ cm$^{-2}$ is a critical value where the phase transition from the amorphous to nanostructured state takes place.

The dispersion of magnetic susceptibility is a consequence of quantum size effects in DNDs and can be used, like other stable parameters of the EPR spectra, for diagnosis of the nanodiamond raw material.[90, 95, 96]

§ Chemical vapor deposition.

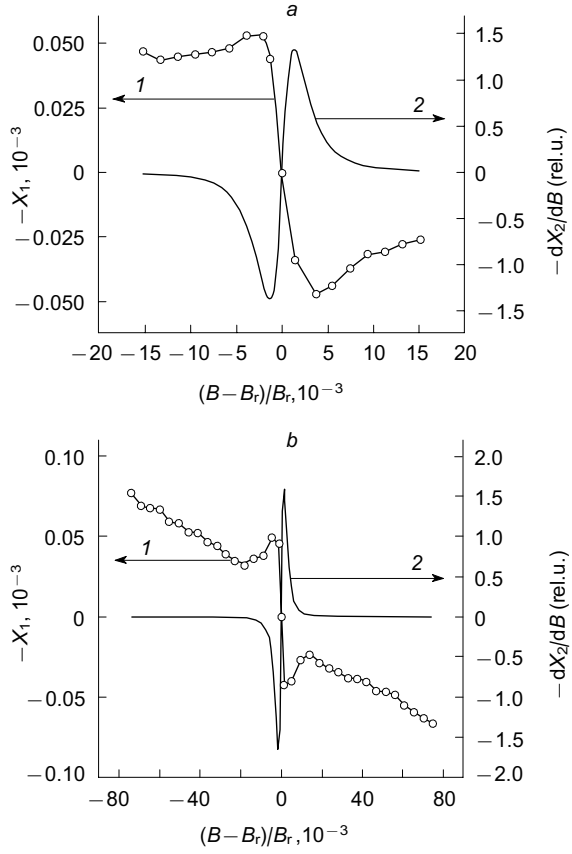



**Figure 7.** Dispersion $X_1$ (*1*) and the EPR spectrum ($dX_2/dB$ is the first derivative of the microwave absorption signal) (*2*) of a DND sample upon variation of the induction of an external magnetic field.[90] Magnetic field sweep: 10 (*a*) and 50 mT (*b*); $B$ is the magnetic field induction, $B_r$ is the resonant magnetic field induction. The authors are grateful to the Editorial Board of the *Journal of Superhard Materials* for the permission to reproduce this Figure.

### 3.4.3. Characteristic features of formation of highly conductive structures in DND powders under conditions of electron paramagnetic resonance

High concentration of paramagnetic centres ($10^{19}-10^{20}$ spin $g^{-1}$) generated by unpaired electron spins in DND samples can be considered as a structure typical of spin glasses, characterized by random distribution of spin – spin interactions and the absence of a long-range order.

Nguyen *et al.*[1] proved the possibility of switching the randomly distributed electron spins in the DND powder to an oriented ordered state; this induces changes in the parameters of EPR spectra and anisotropy of sample properties in the magnetic field. The authors studied a high-purity DND20 powder (0.04 mass % of incombustible impurities) with a mass of 54 mg by EPR spectroscopy. The sample was scanned many times in a continuous mode under resonance conditions and then left under off-resonance conditions in a residual magnetic field of the spectrometer ($\sim$8 mT). After a cycle of measurements, anisotropy of the sample properties was investigated. For this purpose, the sample was rotated in the cavity to make one revolution after each scanning cycle. The spectra were measured after sample rotation by every 45°. In the fourth cycle of measurements, a considerable decrease in the cavity frequency was observed. The cavity Q factor also decreased, as indicated by the change in the amplitude of the EPR signal of the ruby reference. In the fourth cycle of measurements after the sample has been rotated in the magnetic field by 270°, the normally observed symmetrical signal (Fig. 8, line *1*) actually disappeared, particularly, its intensity decreased 400-fold (line *2*). The repeated recording of the EPR spectrum for the same sample orientation showed the presence of a signal (line *3*) related to the paramagnetic centres located in a conductive medium. The spectrum was a dome-shaped line with a strongly asymmetric signal at the top (*g*-factor of 2.00146 and line width of 0.281 mT) with an asymmetry parameter of 4.8 (Dysonian line shape) in the resonant absorption region. The observed sharp change in the EPR spectral parameters attests to a DND phase transition from the paramagnetic state to the state with metallic conductivity.

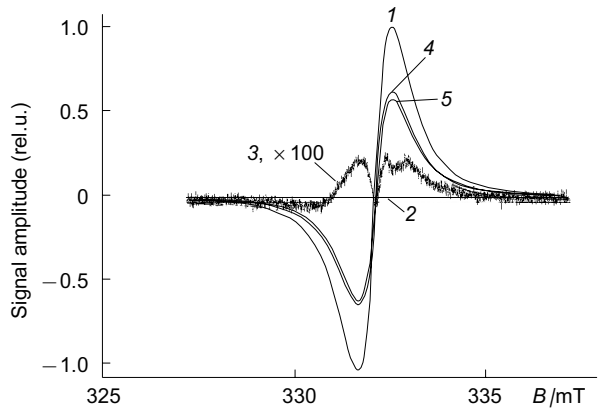



**Figure 8.** EPR spectra of high-purity DND20 sample (without doping) recorded in the final cycle of measurements with sample rotation in the a magnetic field.[1] Rotation angle: (*1*) 225°; (*2*) 270° (first measurement); (*3*) 270° (second measurement) and 315° (first measurement); (*4*) 315° (second measurement); (*5*) 360°.The authors are grateful to the Editorial Board of the *Journal of Applied Spectroscopy* for the permission to reproduce this Figure.

Analysis of the EPR spectra of DND powders leads to conclusions about the influence of magnetic and microwave fields on the formation of highly conductive structures. For these structures, the penetration depth of the microwave field is nearly zero; therefore, paramagnetic centres, most of which are located below the nanodiamond shell, cannot participate in the resonant absorption of microwave energy. The nature of these structures has not been studied; they may represent graphene-like groups inside the DND shell. The presence of the specific asymmetric EPR signal is indicative of the fact that the microwave power is absorbed by surface spins, the symmetry of EPR signals of which is distorted due to the contact with arising conductive areas.[1]

The above results show that EPR spectroscopy is suitable for diagnosis of doping of diamond nanocrystals, for studying kinetic phenomena and phase transitions in DNDs located in a magnetic field, and for diagnosis of nanostructuring of bulk diamond crystals on exposure to ionizing radiation and during the DND synthesis.

### 3.4.4. Thermal stability of detonation nanodiamonds

Dolmatov *et al.*[97] studied the thermal stability of doped DND samples. Exothermic events started to be detected at 30 – 40 °C. The first group of exothermic events ended in the temperature range of 135 – 160 °C, while intense thermal decomposition (oxidation) of the DND diamond phase in air started in the range of 475 – 508 °C. The mass loss of the samples started most often at 50 – 60 °C (desorption of volatile products and water physically bound to the surface). Doping of DNDs with boron or germanium resulted in a pronounced increase in the temperature of the onset of dramatic mass loss (by 100 – 450°) caused by oxidation.

Panova *et al.*[98] investigated the effect of conditions of the detonation synthesis on the state of the DND surface layer. They considered the DND powders provided by SCTB Technolog and LLC SIDAL (Lesnoy, Russian Federation). The intense thermal decomposition (oxidation) of the DND diamond phase in air started in the 475 – 508 °C range.

The purpose of that study[98] was to investigate the possibility of doping DNDs during the synthesis and the effect of introduction of dopants into the explosive charge or the water shell on the diamond surface groups. Nanodiamond powders manufactured by the SCTB Technolog and LLC SIDAL were considered. The authors assumed the possibility of replacing carbon atoms in the nanodiamond lattice by phosphorus, boron, aluminium, silicon, germanium and sulfur heteroatoms during the DND synthesis. They considered two methods for the synthesis of nanodiamonds:

— TH charge was fired in a water shell with solutions of compounds containing phosphorus and boron atoms;

— ammonium hydrogen phosphate, boric acid, germanium oxide or desired heteroatoms as elements (silicon, boron, sulfur, aluminium) were added to the explosive charge as it was formed.[99]

The former process could enable only surface modification of nanodiamonds *via* their contact with boron or phosphorus compounds at the final stage of formation. Using the latter process, it was possible to introduce heteroatoms into the nanodiamond lattice in the chemical reaction zone at temperatures of 3200 – 4300 °C upon decomposition of added compounds or direct atomization

of the added elements. The state of the surface was evaluated by temperature-programmed desorption.[98] The thermograms mainly exhibited three peaks for the desorption of water: the first peak at 80 °C corresponded to desorption of water physically adsorbed on the nanodiamond surface; the second peak at 215 – 265 °C corresponded to desorption of water from meso- and nanopores of aggregated nanodiamonds; and the third peak at 540 – 610 °C was due to desorption of water chemically formed upon decomposition of the remaining oxygenated groups and upon their reactions with the nanodiamond carbon.

Carbon monoxide desorption takes place in the temperature range of 610 – 770 °C with only one maximum; the peaks for atomic oxygen and water are located in the same temperature range. For most modified nanodiamonds, $CO_2$ desorption gives rise to two clear-cut peaks in the 220 – 270 °C and 520 – 660 °C ranges. As a rule, the moderate peak at 220 – 270 °C is caused by physical desorption of carbon dioxide already present on the surface, while the peak at 520 – 660 °C corresponds to chemically formed carbon dioxide (from redox reactions involving the nanodiamond carbon).

In the case of phosphorus-doped DND sample, continuous phosphine ($PH_3$) desorption took place with a maximum at 550 °C, indicating the presence of phosphorus atoms in the DND lattice.

In the case of the DND sample produced by adding aluminium powder to the charge, there is one desorption peak of atomic oxygen in the 240 – 260 °C range; two water desorption peaks (one in the 290 – 310°C range and one in the 610 – 630 °C range); one CO desorption peak in the 310 – 330 °C range; and three $CO_2$ desorption peaks, two of which are already known (about 260 and 520 °C) and the third one is at 900 °C. This attests to the catalytic action of aluminium on the redox reactions of thermal decomposition of nanodiamonds.

### 3.5. Methods for chemical modification of the surface of detonation nanodiamonds

In recent years, the interest in the DND applications has been drifting towards biology and medicine.[46, 100 – 103] A promising and rapidly developing medical application is the use of DNDs as carriers for drug delivery systems.[102]

Nanodiamonds, isolated from the diamond detonation blend and purified by an industrial process involving some oxidative treatment, have a polyfunctional surface composition, which is moreover different for different commercial brands, and this is often responsible for the lack of reproducibility of DND properties. This brings about the necessity for chemical modification of the surface, which can be performed by various procedures. Chemical modification is also necessary for imparting particular properties to DND surface. Owing to high concentration and diversity of functional groups on the nanodiamond particle, a broad range of chemical reactions can be used to modify the particle surface. The carbon atoms of the disrupted shell and the core of the diamond particles do not participate in the chemical reactions of surface groups.

Hydrogenation is the most popular method for modifying the surface of nanodiamonds. The key functionalization reactions of the hydrogenated DND surface are oxidation, halogenation and amination. Usually, hydrogenation is performed by high-temperature molecular hydrogen annealing or hydrogen plasma treatment.

In a number of studies,[103 – 106] tritium was introduced on the DND surface using a thermal activation method. Yakovlev *et al.*[105] noted that the amount of introduced tritium is 3 times greater (up to 90 GBq $g^{-1}$) in the case of pre-hydrogenated nanodiamond than in the case of the pristine sample. The labelling efficiency also increases (up to 2.6 TBq $g^{-1}$) when the surface accessible for tritium is increased by preliminary disaggregation of nanodiamond grains. The chemical properties of the synthesized DND – [$^3$H] are the same as the properties of hydrogenated nanodiamonds, but the presence of radioactive tritium on the surface allows for the use of the material in biomedical research, such as studying cellular interactions, biodistributions, *etc*.

Treatment of DNDs with various oxidants is the simplest and most commonly used method for surface functionalization and hydrophilization. The gas-phase oxidation of nanodiamonds is often carried out using pure oxygen, air, argon with some oxygen, or ozone.[107]

Liquid-phase oxidation is performed using acids, acid mixtures, in some cases, with the addition of transition metal salts. Depending on the oxidation conditions (nature of the oxidant, temperature), the set of oxygen-containing functional groups can vary, which was confirmed by IR spectroscopy.[108]

The DND surface formed after hydrogenation contains inactive C – H functional groups. For conducting chemical reactions on such a surface, it should be activated. An effective way to increase the reactivity of the DND surface is halogenation carried out by some method. In addition, halogenation, especially fluorination, is used to obtain hydrophobic materials. Fluorine, chlorine or bromine atoms can be attached to the DND surface.

Denisov[109] chlorinated the DND surface by treating it with $CCl_4$ vapour (mild chlorination) or with chlorine gas at elevated temperature (severe chlorination). According to experimental results, gas-phase chlorination was more efficient. The experimental data were in good agreement with the thermodynamic estimate of the optimal temperature range for chlorination (400 – 650 °C).

In view of the interest in the biomedical applications of DNDs, which has lately increased, note that the methods chosen for chemical modification should contaminate the nanodiamond as little as possible.[110] Unfortunately, the DND – F product obtained after fluorination was found to contain residual molecular fluorine,[111] which is inadmissible for delivery systems of drugs and biologically active compounds.

Kulakova *et al.*[112] compared the results of chlorination of DNDs of the same brand by different processes: treatment with molecular chlorine in the liquid and gas phases, with $CCl_4$ plasma and thionyl and sulfuryl chlorides. It was shown that the use of thionyl and sulfuryl chlorides results in DND – Cl samples containing a significant amount of sulfur (up to 4 mass %), which is also inadmissible for drug carriers. If chlorination is carried out with a chlorine solution in $CCl_4$, small amounts of covalently bound chlorine are found on the surface, along with chloride anions. The gas-phase chlorination with molecular chlorine at elevated temperature is the method of choice for DND functionalization for biomedical purposes. In addition, gas-phase chlorination reduces the impurity metal content in DND samples.

Amination is also used for the chemical modification of DNDs, since surface-grafted primary amino groups are

convenient anchors for binding various organic compounds, including biomolecules (proteins, enzymes or peptides).[113] Note that DNDs bearing grafted molecules with terminal amino groups are sometimes called in the literature aminated DNDs. The amination of DNDs is usually carried out with ammonia at elevated temperature (425 °C) using prechlorinated DND surface.[108, 109] Unfortunately, attaining complete replacement of surface chlorinated groups by amino groups is a challenging task.

The purpose of DND surface modification by covalent grafting is to obtain surface-grafted compounds. Chemical modification is accompanied by targeted change in the physicochemical properties of DNDs, which gives rise to new materials combining the properties of a carbon matrix and a grafted chemical compound.[114] Extensive studies of the chemical modification of DNDs by covalent grafting are in progress.[97]

A chemical modification method was used [56] to unify the properties of DND samples produced by various manufacturers. For this purpose, the authors employed hydrogen treatment at 850 °C. After high-temperature hydrogenation, all samples had similar surface physicochemical characteristics such as chemical composition of the surface, particle size, ζ-potential and gave stable aqueous suspensions.

These results are in line with the data reported by Denisov.[109] The author noted that chemical modification affects the oxidation stability of DNDs. The UDA-SP nanodiamonds manufactured by the JSC Sinta were treated with hydrogen, chlorinated by two methods and then treated with ammonia. The stability of samples in air was studied by thermogravimetric analysis. The authors concluded that hydrogenation, chlorination and amination of the DND surface is accompanied by increasing thermal stability.

## 4. Applications of detonation nanodiamonds

### 4.1. Fluorinated nanodiamonds as unique neutron reflectors

Neutrons with a wavelength of 0.5 nm and energy of $< 3$ meV are called slow neutrons. At present, the proportion of retained slow neutrons in the corresponding closed systems does not exceed 10% of their initial amount. Furthermore, as the energy of neutrons decreases, the efficiency of their delivery to the target sites sharply drops. Development of efficient reflectors for slow neutrons is one of the methods to increase the neutron flux. Nesvizhevsky *et al.*[115] proposed a new class of reflectors based on fluorinated DNDs (DND – F), which can provide continuous reflectivity with high albedo and serve as an alternative to diffusive slow neutron reflectors. Fluorinated DNDs sharply decrease the neutron absorption, which results in unpredictable albedo for slow neutrons and thus covers the so-called reflectivity gap in the neutron spectrum. As a result, the reflectors can dramatically improve the performance of neutron sources and the efficiency of neutron delivery and, hence, increase the fluxes in neutron devices; this offers prospects for designing a new generation of neutron sources and new experiments.

Detonation nanodiamonds are an obvious choice for slow neutron reflectors, as the absorption cross-section ($C$) in carbon is very low (3.5 mb at the standard neutron velocity of 2200 m $s^{-1}$), the coherent scattering length is very large (6.65 fm), while the volume density (3.5 g $cm^{-3}$) is higher than that for other carbon materials. The characteristic size of DND particles is precisely in the range of optimal theoretical values. Hard fluorination removes all non-diamond components and, hence, it can replace one or several purification stages. All surface hydrogen atoms and hydrophilic groups are replaced by fluorine or removed as gaseous species. The neutron absorption cross-section for fluorine is low (9.6 mb), the inelastic scattering cross-section is markedly lower than that for hydrogen, while the coherent elastic scattering length is large and positive (5.65 fm), unlike the negative scattering length for hydrogen ($-3.74$ fm). Thus, all key properties of fluorine are in line with requirements imposed on materials for efficient nanopowder neutron reflectors.

In intense neutron fluxes, DNDs may become highly radioactive because of activation of certain impurities in their structure.[116] Therefore, it is of interest to manufacture and use highly pure DND powders with minimized contamination. According to X-ray diffraction data, the nanoparticle diamond cores remain unchanged upon fluorination.

The estimated albedo of neutrons from DND – F is close to 100% for very cold neutrons ($< 100$ m $s^{-1}$).[115] The cut-off velocity for DND – F (infinitely thick) reaches 300 – 400 m $s^{-1}$ (the cut-off velocity measured earlier for 3-cm thick untreated DNDs was 160 m $s^{-1}$). Additional benefits of DND – F are low aggregation ability and low water absorption, which make the material preparation easier and more reproducible.

### 4.2. DND – CNT hybrid material

Presently, active studies in the field of synthesis of hybrid carbon nanomaterials based on carbon nanotubes (CNTs) and DNDs are in progress. The driving force is prospect to obtain new composites with markedly improved characteristics, which may considerably expand the scope of their applicability. Hybrid materials with fundamentally new properties can be used in various branches of industry. However, most of currently existing hybrid composites based on nanodiamonds and carbon nanotubes are films and, hence, they cannot be employed in many promising areas, for example, as fillers for composite materials.

It was shown [117, 118] that a homogeneous DND – CNT hybrid material can be prepared as a powder, with CNTs being grown on the DND surface by the CVD method. The purified nanodiamond treated with ammonia at a temperature of ~230 °C and a pressure of 40 – 50 atm served as the diamond raw material for the preparation of DND – TAN ¶ by the SCTB Technolog. The nanodiamond surface was coated by a cobalt nanolayer, which catalyzed the vapour deposition of CNTs. The content of deposited nanotubes in the ready composition was 32 mass %. The resulting hybrid composite was an ultrafine black-coloured powder.

Multi-walled nanotubes uniformly coated the aggregated nanodiamonds, the resulting composite was homogeneous, and the particle size of the hybrid composite was ~10 μm.[118] The specific surface area of the material (calculated by the Brunauer – Emmett – Teller method) was close to 225 – 230 $m^2$ $g^{-1}$. The pore volume in the DND – CNT sample depended on the pore size, being as follows:

¶ DND – TAN are detonation nanodiamonds obtained by detonation synthesis followed by one-stage chemical purification with dilute nitric acid (with the addition of ammonium nitrate) and treatment with ammonia at high temperature and pressure. As a result, the surface of these DNDs contains a large number of amino groups.

| Pore type and size | Specific pore volume /cm$^3$ g$^{-1}$ |
|---|---|
| Micropores ( < 2 nm) | 0.01393 |
| Mesopores (2 – 5 nm) | 0.44737 |
| Macropores ( > 50 nm) | 0.20358 |
| Total | 0.66488 |

The highly aggregated nanodiamond powder is rapidly precipitated in water, whereas the DND – CNT hybrid forms a stable aqueous suspension. No precipitate was observed even after this suspension was allowed to settle for 20 days. Ultrasonic treatment of the suspension did not affect its state either. This attests to high strength of binding between nanotubes and the nanodiamond surface. The hybrid composite dried to the powdered state can also be introduced into water to form a stable suspension upon a moderate ultrasonic treatment. With this treatment, the aggregated hybrid composite particles with a diameter of several micrometres are split into 50 – 60 nm particles giving a stable aqueous suspension.

Thus, a method for preparation of a new hybrid carbon material consisting of carbon nanotubes and nanodiamonds was developed for the first time.[117, 118] The method is based on the CNT preparation on the cobalt-activated DND surface. The composite is obtained as an ultradispersed black powder capable of forming a stable aqueous suspension.

## 4.3. Electrochemical metal – diamond coatings

### 4.3.1. Chromium – diamond coatings

Chromium-diamond composite coatings, which have been successfully implemented in industry, provide a severalfold increase in the service life of tools and parts of machines and mechanisms, owing to the enhanced microhardness and wear resistance of the composite electrochemical coatings (CEC) containing DNDs.[5] Typically, DNDs account for $\leqslant$1 mass % of the coating. Hence, the new properties of CEC cannot be attributed to the hardness and low friction coefficient inherent in diamond. It was shown that chromium – diamond coatings have a chromium specific microstructure and texture, whereas no single DND particles can be detected in the coating.

Apparently, the influence of diamond particles on the CEC properties starts in the near-electrode layer where complex discharge processes of chromium ions take place. The DND surface interacts with the chromic acid anion and is thus activated. The activated DND particles, which are co-precipitated with chromium, initiate the dispersion strengthening effect, which is manifested as decreasing grain size of electrolytic chromium. In addition, chromium microcrystallites are highly disordered. Apparently, such texture of the coating is caused by the structuring effect of DND particles on the near-electrode electrolyte layer. As a result, performance characteristics of the coatings are markedly improved.

Aleksandrova *et al.*[119] used phosphorus-doped DNDs as aqueous suspensions for a standard electrolyte. The dependences of the coating microhardness on the additive concentration have two maxima (1 and 5 g L$^{-1}$), which can be attributed to the action of DNDs as surfactant particles in the electrical double layer when their content is low ($\sim$1 g L$^{-1}$). As the additive concentration increases, they are aggregated, while the aggregates are physically captured by the growing chromium precipitate. The microhardness of the coatings obtained without DNDs is 855 kgf mm$^{-2}$, while those of the coatings obtained under the same conditions using DND – TAN and DND – P are 1150 and 1017 kgf mm$^{-2}$, respectively. As compared with the chromium coating without additives, the maximum wear resistance increases 12-fold for the use of DND – P and 5-fold for the use of DND – TAN or DB. The highest corrosion resistance in the salt spray chamber is inherent in chromium coatings with boron-doped nanodiamonds (DND – B) (0.08 mass % boron). The concentrations of this additive were 2.5, 5.0 and 10 g L$^{-1}$; the studies were performed using hard and wear resistant chromium plating. The corrosion resistance was 3 times as high as that of the chromium coating without additives; the coating is denser and has no through thickness cracks. The thickness of the chromium coating with boron-doped (DND – B) or phosphorus-doped (DND – P) nanodiamonds can be reduced to 20 – 50 μm.

In the presence of additives, the coatings are more shiny, smooth and more uniform; they have no low-quality areas at the electrode edges, which are especially characteristic for high current densities in pure solutions. Due to the change in the structure of precipitates, the microhardness of chromium coatings increases from 855 kgf mm$^{-2}$ for pure chromium to 1300 kgf mm$^{-2}$ for chromium with DND – B additives.

Burkat *et al.*[120] used dry products containing the following components:

— DND obtained from a TH mixture, a surfactant, sodium carbonate and citric acid; the DND content is 62%;

— DB obtained by tetryl detonation; the DND content is 62%.

The microhardness of solid chromium increased from 9.5 to 13.6 GPa in the presence of DNDs and from 9.3 to 13.2 GPa in the presence of DB; in the case of wear-resistant chromium, the microhardness increased from 8.0 to 13.6 GPa in the presence of DNDs, while wear decreased from 3.0% to 0.8% (for DNDs and DB).

Thus, the use of economically preferable dry diamond-containing formulations resulted in high quality characteristics of chromium – diamond coatings; the DB obtained by detonation of tetryl was used for the first time.

### 4.3.2. Nickel – diamond coatings

A study of Dolmatov *et al.*[121] was aimed at substantially increasing the microhardness, wear resistance and corrosion resistance characteristics of nickel – diamond coatings by adding phosphorus-doped DNDs. The modified detonation nanodiamonds (MDNDs) were prepared by detonation of an explosive charge (50 : 50 TH; 2 mass % – 10 mass % $NH_4H_2PO_4$) in an aqueous urotropin solution shell. The DB formed after explosion was purified by the standard chemical procedure to attain a phosphorus content of 0.06 mass % to 0.21 mass % in DNDs. The electrochemical nickel plating was carried out using a standard electrolyte of the following composition /g L$^{-1}$: $NiSO_4 \cdot 6H_2O$, 250 – 300; $NiCl_2$, 35 – 55; $H_3BO_3$, 30 – 45; MDNDs, 2 – 7; RADO-57M, 4 mL. The nickel plating was carried out at pH 5 and a temperature of 25 °C. The physicomechanical characteristics of the electrochemical composite nickel coatings are mainly influenced by the DND concentration in the electrolyte and the current density. The introduction of MDNDs gives the smallest grain size, provides a 2.5-fold increase in the microhardness and a 8-fold decrease in wear.

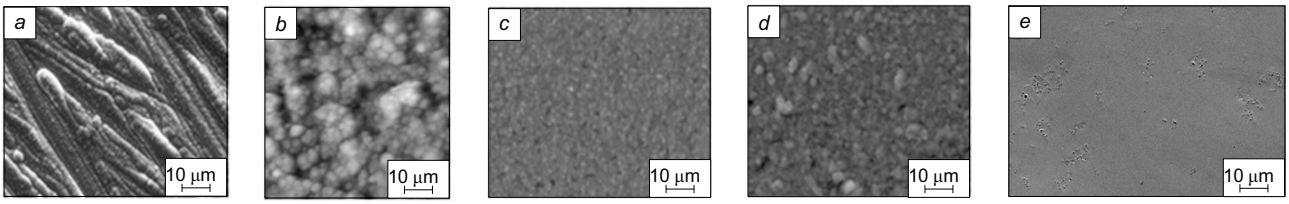



**Figure 9.** Micrographs of surfaces (*a*, *b*) and micro-slices (*c* – *e*) of coatings deposited from an electrolyte without additives (*a*, *c*), with added DND (*d*) and with added DND – P (*b*, *e*).[121] The authors are grateful to Springer and *Journal of Superhard Materials* for the permission to reproduce this Figure.

The micrographs of the nickel coating with modified and pristine DNDs are depicted in Fig. 9.[121] The properties of these coatings varied in the following way:

| Panel in Fig. 9 | *a*, *c* | *d* | *b*, *c* |
|---|---|---|---|
| Microhardness /kgf mm$^{-2}$ | 268 | 381 | 660 |
| Wear (%) | 14 | 3.8 | 1.7 |

When coupled with iron, nickel is the cathode, as it has a more electropositive potential. Nickel can protect steel only physically; hence, the coating should have no pores. The nanodiamond additives act as surfactants and thus decrease the porosity of nickel coatings. The samples coated by nickel from an electrolyte containing nanodiamonds showed much better characteristics. When only MDNDs were used, the corrosion resistance increased 5 – 9-fold, while the use of the MDND + RADO-57M composite additive induced a 35 – 70-fold increase.

Combined use of MDNDs and RADO-57M produced the following effects:

— the microhardness of the coatings increased 1.75-fold compared with the best of previous results (Ref. 122).

— the MDND consumption decreased: it was 6 times lower than those in all previous studies (Refs 122, 123);

— the low current density was used [$i$ = 2.5 A dm$^{-2}$, which is 2 – 6 times lower than in other studies (Refs 122, 123)];

— there was no need for complex MDND pretreatment for introduction into electrolyte (immediately after chemical purification, the MDND suspension was added to the electrolyte for coating deposition);

— a simpler and cheaper electrolyte composition; a nearly room temperature for deposition (25 °C); therefore, the energy expenditure was markedly reduced; a standard electrolyte nickel plating electrolyte was used.

#### 4.3.3. Electrochemical diamond-containing anodized aluminium oxide coatings

The most important issues are increasing the corrosion resistance, wear resistance and strength of anodized oxide coatings made of aluminium and its alloys, while enhancing the dielectric properties of the coatings. A process has been developed comprising electrochemical oxidation in a sulfuric acid electrolyte containing 0.5 – 10.0 g L$^{-1}$ of DNDs modified by ammonia, antimony or boron.[124]

The process was conducted using DND – TAN, antimony-doped diamond blend (DB – Sb) and DND – B.

The DND – TAN surface has a large number of amine and amide functional groups. The least expensive, widely used and environmentally safe procedure is anodic oxidation in aqueous sulfuric acid of 180 – 250 g L$^{-1}$ concentration at a current density of up to 2.0 A dm$^2$, maximum voltage of ~24 V and temperature of 10 – 20 °C carried out for 15 – 60 min. These conditions were patented.[124]

In electrolytes, modified DNDs (DND – TAN, DB – Sb or DND – B) form sedimentation- and coagulation-stable systems at working concentrations of 0.5 – 10.0 g L$^{-1}$. The negative charge of nanodiamond additives is the driving force of penetration of DB or DNDs into the pores formed on exposure of the aluminium surface to the acid. When MDNDs are used in the electrolysis, owing to higher affinity for the oxide film, higher mobility in the electrolyte, the presence of amine and amide groups (in the case of DND – TAN) or antimony- and boron-containing groups (in the case of DB – Sb and DND – B) on the nanodiamond surface, the resulting coatings have high microhardness, low porosity and enhanced corrosion resistance, with the consumption of nanodiamond raw materials being low

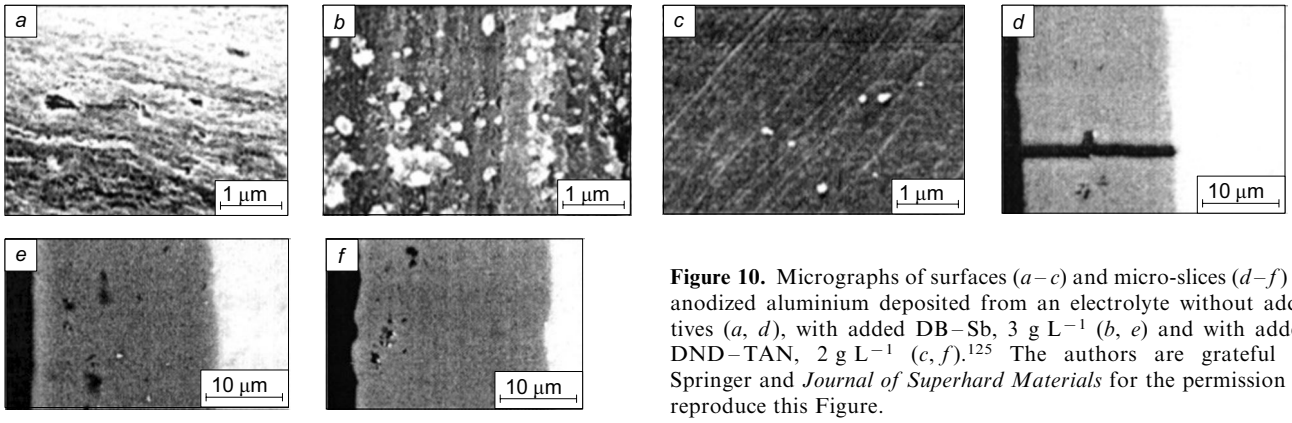



**Figure 10.** Micrographs of surfaces (*a* – *c*) and micro-slices (*d* – *f*) of anodized aluminium deposited from an electrolyte without additives (*a*, *d*), with added DB – Sb, 3 g L$^{-1}$ (*b*, *e*) and with added DND – TAN, 2 g L$^{-1}$ (*c*, *f*).[125] The authors are grateful to Springer and *Journal of Superhard Materials* for the permission to reproduce this Figure.

**Table 6**. Change in the surface properties of anodized aluminium with DND – TAN and DB – Sb.[125]

| Item in Fig. 10 | Microhardness /kgf mm$^{-2}$ | Porosity (%) | Corrosion resistance /h (40°) |
|---|---|---|---|
| *a*, *d* | 623 | 0.025 | 92 |
| *b*, *e* | 1003 | 0.011 | > 220 |
| *c*, *f* | 1020 | 0.009 | > 220 |

(0.5 – 10.0 g L$^{-1}$). The presence of nanodiamonds does not affect the growth rate of the protective film, but provides the film filling during the electrolysis.

The use of DB – Sb decreases the porosity ~2.3-fold compared with the porosity of anodized aluminium. The corrosion resistance of anodized aluminium deposited from an electrolyte containing DND – TAN and DB – Sb is ~2.4 times higher than the corrosion resistance of coatings without additives. As the electrolysis temperature decreases (down to 5 – 7 °C), the microhardness of the coatings increases. An increase in the current density also leads to increasing microhardness (Fig. 10). The data demonstrating the change in the surface properties of anodized aluminium containing DND – TAN and DB – Sb are summarized in Table 6.[125]

The increase in the microhardness of anodic aluminium coatings is due, first of all, to the presence of DB – Sb and DND – TAN in the oxidation electrolyte; in the recommended concentration range of 0.5 – 10 g L$^{-1}$, a stable 1.5-fold increase in the microhardness is observed.

#### 4.3.4. Silver – diamond coatings

The use of relatively non-toxic non-cyanide electrolytes for silver plating affords coatings that are inferior in the set of electrophysical and mechanical characteristics to silver precipitates obtained from highly toxic cyanide baths. A process has been patented[126] for the deposition of a silver – diamond coating with a low resistivity, high wear resistance, low porosity and, hence, enhanced corrosion stability for low consumption of a cheap modified DB. These coatings significantly increase the service life of items and expand the scope of their application. If the silver coating contains graphene apart from DNDs, the coating electrical conductivity markedly increases. The production process of the coatings includes the electrochemical deposition from an electrolyte containing silver ions and DB of the detonation synthesis pretreated with 5% – 30% nitric acid. Electrolyte composition/g L$^{-1}$: $K[Ag(CN)_2]$ (in terms of Ag), 20 – 35; $K_2CO_3$, 40 – 50; KCNS, 150 – 200; DB, 0.2 – 2.0; temperature of 18 – 25 °C and cathodic current density of 0.5 – 2.0 A dm$^{-2}$. The diamond blend contained 40 mass % – 50 mass % DND and 50 mass % – 60 mass % non-diamond carbon. For the removal (oxidation) of the disordered carbon and retention of graphene-like structures, DB is treated with dilute nitric acid.

The addition of DB to a dicyanoargentate electrolyte was found to induce the following beneficial effects: a 1.5 – 3.0-fold increase in the electrical conductivity of silver coatings; a 3 – 6-fold increase in the coating wear resistance (1.5 g L$^{-1}$ of DB); a 5-fold decrease in the coating porosity (with a parallel increase in the corrosion resistance) (0.5 g L$^{-1}$ of DB; $i$ = 0.3 A dm$^2$); and a 2-fold increase in the throwing power (coating uniformity across the thickness). A 3-fold decrease in the grain size is attained when the DB concentration in the electrolyte is 0.2 to 2.0 g L$^{-1}$. The microhardness of the coatings increases up to 1.5-fold (from 80 to 118 kgf mm$^{-2}$).

A simple process has been developed[127] for the fabrication of a silver – diamond coating with high wear resistance, low porosity and, hence, enhanced corrosion resistance for a low consumption of diamonds, which considerably increases the durability of items coated by this material. The proposed method includes the coating deposition at a temperature of 18 – 25 °C and current density of 0.3 – 2.0 A dm$^{-2}$ from the electrolyte containing /g L$^{-1}$: $K[Ag(CN)_2]$ (in terms of Ag), 20 – 35; $K_2CO_3$, 40 – 50; KCNS, 150 – 200; DND – TAN, 0.2 – 2.0. The adsorption capacity of DND – TAN is 1 to 10 μg-equiv. m$^{-2}$; they can adsorb 20 to 380 mg of silver per gram of the added nanodiamonds and participate in the transport of silver ions towards the cathode surface.

As the concentration of DND – TAN additive increases, the activation energy increases ~3-fold. Hence, there is an additional potential barrier that hampers the ion discharge. It was found that the silver coating samples obtained without DND – TAN have a clearly coarse crystalline structure, while the samples obtained in the presence of DND – TAN possess a uniform dense structure. The microhardness of the silver coating increases in the presence of DND – TAN from 80 (without the additive) to 155 kgf mm$^{-2}$.

By using DND – TAN in the dicyanoargentate electrolyte, the authors attained a ~30-fold increase in the wear resistance of the silver coating; a 2 – 7-fold decrease in the coating porosity (with a parallel increase in the corrosion resistance); a 1.6 – 1.7-fold increase in the throwing power (coating uniformity across the thickness); and a 4-fold decrease in the grain size (for the 0.2 to 2.0 g L$^{-1}$ concentration of DND – TAN in the electrolyte).

#### 4.3.5. Gold – diamond coatings

Electrochemical gold plating has been studied[128, 129] in two standard electrolytes, citric acid and phosphoric acid, in the presence of DNDs doped with boron and phosphorus (from 0.2 to 5.0 g L$^{-1}$). Also, DND – TAN was used.[130] In addition, DNDs crushed to the nanometre state using Ōsawa and co-workers[131] and Vul' – Aleksenskii[132] methods were employed.

The advantages of the proposed process over the existing methods for the manufacture of gold coatings are as follows:

— almost no wear in the case of using either boron-doped DNDs crushed by the Vul' – Aleksenskiy method or a dispersed dry DND powder (DND – B) in a cavitational dispersing system;[129]

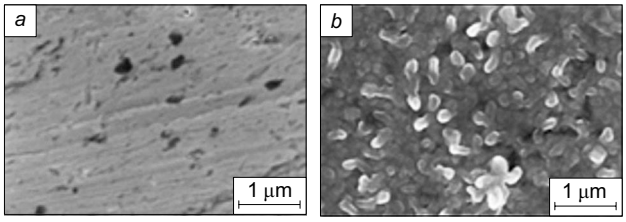



**Figure 11.** Surface micromorphology of gold coatings obtained without additives (*a*) and with added (1 g L$^{-1}$) DND – B (*b*).[129] The authors are grateful to Springer and *Journal of Superhard Materials* for the permission to reproduce this Figure.

— increase in the microhardness of gold coatings by 20% – 60% (up to 220 kgf mm$^{-2}$) compared to that of pure gold;

— the composition gold plating requires conventional galvanic equipment and basic chemicals used for gold plating.

The implementation of this new process may decrease the thickness of the gold coating 2 – 3-fold, which would save the precious metal, reduce the electrical energy and labour expenditures by a large factor and decrease the environmental impact. All this leads to higher quality and competitive capacity and expands the market outlet for gold – diamond-coated items. This is exemplified by Fig. 11, which shows the micrographs of the surface of gold coatings without additives and with the addition of boron-doped DNDs. The properties of these coatings varied in the following way:[129] the microhardness was 180 and 214 kgf mm$^{-2}$ and wear was 2.8% and 1.0%, respectively, for samples presented in Fig. 11 *a*,*b*.

#### 4.3.6. Zinc – diamond coatings

The use of zinc is due to the properties of inorganic zinc compounds such as environmental stability and low cost. Zincate electrolytes are more preferable from the environmental standpoint than the cyanide electrolytes used formerly. A biologically soft polymer additive A1DM, decomposing in the environment, was found and used for zincate electrolytes. A study of Burkat *et al.*[133] was aimed at elucidating the effect of A1DM and boron-doped (0.45 mass %) DNDs on the corrosion resistance of zinc coatings. The coatings were deposited from an electrolyte containing /g L$^{-1}$: ZnO, 6 – 12; NaOH, 75 – 120; A1DM, 8 – 12; DND – B, 0.5 – 7. The addition of DND – B markedly hampers zinc ionization in comparison with the addition of only A1DM and results in a denser coating. The corrosion currents in a 3% NaCl solution decrease virtually 3.6-fold on the zinc coatings produced in the presence of DND – B. In a salt spray chamber, corrosion was lower for zinc coatings produced from electrolytes containing boron-doped nanodiamonds in at concentration of 5 and 7 g L$^{-1}$ (corrosion decreased 3.1 – 3.4-fold), which is in good agreement with the data on corrosion currents.

Thus, the combined use of A1DM and DND – B additives in the zincate electrolyte had the following benefits: the uniformity of coating deposition increased 2.5 – 4.0-fold; the corrosion resistance increased 2.5 – 3.0-fold; and the microhardness increased by 10%. Recommended electrolyte composition /g L$^{-1}$: ZnO, 10; NaOH, 100; A1DM, 6; DND – B, 5 – 7; deposition conditions: $i$ = 3 A dm$^{-2}$, $T$ = 25 °C.

### 4.4. Bulk metal – nanodiamond composites

Copper, aluminium and their alloys are of particular interest as the bases for bulk composite materials.[134] The addition of nanodiamond powders to the aluminium matrix makes it possible to obtain materials with high thermal conductivity and specific strength, which are necessary for aircraft, nuclear and electronic industries. The physical doping *via* milling of DND aggregates together with the copper M1 or brass L62 particles, accompanied by strain-induced destruction and welding, gives a granular composite material. Up to 20 vol.% DNDs are added to a mixture of copper and brass powders. After treatment for 100 min, the granular product acquires an equiaxed shape and a homogeneous structure. The composite material was obtained by mechanical mixing in a Retch PM-400 planetary mill. When the DND content was up to 10 vol.%, a uniform distribution of non-agglomerated nanodiamonds in the metallic matrix could be obtained on long-term treatment. It was shown that the increase in the DND content in the composite above 20 vol.% results in significantly decreasing homogeneity, so that DNDs appear on the surface of the granular material as a separate phase.[59]

The following specific features of using DNDs were noted:[134]

— important engineering factors are the decrease (down to zero) of adhesion of the raw material (together with nanodiamonds), intermediate and final products to the process equipment surfaces; the absence of product lumping in any stage of processing;

— a chemical engineering factor is enhancement of oxidative process (for aluminium, nickel and copper) in the case of high DND content.

The fracture testing of the resulting composite material showed two types of fracture: a lusterless and a bright fracture. When 10 vol.% DNDs are used, the fracture affects the material bulk rather than the boundaries of granules. The fracture involves the granule boundaries only if the DND concentration in the composite is $\geqslant$20 vol.%. In this case, the reinforcing particles are distributed non-uniformly. When the DND content is 10 vol.%, it is possible to reduce the mixing and milling time down to 1 h (for copper and aluminium). The results of compression tests confirmed this conclusion. The application of DNDs decreases the linear thermal expansion coefficient of the composite.

Meanwhile, in the fabrication of the nickel-based composite, a uniform distribution of nanodiamonds throughout the composition is achieved over a much longer time than in the case of an aluminium or copper matrix.[135]

Elomaa *et al.*[136] described a process for the vapour deposition of the standard diamond coatings. In order to enhance adhesion between the deposited polycrystalline diamond film and the substrate, the latter was manufactured from a composite with a metal or non-metal binder and DNDs, the volume fraction of which was 5% to 90%. The resulting composite contained at least one metal (silver, gold, platinum, copper, aluminium, nickel, cobalt, tantalum, yttrium, zinc, tin or lead). This composite can also be manufactured by mechanical doping.

### 4.5. Composite materials based on polymers

The applications of DNDs for the fabrication of various types of composites based on polymers are described in several reviews (see, *e.g.*, Refs 137 – 140). However, despite the large number of scientific publications, the level of industrial application of these composites is markedly lower than that of, for example, technical carbon. One of the causes for this is the abundance of diverse functional groups on the DND surface, with the type and the quantity of functional groups being appreciably dependent on the preparation prehistory, purification method and subsequent functionalization of the DND surface.[141 – 143] Meanwhile, the change in the functional composition of the initial DNDs is often a necessary condition for achieving a higher level of compatibility between the filler and the polymer matrix.

Furthermore, the production cost of not only purified DNDs, but also DB is many times higher than the production cost of the same amount of the polymer used as the

matrix component. It appears that composites based on epoxy resins, elastomers and some types of thermoplastic,[144] tribological, biomedical [144] and special-purpose materials, the manufacture of which does not require large amounts of nanodiamonds, would be the most promising DND-containing new materials with improved properties and characteristics.

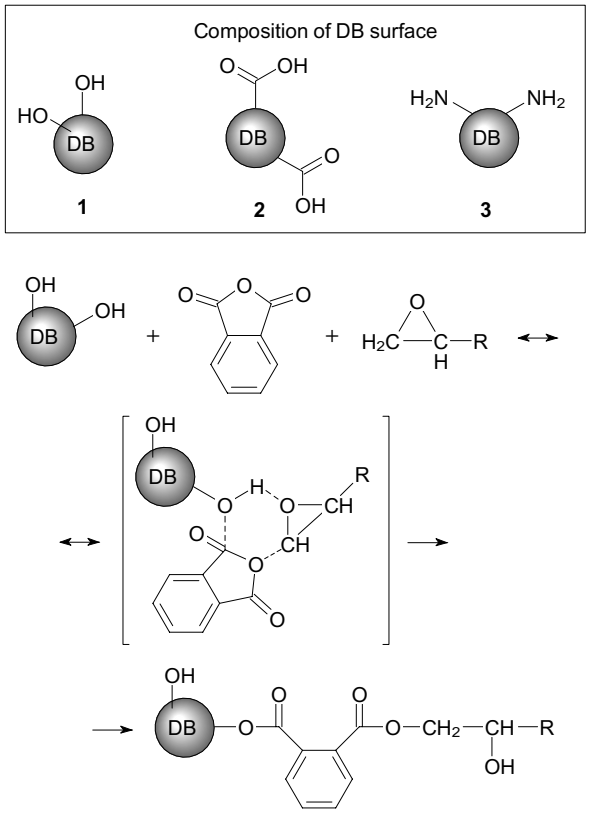
The most pronounced changes in the properties and characteristics of polymer matrix materials (*e.g.*, mechanical properties) caused by doping or filling with finely dispersed DNDs were ascertained for the polymer matrices with initially low mechanical characteristics (epoxy resins, elastomers). Doping of high-strength or high-modulus polymer matrices with nanodiamonds proved to be less efficient. Studying of the effect of the composition of nanodiamond surface on the properties and characteristics of the obtained polymer composites is a key task of the research related to DND-containing composites. Rakha *et al.*[145] used treatment with ozone followed by surface amination with excess triethylenetetramine (TETA) and treatment with a mixture of nitric and sulfuric acids for 24 h for functionalization of the DND surface. The composites were prepared using diglycidyl ether of bisphenol A (DGEBA) as the matrix component and TETA as the curing agent. The attachment of functional groups to the DND surface, providing adhesion between the nanoparticle and the epoxy matrix, was proved by Fourier transform IR spectroscopy. The mechanical characteristics of the composites were determined by the three-point bending method. The bending strength, elastic modulus and impact strength of the nanocomposites containing 0.1 mass % of ozone-treated DND increased by 85%, 57% and 39%, respectively. This degree of filling of the composite proved to be optimal. At higher DND contents, the mechanical properties of composites were deteriorated.

The effect of DB and DNDs, obtained by oxidation of DB at 435 °C followed by treatment with a nitric and sulfuric acid mixture, on the mechanical characteristics of an epoxy matrix based on DGEBA and methylhexahydrophthalic anhydride (as a curing agent) was studied by Haleem *et al.*[146] For composites containing 1 mass % of the filler, the tensile strength increased 1.5-fold.

Several groups of researchers studied the effect of DND as a functional reactive dopant in composite systems. For example, Aris *et al.*[147] used three types of DNDs (with pristine, oxidized and aminated surface) to study the curing kinetics of the EPON™828 epoxy resin (using TETA as the curing agent). The differential scanning calorimetry experiments on the curing kinetics of the epoxy resin demonstrated that adding DNDs to the reaction system did not change the curing mechanism, but affected the kinetics. Analysis of the kinetic curves by the isoconversion method showed that in the presence of nanodiamonds, the activation energy for the cross-linking of epoxy resin decreases, this decrease being most pronounced in the case of DND particles with polar amino groups on the surface (due to acceleration of the epoxide ring opening with an amine curing agent).

The mechanism of curing of multicomponent thermosetting binders in the presence of highly dispersed DB particles was studied in detail by Tikunova *et al.*[148] As investigation objects, the authors used dispersion filled polymer binders based on the Epikote 828 epoxy resin and the Epikote 154 novolac resin. Cyclic anhydrides (isomethyltetrahydrophthalic and endic anhydrides) were used as curing agents and

**Scheme 1**




undecylimidazole served as the catalyst. The epoxy resin curing process was carried out in the presence of highly dispersed DB powder (manufactured by CJSC Elektrokhimpribor, Lesnoy, Russian Federation). According to high-temperature FT IR spectroscopy and attenuated total reflection data, the diamond blend additive induces an increase in the rate of polyester formation and accelerates the composite curing in the temperature range of 85 – 165 °C. The maximum degree of conversion of the anhydride groups was observed for DB content of only 0.05 mass %. The authors suggested that the curing of DB-filled binders results in the formation of stable complexes involving the anhydride groups of the curing agent and the functional groups present on the surface of DB particles (see, for example, structures **1** – **3**), which are in turn complexed with epoxide groups (Scheme 1).

The following two important conclusions were drawn in the above publications devoted to DND-doped epoxy resins:

— DNDs can act in these systems as not only active functional fillers, but also as (co)catalysts of the involved polymerization processes;

— the DND concentration (load) is moderate and should be optimized for producing the maximum effect.

#### 4.5.1. Elastomer – diamond composite materials

Shakun *et al.*[149] analyzed the results obtained by using DNDs and DB as fillers for various elastomers for common and special purposes, including polyfluorinated elastomers, polysiloxanes, polyisoprenes, styrene – butadiene rubber and polyurethane. Generally, the use of DNDs and DB enhanced the strength and tribological characteristics, increased the tensile strength and improved the processability.

Hajiali and Shojaei [150] investigated the effect of DNDs on the formation of a network of entanglements and the kinetics of cross-linking of an elastomer mixture (natural rubber and styrene butadiene rubber) during mechanical mixing and vulcanization by sulfur-containing cross-linking systems. The uniform distribution of the filler throughout the elastomer matrix (5 parts of DNDs per 100 parts of the elastomer) was confirmed by high-resolution field emission scanning electron microscopy (FESEM). The curing of rubber mixtures in the presence of DNDs had a shorter induction period and a higher rate with a low activation energy for all vulcanizates. The authors attributed this result to adsorption of the vulcanization accelerator on the DND surface.

The introduction of pristine DND and DND doped with 1.45 mass % – 4.25 mass % vinyltrimethoxysilane (VTMOS) results in polydimethylsiloxane (PDMS) reinforcement. The improvement of dispersion of doped DNDs in PDMS upon mechanical mixing of the components was evidenced by FESEM. The introduction of DNDs and DND – VTMOS into PDMS is accompanied by increasing tensile strength of organosilicon rubber by 45% and 70%, respectively. The most pronounced increase in the strength of filled PDMS in the studied range of compositions (0.2 mass % to 1.5 mass % doped DNDs) was found for the lowest (0.2 mass %) degree of filling.

#### 4.5.2. Polymer – diamond composites based on thermoplastics

Apart from functional groups, the DND surface contains uncompensated (usually positive) surface charges, which is a consequence of acid treatment during the purification procedure.[117] It is not surprising that a much more pronounced effect of DNDs on the properties of thermoplastics was usually observed for polymers with so-called polar matrices (polyamides, polyvinyl alcohol, butadiene – styrene thermoplastic elastomer, *etc.*) rather than non-polar matrices (polyolefins, perfluorinated polymers, *etc.*).

Morimune *et al.*[151] investigated isotropic composites of polyvinyl alcohol (PVA) with DNDs (PVA – DND) that were cast from an aqueous solution of the polymer containing dispersed DND particles. The most pronounced (2.5-fold) increase in the initial elastic modulus of the composite relative to the reference sample (pristine PVA) was found for a DND content of 1 mass %. The tensile strength for this degree of filling also increased (~1.25-fold). A further increase in the degree of filling did not lead to a considerable change in the elastic and strength characteristics; the authors attributed this to aggregation of the filler. It should be noted that absolute values of the elastic modulus and tensile strength of the reference sample were moderate, 4 GPa and 95 MPa, respectively; therefore, the absolute values for these characteristics attained for the composite with the optimal component ratio were also moderate: 10 GPa and 120 MPa.

A study of the morphology and mechanical properties of the PA6 polyamide composites with DND – COOH and DND – $NH_2$ prepared by the melt mixing method demonstrated [152] that the use of DNDs with carboxylated surface results in composite embrittlement and the elongation at break of this composite decreases with increasing degree of filling. In the case of DND – $NH_2$ composite (0.25 mass % degree of filling), the initial elastic modulus increases 1.25-fold with virtually invariable tensile strength and elongation at break.

Kurkin *et al.*[153, 154] demonstrated for the first time that not only the DND content in the system but also the sign of the uncompensated surface charge of DND particles can considerably affect the properties of the polymer – DND composite. The authors studied the influence of DNDs on the adhesive strength of PVA fibre in the epoxy matrix. Diamond blends of two types were used as modifying fillers, one with positively [DB(+)] and one with negatively [DB(−)] charged surface (according to dynamic light scattering, the ζ-potential in DMSO was +20 and −26 mV, respectively). The system included the following components: ED-20 epoxy resin served as the model binder, *m*-phenylenediamine (MPD) was the curing agent and diethylene glycol diglycidyl ether (DGDE) served as the plasticizer. The mass composition of the cured resin was as follows: ED20 : MPD : DGDE = 100 : 20 : 15. Diamond blends of two types were added to PVA fibre and to the epoxy matrix in various combinations (totally 9 variants). The DB content in the epoxy binder was 0.05 mass % and that in PVA fibre was 2.8 mass %. The adhesive strength of the PVA fibre in the epoxy matrix was determined by the pull-out method after curing the binder under standard conditions. Modification of the matrix component virtually did not affect its mechanical characteristics, while modification of the fibre component by adding DB (+) caused a 1.6-fold increase in the tensile strength of the PVA fibre and a ~2-fold increase in the elongation at break (Table 7).

**Table 7**. Mechanical characteristics of modified components of polymer systems.[154]

| Component | Tensile strength /MPa | Elongation at break (%) |
|---|---|---|
| *Epoxy matrix* | | |
| ED20 | 97 ± 3 | 2.2 |
| ED20 + 0.05 mass % DB(+) | 98 ± 2 | 2.1 |
| ED20 + 0.05 mass % DB(−) | 100 ± 2 | 2.2 |
| *PVA fibre* | | |
| PVA | 634 ± 15 | 4.8 |
| PVA + 2.8 mass % DB(+) | 1038 ± 50 | 6.4 |
| PVA + 0.05 mass % DB(−) | 590 ± 30 | 6.1 |

The adhesion strength at the PVA fibre/epoxy matrix interface also strongly depended on the variant of modification (Table 8).

The maximum adhesion strength at the polymer/binder interface increased ~4-fold (42 MPa), with DB(−) being distributed in the epoxy binder and DB(+) being distributed in the fibre, in comparison with the interfacial strength of pristine components (10.5 MPa).

Composites based on thermoplastics and DNDs showed a nontrivial result of increasing deformation energy at break of PVA – DND composites upon the addition of

**Table 8**. Interfacial adhesion strength (MPa) for the initial and modified components of epoxy systems.[154]

| Component | PVA | PVA + DB(+) | PVA + DB(−) |
|---|---|---|---|
| ED20 | 10.5 ± 0.5 | 23 ± 2 | 16 ± 1 |
| ED20 + DB(+) | 37 ± 2 | 19 ± 3 | 33 ± 1 |
| ED20 + DB(−) | 16 ± 1 | 42 ± 2 | 17 ± 2 |

DNDs;[152–155] most often, the introduction of an inorganic component to the polymer system leads to embrittlement. In the case of filled composites, the elastic modulus usually increases, the tensile strength either remains unchanged or decreases, while the elongation at break sharply decreases almost in all cases. A possible explanation to the improvement of elasticity of PVA fibres upon the addition of DNDs is the formation of so-called sliding links of chain entanglements (possibly represented by functional groups of doped DND particles), which react with the PVA hydroxyl groups. Previously, a similar effect of increasing deformation energy at break of a filled composite was observed for the butadiene–styrene thermoplastic elastomer filled with DNDs and DB.[156]

#### 4.5.3. Tribology of polymer composites

A large number of studies address the potential promising tribological applications for DNDs (*e.g.*, Ref. 157).

A study of the tribological properties of epoxy matrices filled with pristine DNDs and modified DNDs with an aminated surface (ethylenediamine) [155] showed a significant decrease in the wear and friction coefficient compared to those for an unfilled material. Tribological characteristics were determined for different characteristic size scales using the pin-on-disk method in a composite–metal dry friction pair with aluminium or steel spheres as counter-bodies, the nanoindentation method and atomic force microscopy. The use of surface-aminated DNDs for improving the tribological characteristics of composites proved to be more efficient than the use of pristine DNDs, which was explained by the formation of a stronger particle/matrix interface. Unfortunately, significant changes in tribological characteristics were found only for high degrees of filling of the polymer composites ($\geqslant$7.5 mass % DND), which limits their practical applicability in friction pairs.

Ayatollahi *et al.*[158] studied the tribological properties of epoxy-based composites with DNDs at low contents of the filler. The addition of only 0.1 mass % DNDs with the surface modified by cetyltrimethylammonium bromide resulted in a 50% decrease in the friction coefficient for the epoxy matrix–carbon steel dry friction pair and a 84% decrease in wear. A further increase in the DND content in the system did not improve the tribological characteristics, probably, due to the local aggregation of DND particles.

Golchin *et al.*[159] used the pin-on-disk method to study the tribological characteristics of DND-filled ultrahigh molecular weight polyethylene (UHMWPE) in water-lubricated sliding contacts. Inconel 625, an acid-resistant nickel–chromium alloy containing niobium and molybdenum, was used as the counter-body. For the introducion into UHMWPE, the nanodiamonds were dispersed in ethanol using an ultrasonic bath and blended with dispersed polymer particles. The subsequent drying and consolidation gave the composite material. The composite containing 1 mass % DND had a 72% lower wear and a 24% lower friction coefficient than the pristine UHMWPE. On further increase in the DND content, the modification effect disappeared, which was attributed to inefficient dispersion of DNDs in the composite.

The tribological properties of the PA6/DND–COOH and PA6/DND–$NH_2$ systems were studied by the pin-on-disk method in a dry friction pair with the AISI 52100 stainless bearing steel.[160] The composites were synthesized by the melt mixing method. It was shown that PA6 filled with carboxylated DNDs (1 mass %) were characterized by a 30% decrease in the wear rate and a 60% decrease in the friction coefficient compared with those of unfilled PA6 polyamide. For comparable degrees of filling, the introduction of surface-aminated DNDs into the composite led to a lower wear than the introduction of surface-carboxylated DNDs. The authors attributed this to better dispersion of modified DND in PA6 polyamide. For the PA6 composite containing 1 mass % carboxylated DNDs, the friction coefficient and wear rate were shown to gradually decrease in long-term tribological tests. In the authors' opinion, a possible explanation to this result is the formation of a strong contact friction layer, which contains nanodiamond particles and determines the self-lubrication effect and high thermal conductivity.

#### 4.5.4. Polymer – DND composites for special applications

Highly thermally stable poly[2,2′-(*p*-oxydiphenylene)-5,5′-bibenzimidazole] (OPBI) was synthesized in polyphosphoric acid in the presence of DNDs to give *in situ* the DND–OPBI/OPBI nanocomposite by the Friedel–Crafts reaction.[161] The covalent attachment of DNDs to the polymer was proved by NMR spectroscopy, X-ray photoelectron spectroscopy and X-ray diffraction. A scanning electron microscopy examination confirmed efficient dispersion of DNDs in the polybenzimidazole matrix. It was shown that DNDs efficiently reinforce the polymer matrix. A 30% increase in the elastic modulus and tensile strength without the loss of ductility was found for the modified polymer containing 1 mass % DNDs. The DND-grafted composites had a higher thermal stability than the pristine polymer. For the composites with the same DND content prepared by mechanical mixing, no practically significant changes in the polymer matrix properties were observed.

Branson *et al.*[162] reported an attempt to produce DND-containing nanofluids with high thermal conductivity. Stable ethylene glycol dispersions of DNDs were prepared using the technique of formation of polymer brushes on the surface of nanodiamond particles. For the preparation of such particles, a dispersion of DNDs in DMSO was treated with glycidol at elevated temperature; the process was accompanied by covalent condensation of glycidol monomers with the DND carboxyl groups followed by ring opening oligomerization of glycidol to give polymer brushes composed of polyglycidol molecules. The replacement of DMSO by ethylene glycol resulted in the formation of the target nanofluids, which showed an increase in the heat conductivity of the medium by 12% for the DND content of 0.9 vol.% in comparison with pure ethylene glycol. The authors believe that improvement of the covalent DND modification procedure, which optimizes the nanodiamond solvation process, could result in the preparation of cooling fluids with high thermal conductivity.

A practically important example of industrial use of DNDs in polymer systems was described by Bhadra *et al.*,[163] who examined the possibility of DND immobilization in the Celgard type X30–240 distillation membrane for improving the water desalination process. The nanodiamonds were inserted into the membrane by forcing a DND dispersion in an acetone solution of polyvinylidene fluoride through the membrane. All performance characteristics were higher for the modified desalination membrane containing only 2 mass % DND than for the pristine membrane. In the described experiments, the permeate flux reached a maximum value of 13.8 L $m^{-2}$ $h^{-1}$ at the degree of desalination of 99.9%. The mass transfer coefficient for

the modified membrane at 90 °C reached a maximum of $5.47 \times 10^{-8}$ kg m$^{-2}$ s$^{-1}$ Pa$^{-1}$ and, depending on the flux, it was 1.4 – 1.8 times higher than this value for the pristine membrane. In the authors' opinion, the introduction of DNDs has a favourable influence on the interaction of water with the hydrophobic membrane, thus improving the water vapour permeability of the membrane and preventing the penetration of liquid water into the pores.

It is known [164] that DNDs are more biocompatible materials than carbon nanotubes or technical carbon. Considering the DND biocompatibility and the wound-healing ability established for the bacterial cellulose/chitosan composites, Ostadhossein *et al.*[165] made an attempt to fabricate composite films based on polysaccharides containing nanodiamonds, which could become a flexible platform for the development of new promising types of medical dressings. The chitosan/bacterial cellulose/DND composite films containing 1, 2, 3 and 4 mass % DNDs were cast from solutions. Upon the addition of 2 mass % DND, the elastic modulus of the cast composite film increased 3 – 5-fold, while the tensile strength of the material and the elongation at break decreased by 25%. Analysis of mitochondrial activity of L929 fibroblast cells showed that the nanocomposite films remain biocompatible (> 90%) even after 24-h incubation. The developed materials can be used for the manufacture of medical dressings, including those providing transdermal drug delivery.

Delavar and Shojaei [166] investigated the possibility of changing the mechanical characteristics of biomedical chitosan – DND composites by varying the degree of oxidation of filler particles. The controlled oxidation of the DND surface was carried out at 420 °C for various periods of time. Nanodiamond-containing composite films were prepared by casting from a solution. The most pronounced increase in the tensile strength (up to 85%) and tensile modulus (up to 125%) was found for the composite that contained 1.5 mass % DND oxidized for a long period of time (4.5 h). Meanwhile, the elongation at break decreased by 300%.

Angjellari *et al.*[167] reported the use of the PVA/DND dispersion as a new type of ink for 3D printing of items of various shapes. Analysis of the mechanical properties of three-dimensional printed objects showed that the average elastic moduli determined by the contact resonance of the calibrated cantilever of a Solver atomic force microscope (NT-MDT, Russian Federation) were greater by 22%, 44% and 200% for PVA – DND nanocomposites with 0.5 mass %, 1 mass % and 5 mass % filler contents, respectively, than for pristine PVA. It was assumed that the developed PVA – DND composites would be widely used for 3D printing.

### 4.6. Antifriction oil compositions with detonation nanodiamonds

Diamond blend is often used as a multifunctional lubricating oil additive. Fractal carbon particles with a developed periphery have a strong structuring effect on the oil, which largely changes the friction mechanism.[168] Apart from the dispersion of carbon particles, tribochemical reactions, including unexpected ones, take place in the friction zone with local heating and loads. Simulation of the friction conditions (high pressure and temperature) for the DB – hydrocarbon systems revealed considerable changes in the phase composition of carbon, in particular, appearance of graphene-like structures as a result of recrystallization of a part of amorphous carbon. Hence, in the tribological contact area, a carbon particle is transformed into a graphene-like cluster with specific lubricating properties, caused by the layered structure of graphene. Apparently, the graphene-like structures are generated in a repeated manner, which ensures long-term performance of the additive.

Apart from the decrease in the friction coefficient, the addition of nanodiamonds to the lubricant causes a considerable decrease in the wear of the friction pair. This raises the temperature limit of applicability of the lubricant composition. Ivanov [169] proposed a mechanism of DND action on the friction surface of the pair depending on the applied load. It is believed that the lubrication mechanism in the presence of DNDs is related to incorporation of DNDs into the tribological surface. The size, strength and the round shape of nanodiamonds make them an effective antiwear and antifriction additive to quite a number of lubricants. In a diamond blend with, on average, 40 mass % – 60 mass % nanodiamonds and, correspondingly, 60 mass % – 40 mass % graphite/graphene structures, the former exhibit weak microcutting properties, which are, however, sufficient for polishing of contact surfaces. This process is of short duration and ensures the largest contact area and, hence, a semifluid or fluid lubrication regime. The remaining carbon of the diamond blend undergoes adhesive interaction with the new surface of the friction pair, with high temperatures arising upon friction.

The chemically reactive components, first of all carbon, present in the lubricant saturate the friction pair surface with atomic carbon. Thus, austenite and martensite structures or white spots are formed on the surface layer. This is accompanied by a decrease in the friction coefficient because of decreasing adhesion and specific surface energy.

Ivanov [169] studied the friction pair consisting of steel ShKh15 (GOST 801) and steel 45 (GOST 8509-86) in the presence of the I-40A lubricant containing 0.08 mass % – 0.48 mass % diamond blend manufactured by the SCTB Technolog, composed of 56 mass % nanodiamonds and 44 mass % graphite/graphene carbon. The authors showed that the DB content of not more than 0.1 mass % is the maximum effective concentration for tribocoupling. An excess over this concentration does not affect friction parameters of this contact pair. It was shown that at a moderate pressure on the contact pair, the nanodiamond crystallites in the oil composition act as a micro abrasive component, actually grinding and polishing the surface. As the pressure on the friction pair increases, the crystallites of the nanodiamond penetrate into the metal surface, that is, into surface defects or lower-density areas. Gradually, this process would give rise to a continuous layer of diamond nanoparticles. This would first happen to the friction pair part characterized by higher plasticity. After the whole surface of this part is coated by nanodiamond particles, the other part (which was initially harder) would start to behave similarly to the first part and the surface impregnation with nanodiamonds would continue. Thus, actually one gets a diamond – diamond friction pair instead of the initial steel – steel pair; therefore, the friction coefficient decreases and the wear resistance increases.[168]

However, the use of DB rather than DNDs as the additive is much more efficient. In this case, both the wear rate of the friction surface and the friction coefficient decrease to even a greater extent, while the pressure on the friction pair can be higher. Indeed, the friction coefficient in

the contact pairs decreases by 25% – 35%, wear resistance increases 2.1 – 2.6-fold and the noise during friction decreases. Due to their clear-cut structuring impact on any systems, nanodiamonds both in the pure state and in the blend also efficiently operate in greases, where they participate in the formation of a structural framework. Here a similar effect is observed: the addition of the blend induces a 25% – 35% decrease in the friction coefficient and a 1.4 – 3.1-fold increase in the wear resistance of contact pairs; this enables operation at higher pressures.

Good prospects are offered by modification of nanodiamonds by complex lanthanide sulfonates to give stable dispersions in oils. The new DND – La complexes may be considered as environmentally benign anticorrosion additives and, of course, may decrease the friction coefficient.[169] A new method was elaborated for the preparation of lanthanide sulfonates for the subsequent grafting to the nanodiamond surface in order to produce stable oil suspensions. It was shown that the addition of complexes grafted to the nanodiamond surface not only gives a stable suspension, but also efficiently decreases the friction coefficient of the contact pair. A more complex composite material consisting of nanodispersed polytetrafluoroethylene (NPTFE) and nanodiamonds with lanthanum – magnesium complexes deposited on the surface was studied as an antifriction oil additive. High efficiency of this additive was shown, in particular, for two-stroke engine cylinders and pistons.

The base oil used for the above compositions was I-12A or I-20A oil (GOST 20779-75). The additive concentration in the oil was always 2%. It was found that a considerable increase in the seizure load up to 5.0 kN is caused by introducing lanthanum magnesium sulfonate to oil. The addition of NPTFE to the composition changes the friction mechanism of contact pairs.

Thus, a considerable decrease in the friction coefficient down to 0.011 and retention of this level throughout the tribological tests was found for the composition containing 0.026 mass % nanodiamond together with NPTFE in the I-12A industrial oil. The coefficient of friction for the same composition without the nanodiamond additive increased almost 4-fold. This naturally affected the temperature in the contact zone of friction pairs: when the composition without nanodiamonds was used, the temperature was 2 times higher than in the case of the nanodiamond-containing composition.

Full-scale tests confirmed the obtained results: when the DND additive was used together with NPTFE, the maximum crankshaft speed increased, while the engine temperature decreased. It was shown that nanodiamonds used in combination with NPTFE give suspensions stable for up to 12 months. In view of the pronounced and poorly reversible aggregation of dry diamond nanoparticles, aqueous suspensions of nanodiamonds should be used to prepare these compositions. It was shown [169] that the preparation of oil compositions that induce the highest seizure load requires the addition of La/Mg complexes to DNDs, while for decreasing the friction coefficient, it is more appropriate to use the DND + La/Mg + NPTFE additive.

The foregoing provides the following conclusions:

— diamond blend and nanodiamond additives can generate a new (juvenile) friction surface in the contact pairs by means of nanodiamonds that penetrated into the surface; this, in turn, leads to decreasing wear and friction and increasing pressure of seizure. The friction coefficient decreases by 25% – 35%, the service life of contact parts increases 4 – 4.5-fold, the wear of contact parts decreases 1.4 – 3.1-fold, and load on the contact pairs may be increased by a factor of ~4.1;

— nanodiamonds modified by lanthanide derivatives form dispersions in industrial oils stable for up to a year; the friction coefficient in contact parts decreases to 0.011;

— the recommended amount of diamond blend that should be added to oil is 0.03 mass % to 0.55 mass %, depending on the operating conditions.

### 4.7. Catalysts based on detonation nanodiamonds

Veretennikov *et al.*[170] studied the effect of catalytic amounts of DNDs, the reaction temperature and the intensity of stirring on the ratio of the *ortho* and *para* isomers of mononitrotoluene in the products of toluene nitration with a sulfuric and nitric acid mixture. The introduction of DNDs results in a significant decrease in this ratio in mononitration products compared with conventional nitration over the whole temperature range.

Like other carbon nanomaterials, DNDs are of interest as catalysts and active phase supports, in particular, for platinum group metals. Metal catalysts supported on DND particles are obtained by various methods, for example, by chemical reduction of salts added to an aqueous suspension of DNDs, electrophoresis of metal nanoparticles or direct electrochemical reduction of metal ions on the DND particle surface.[171] High-performance catalysts for the oxidation of methanol in fuel cells were obtained and studied.

Highly sensitive sensors for determination of CO in the atmosphere were manufactured using DND particles coated by a platinum layer. The sensor operation is based on the oxidation of carbon monoxide to carbon dioxide according to the fuel cell principle, which does not require additional power supply.[171]

The DND – Pd complexes exhibit a very high catalytic activity towards hydrogenation of unsaturated hydrocarbons, which makes it possible to carry out the reaction even at room temperature.[172]

### 4.8. Polycrystalline materials made of nanodiamonds

The use of high pressures and temperatures for the formation of nanostructures in diamond-based polycrystalline superhard materials is associated with the possibility of consolidation of the initial nanopowders under these conditions.

Studies of polycrystals obtained by sintering of DND powder at high pressure (4.5 and 8 GPa) and high temperature (1000 – 2300 °C) were reported.[173, 174] It was shown that sintering is accompanied by structural rearrangements that are typical of sintering of dispersed powders with a two(or more)-level initial substructure, that is, grains → aggregates I → aggregates II. The sintering takes place first in the bulk of aggregates I and then between these aggregates, *i.e.*, in the bulk of aggregates II. When the pressure is 8 GPa and the temperature is 1500 °C, the proportion of aggregates II is 20%. The consolidation of DND particles is accompanied by the diamond → graphite phase transition, which starts at ~1000 °C.

The synthesis of polycrystalline materials from DNDs was carried out in a high-pressure apparatus (HPA).[174] As a rule, the high-pressure cell is charged by a conventional procedure in air. If no measures are taken to reduce the amount of gases adsorded by the developed surface of the powders during charging, sintering of diamond crystals at

high temperature is deteriorated, because they chemically react with gases (first of all, oxygen), which are desorbed under these conditions from the surface of diamond particles and are located in the pores.

It was shown[175] that the kinetics of compaction of the diamond powder under the action of high pressure and temperature can be described in terms of the simple model of viscoplastic medium.

The major obstacle to increasing the density of polycrystals produced from DNDs that were prepared for sintering by degassing and vacuum thermal treatment of the particle surface with sealing of the HPA operating volume is the structure of pores between the single crystals formed by agglomerates of initial diamond nanoparticles.[176] This gives rise to the counteraction of capillary forces to the forces arising due to external pressure. In the absence of chemical reactions between oxygen and the diamond, the backpressure, which arises due to the presence of air in the pores, insignificantly decreases the density of polycrystals in comparison with graphitization of diamond nanoparticles caused by the above-mentioned reactions. The gas backpressure is much lower than the Laplace pressure, which appears in the pores formed by recrystallized agglomerates of the initial diamond nanoparticles. One way of enhancing physicomechanical properties of sintered polycrystals is to considerably increase the operating pressure in the HPA.

Without increasing the HPA pressure, the only method for improving the physicomechanical properties of polycrystalline materials obtained by sintering DND powders is to search for additives that would promote the formation of the required composite structure. First of all, these are additives that form chemical compounds with carbon during sintering and thus fasten the diamond particles. The addition of tungsten or tungsten oxide activates sintering of the DND powder in a high-temperature region.[177]

A study of the oxidation kinetics of diamond nanopowder demonstrated that in the presence of tungsten, the rate of this process decreases,[178] because of chemical modification of the diamond nanoparticle surface by tungsten to give W–O and W–C bonds, which were identified by IR spectroscopy.[179] In a study of the phase composition of the composite samples obtained by high-pressure sintering of a hydrogen-reduced mixture of a DND powder with a $WO_3$ nanopowder, it was shown that the composite contains the carbide WC and the oxide $WO_3$. Tungsten carbide is formed both upon direct reactions between diamond and tungsten and upon reactions in the W–C–O system. Calculations showed[179,180] that the introduction of tungsten into the considered system at high pressure markedly decreases the Gibbs free energy as a result of reactions of carbon dioxide and carbon monoxide with tungsten. The reactions afford solid-phase WC and $WO_3$, *i.e.*, tungsten binds the gaseous products of diamond oxidation, thus retarding (or suppressing) its graphitization.

Bochecka *et al.*[174] investigated the thermal stability of DND–WC composite samples. The thermal stability coefficient of these samples is 0.86, which is classified as high thermal stability.[181]

Further improvement of the synthesis of the diamond–tungsten carbide nanocomposite consisted in the use of tungsten nanopowder prepared by electric spark dispersion of tungsten electrodes.[182] As a result, the fracture toughness of the composite increased to 7.0 MPa $m^{1/2}$.

Testing of the working parts of tools manufactured from the developed diamond–tungsten carbide nanocomposite showed good applibility of this material for the finish turning of non-ferrous metals.[183–185]

### 4.9. Modified detonation nanodiamonds for biomedical applications

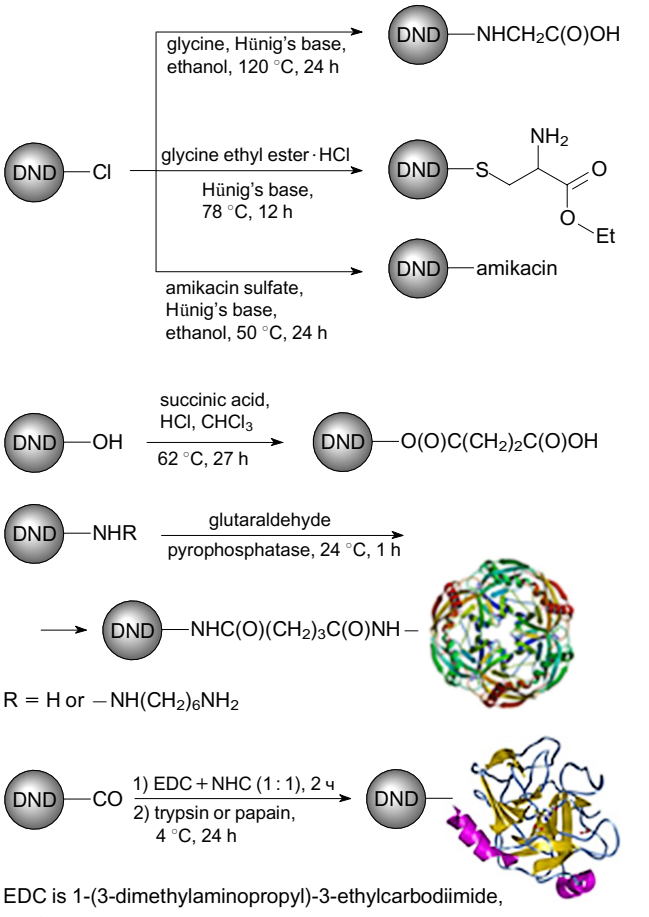
The interest of researchers in the use of DNDs for biological and medical applications has increased in recent years.[117] This is caused by the optimal combination of physicochemical and biopharmaceutical properties of DNDs: they possess no carcinogenic or mutagenic action and they are nontoxic and biocompatible. Presumably, DNDs could become a perfect platform for the development of targeted drug delivery systems.

The possible biological applications of new copper composites with DNDs were considered in a patent.[135] In view of the enhanced oxidation of these materials, they were proposed as anti-biofouling coatings for marine facilities. The basics of application of copper(I) oxide is rather simple: $Cu_2O$ particles inserted into the coating material repel marine organisms.

The problem is that $Cu_2O$ particles are washed away with water; this causes a new attack of the fresh surface with a marine organism up to new $Cu_2O$ particles, and this cycle is continuously repeated. This brings about the necessity of applying the coating once again after 1–2 years. The new composite material is not brittle and is not degraded by water; therefore, water can hardly affect it. Thus, the service life of the coating is substantially extended.

The development of systems for targeted delivery of biologically active and medicinal substances is a relevant

**Scheme 2**




EDC is 1-(3-dimethylaminopropyl)-3-ethylcarbodiimide, NHC is *N*-hydroxysuccinimide

challenge of nanomedicine. Among various sorts of nanocarbon, nanodiamonds are most promising as platforms for the design of such systems. The advantages of DNDs are caused by the considerable quantity and possible specific transformations of functional groups. The applications proposed for DNDs include the development of biomarkers, biosensors, potent adsorbents, *etc*.

A series of studies performed at the M.V.Lomonosov Moscow State University and the Ryazan State Medical University named after Academician I.P.Pavlov resulted in the production and investigation of drug delivery systems based on the nanodiamond platform for the delivery of glycine (central neurotransmitter) and cysteine (drug for the treatment of cataract).[78, 102, 108, 186, 187] A number of conjugates were patented.[188 – 197] The conditions for grafting of these compounds are depicted in Scheme 2.

The advantages of covalent attachment of biological macromolecules to the DND surface are obvious: the product has a higher stability, which is provided by strong covalent bonds rather than electrostatic interaction. However, noncovalent modification, that is, adsorption of particular molecules on the surface, also has benefits in some cases, for example, for the design of targeted drug delivery systems.

Using covalent and noncovalent binding methods, the DND surface can be modified by both small molecules[101, 113] and biological polymers: proteins and nucleic acids. The biological and medical applications of DNDs, like those of other materials, mainly include the following purposes:

— as auxiliary materials in the laboratory and medical practice, *i.e*., without contact with biological objects, as external sensors, chips, *etc*.;

— for direct contact with biological objects; in this case, there are two possible options:

*in vitro* as intracellular probes, labels, *etc*.; and

*in vivo* as therapeutic agents, carriers of targeted drug delivery systems, diagnostic agents, *etc*.

#### 4.9.1. Nanodiamonds as fluorescent labels

The importance of development of new types of fluorescent markers for biology and medicine is due to the fact that the widely used indicators based on fluorescent dyes have a number of drawbacks, in particular, they are largely affected by solution acidity and are also, photo-unstable and toxic for living systems.

The use of DNDs as labels for biological systems offers obvious advantages.[198] The size of the nanodiamond cores of primary particles provides a highly developed polyfunctional surface of the material. The very high fluorescence of DNDs makes them suitable for biomedical diagnostic purposes as optical markers.[198, 199] Usually, biomedical experiments on luminescent DNDs make use of highly efficient luminescence of NV centres and intense broad-band fluorescence, presumably, associated with structural defects of the DND surface. In particular, targeted fabrication of 'carbon dots', that is, fullerene-like structures of $\sim$1 nm size on DND surface, through diamond blend oxidation enhanced the broad-band fluorescence more than 20-fold.[200]

It was shown that DND particles represent a platform for multifunctional markers with different approaches to particle detection. Apart from fluorescence, Raman light scattering in diamond is used to detect DND particles in biological specimens. High-contrast images of nanodiamonds in cells were obtained by time-delayed fluorescence detection of DNDs.[201] The fact is that fluorescence lifetime of the NV centres ($\sim$20 nm) is an order of magnitude longer than the cell intrinsic fluorescence lifetime.

Nanodiamonds containing NV centers possess strong fluorescence, which is quite sufficient for monitoring a single particle in a cell. Furthermore, fluorescence persists for 300 s, whereas for common organic dyes this time is $\sim$10 s.[198] The first advantage of nanodiamonds as fluorescent probes is that they emit light in the red region (575 – 750 nm). This makes it possible to operate beyond the intrinsic fluorescence region of cells (300 – 500 nm). Second, these emitters are photo-stable.[199]

Fluorescence of nanodiamonds may also be due to the presence of silicon vacancy (SiV) complexes.[201, 202] Data on the synthesis of $\sim$1.6 nm nanodiamonds ($\sim$400 carbon atoms) with stable photoluminescent centres based on SiV complexes were reported.[117, 202, 203] Each nanocrystallite can include one or several centres of this type, with fluorescence being stable with time. Nanodiamonds can be used as contrast agents for magnetic resonance imaging. For this purpose, a residue capable of chelating the $Gd^{3+}$ ion[204] is attached to nanodiamonds (4 – 5 nm). A more complex procedure of synthesizing the gadolinium-containing contrast was discussed in the literature.[205, 206]

Meanwhile, radioactive labelling has always been the most convenient and sensitive method for monitoring a substance in the body. Girard *et al*.[207] described the synthesis of tritium-labelled DNDs. The authors showed that some of tritium (up to 7%) diffuses into DND particles; therefore, surface functionalization does not affect the label. This method is suitable for preparing up to several hundred milligrams of DND-based labels and can be used to trace the distribution of nanodiamonds in various tissues of the body.

The successful use of any material for biological and medical purposes is determined by their two properties: lack of toxicity and biocompatibility. Detonation nanodiamonds can be employed in any *in vitro* system, in particular, for the delivery of substances into cells and for the design of diagnostic systems. Before the problems of DND metabolism or excretion from the body are solved, it is already possible to use them in composites for external application.

#### 4.9.2. Nanodiamonds for drug delivery

The relative ease of penetration of nanodiamond particles into cells has become the base for the development of DND-based drug delivery methods. One more important factor is that a DND-immobilized compound (*via* covalent or other type of bond), even a very complex one (such as proteins and enzymes), retains the natural activity almost completely.[108, 141] Non-covalent attachment is used most often; this facilitates the release of the active component near the target. For example, DNDs form adducts with the anticancer drug doxorubicin *via* ionic bonds.[208] This process is reversible and can be controlled by the concentration of $Cl^-$ ions. It was shown experimentally that binding to DNDs promotes penetration of doxorubicin into mouse macrophages and tumour cells. In the authors' opinion, this composite could be used for drug delivery to colorectal carcinoma cells.

An eye is a fairly isolated system in the body; therefore, treatment of eye disorders requires, most often, systemic administration of large doses of pharmaceuticals, which may cause adverse effects. The topical administration of

drugs as eye drops or drug-loaded contact lenses usually produces only a short-term effect due to washing out of the drug. In these cases, it is appropriate to use depot forms, *e.g.*, those based on a nanogel prepared by cross-linking of polyethyleneimine-coated nanodiamonds and partly *N*-acetylated chitosan in the presence of timolol maleate.[209] This gel is applied as a constituent for the fabrication of contact lenses, from which the drug is washed out under the action of lysozyme contained in the lacrimal fluid, as the chitosan – nanodiamond matrix is being degraded. It was shown that nanodiamonds can serve as a platform for nonviral vectors in gene delivery systems using basic peptide (such as Arg8, Lys8, His8) residues at the end of polyglycerol chains.[209] The use of this approach with the addition of doxorubicin at the last stage resulted in the development of targeted drug delivery systems for anticancer drugs.[210]

Nanodiamonds were employed as adsorbents in experiments on the development of a bone tissue regeneration system based on the bone morphogenetic protein.[211] A drug delivery system comprising a composite with a fluorescent nanodiamond core and a porous silica shell was proposed.[212] The thickness of the porous layer can be varied during the synthesis, which makes it possible to control the nanoparticle size. Using this composite, it is possible to monitor the drug delivery process by recording a stable fluorescence image of DND distribution in the cell. Hence, this composite can be classified as a theranostic, that is, a carrier functioning simultaneously for therapeutic and diagnostic purposes.

#### 4.9.3. Imaging of nanodiamonds

The key methods for imaging of DND particles suitable for both *in vitro* and *in vivo* experiments include the following:[104, 108]

— tritium labelling;

— covalent binding of a radiocontrast agent, triiodobenzyl alcohol;

— formation of a luminescent label on the nanodiamond surface as a result of oxidation.

The replacement of protium in the C—H groups on the nanodiamond surface by tritium does not change the particle structure and does not affect the reactivity of the surface. Yakovlev[108] reported the results of DND – [$^3$H] biodistribution in the body of laboratory animals. The experiment that lasted for 6 months established the regularities of nanodiamond accumulation and excretion. As an example, Fig. 12 shows the data on DND – [$^3$H] distribution in a rat body upon intravenous administration. The highest amount of the nanodiamonds is accumulated in the lungs; it is 10 times higher than the amounts located in other organs.

The author[108] studied the effect of the nature of drug substances (glycine and amikacin) covalently grafted to the nanodiamond surface on the dynamics of penetration of the obtained conjugates into HeLa cells (Table 9).

DND conjugates with inorganic pyrophosphatase (PPase) were obtained[186, 213] by covalent grafting to the aminated nanodiamond. The greatest amounts of the enzyme in the samples were $0.80 \pm 0.05$ and $0.60 \pm 0.02$ mg of PPase per mg of DND—$NH_2$ and DND—$NH(CH_2)_6NH_2$, respectively. The catalytic activity of the resulting PPase-containing samples was, on average, higher than that for non-covalent immobilization. It is

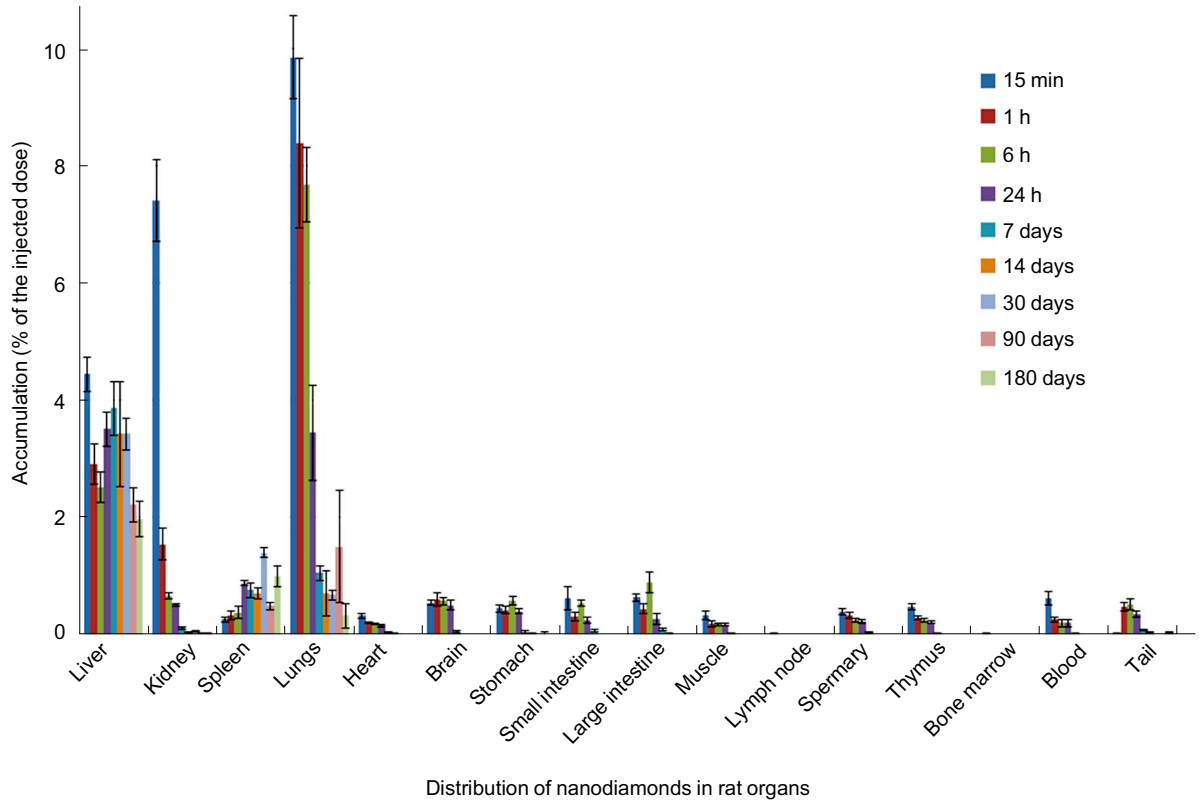



**Figure 12.** DND – [$^3$H] distribution in rat organs upon intravenous administration.[108] The volume of added DND – [$^3$H] hydrosol was 100 μL and the specific radioactivity was 0.61 mCi $mL^{-1}$.

**Table 9**. Effect of the nature of immobilized drug on the dynamics of DND penetration into HeLa cells on incubation for 24 h.[108]

| Sample | Percentage of cells with DND (%) during incubation | | | |
|---|---|---|---|---|
| | 15 min | 2 h | 4 h | 24 h |
| Pristine DND | 38.9 | 85.7 | 90.2 | 88.7 |
| DND – glycine | 2.9 | 3.9 | 6.9 | 70.7 |
| DND – amikacin | 3.8 | 44.8 | 45.3 | 87.3 |

worth noting that the activity of covalently grafted PPase is better retained in the presence of a linker: up to 65% of the enzyme activity was retained when DND – $NH_2$ was used and up to 95% was retained in the case of DND – $NH(CH_2)_6NH_2$.

#### 4.9.4. Specific *in vivo* activity of DND – glycine conjugate

Studies of the pharmacological action of the DND – glycine conjugate [56, 108, 193] demonstrated that the conjugate, unlike pure glycine, exhibits a potent anxiolytic effect, which does not decrease over a period of 24 h.[193, 214] The conjugate of glycine and DNDs surpasses glycine in the antidepressant effect, providing statistically significant increase in the life span of test animals.[195]

The most severe consequence of blood vessel diseases is hemorrhagic stroke, which may occur irrespective of age. The glycine – nanodiamond conjugate in a dose of 4 mg $kg^{-1}$ has an anti-stroke effect and decreases the mortality of animals from 70% to 40%.[214] The frequency of severe complications of the hemorrhagic stroke decreases by more than 80%.[214]

The tests showed that daily intraperitoneal administration of the DND – glycine conjugate in a dose of 4 mg $kg^{-1}$ for a week after a stroke has a clearly defined therapeutic action: the mortality of animals after a stroke decreases. [214]

## 5. Conclusion

This review of the state-of-the-art studies in the field of detonation nanodiamonds reflects the achievements made in the theory and practice of detonation synthesis. Studies on the theoretical issues of detonation synthesis aimed at gaining more in-depth knowledge on the mechanism of DND formation are in progress. It was shown that carbon nanoparticles are formed directly behind the detonation wave front and that their growth stops after 3 – 4 μs far beyond the Chapman – Jouguet plane. The thermochemical calculations showed that complete degradation of the original explosive requires much more energy than is released upon detonation of these compounds. The nucleation and subsequent growth of nanodiamond particles occur *via* chemical reactions. The $C_2^{\bullet}$ dimer radical is, most likely, the initial species for the formation of DNDs. The adamantyl radical may be the parent structure for DNDs. The growth of DND particles stops ($\leqslant$8 nm) due to disruption of long-range order and accumulation of defects in the crystallite structure and due to exhaustion of the radicals during particle growth in post-detonation processes.

The explosive charges with optimal nature and oxygen balance as well as with optimal composition, specific power and density were identified for the synthesis of nanodiamonds. The highest yields of DNDs can be obtained by using tetryl (extracted from ammunition), TNT – RDX mixtures (50 : 50 and 40 : 60 TH) or binary and ternary tetryl-based charges. Analysis of the influence of composition of the explosive charge shell and the heat capacity of the gas medium in the explosion chamber on the result of detonation showed that the DND yield and purity can be controlled by introducing reducing agents into the charge armour (aqueous solutions of urotropin, urea and hydrazine are compounds of choice).

A new highly economical and environmentally safe process was developed for the chemical purification of DND by treatment with the dilute $HNO_3$ with addition of $NH_4NO_3$ at 200 – 260 °C. During this process, not only are non-diamond carbon species completely oxidized, but also inorganic impurities present in DB are almost completely dissolved; the corrosion of equipment is virtually absent and only nitrogen gas is released.

Under optimized synthesis and purification conditions, boron-, phosphorus- and aluminium-doped DNDs were synthesized for the first time. Doping of DNDs results in considerable changes in the EPR spectral parameters: the hyperfine structure typical of point defects in crystals is recorded; the concentration of paramagnetic centres decreases; the dispersion of magnetic susceptibility depends on the sort of doping atom. The non-monotonic change in the cavity frequency on passing through resonance, which is observed only in nanostructured systems, was detected for the first time. Currently, DNDs have been recognized as highly promising materials for the design of single-photon emitters. The applicability of DNDs as efficient continuous slow neutron reflectors with high albedo was demonstrated.

New materials based on DNDs were developed and their performance characteristics were described. These materials are DND – CNT composites, new electrochemical coatings, bulk metal – nanodiamond composites, polymer composites (in particular, those containing DB) and efficient antifriction oil compositions. The use of doped DNDs for electroplating of chromium, nickel, zinc, silver and gold produces more uniform and less porous coatings with enhanced operational characteristics such as microhardness, wear resistance and corrosion resistance. The DND addition affects oxidized aluminium in a similar way. The synthesis of metal – nanodiamond composites was developed. The obtained composites based on copper, nickel and aluminium showed almost no adhesion between the material being processed and the processing tool.

Numerous studies deal with the application of DNDs in non-traditional areas. DNDs were shown to be efficient in catalysis as both catalysts and supports for industrially important processes: conversion of aliphatic alcohols, toluene nitration, hydrogenation of unsaturated hydrocarbons, methanol and carbon monoxide oxidation, hydrodechlorination of organic compounds, *etc*. Catalysts based on DNDs are highly active and selective.

Considerable advances were made in biomedical applications of DNDs. Currently, a variety of these applications have been proposed such as the design of biomarkers, biosensors, highly efficient adsorbents, coatings for surgical tools, cosmetic compositions, anti-UV creams and additives to dental materials. An efficient copper – nanodiamond composite for anti-biofouling coatings of marine facilities was developed. New chitosan/bacterial cellulose/DND composite films were proposed, suitable for the manufacture of medical dressing materials, including those providing the transdermal drug delivery.

Methods for imaging of DND particles (tritium labelling, introduction of radiocontrast agents, oxidation) suit-

able for *in vitro* and *in vivo* experiments were developed. It was found that DNDs penetrate into cells, where they are not surrounded by a membrane, freely occur in the cytoplasm and do not get into the nucleus or mitochondria. The DND distribution among organs of animals upon intravenous administration was studied. The greatest amount of DNDs is accumulated in lungs; this is an order of magnitude higher than the amounts of nanodiamonds in all other organs. This implies that new DND-based dosage forms could be developed for the treatment of severe lung diseases such as tuberculosis and COVID-19.

Using chemical modification of DNDs, new materials combining the properties of the carbon matrix and the grafted compound were elaborated. The DND – glycine conjugate was found to change the intensity and spectrum of the specific drug activity upon immobilization on the diamond nanoparticle; the action of the conjugate was found to exceed the action of glycine, even when used in a lower dose, and, in some cases, there appears a new type of pharmacological activity that is not inherent in native glycine. The DND – glycine conjugate in a dose of 4 mg $kg^{-1}$ possesses a clear-cut anti-stroke effect (against hemorrhagic stroke): the survival rate of animals increases from 7% to 40% in the presence of the conjugate, while the frequency of severe complications in survivals decreases by more than 80%.

It seems that in the near future, it would be most important to continue studies on the use of DNDs in medicine, polymer – diamond systems, electroplating and in fuel compositions for various purposes.

## References

1. T.T.B.Nguyen, V.Yu.Dolmatov, N.M.Lapchuk. *J. Appl. Spectrosc.*, **84**, 999 (2018)
2. V.Yu.Dolmatov. In *Nanodiamonds Advanced Material Analysis, Properties and Application*. (Ed. J.-C.Arnault). (Amsterdam: Elsevier, 2017). P. 391
3. *Detonatsionnye Nanoalmazy. Tekhnologiya, Structura, Svoistva i Primenenie*. (Detonation Nanodiamonds. Technology, Structure, Properties and Application). (Eds A.Ya. Vul', O.A.Shenderova). (Saint Petersburg: A.F.Ioffe FTI, 2016)
4. V.Dolmatov. In *Carbon Nanomaterials Sourcebook: Graphene, Fullerenes, Nanotubes and Nanodiamonds* (Ed. K.D.Sattler). (Boca Raton, FL, London, New York: CRC Press, Taylor and Francis Group, 2016). P. 509
5. V.Yu.Dolmatov. *Russ. Chem. Rev.*, **76**, 339 (2007)
6. V.V.Danilenko. *Vzryv: Fizika, Tekhnika, Tekhnologiya*. (Explosion: Physics, Engineering, Technology). (Moscow: Energoatomizdat, 2010)
7. V.Yu.Dolmatov. *Detonatsionnye Nanoalmazy. Poluchenie, Svoistva, Primenenie*. (Detonation Nanodiamonds. Synthesis, Properties and Application). (Saint Petersburg: NPO 'Provessional', 2011)
8. M.Van Thiel, F.H.Ree *J. Appl. Phys.*, **62**, 1761 (1987)
9. A.N.Dremin, S.V.Pershin, S.V.Pyaternev, D.N.Tsaplin. *Fiz. Goreniya i Vzryva*, **25** (5), 141 (1989)
10. A.G.Antipenko, S.V.Pershin, D.N.Tsaplin. In *IX Vsesoyuznyi Simpozium po Gorenoyu i Vzryvu*. (The IXth All-Union Combustion and Explosion Symposium). (Chernogolovka, 1989). P. 104
11. S.V.Pershin, D.N.Tsaplin, A.G.Antipenko. In *V Vsesoyuznoe Soveshchanie po Detonatsii*. (The Vth All-Union Detonation Meeting). Vol. 2. (Chernogolovka: MP IMTEKH, 1991). P. 233
12. S.V.Pershin, D.N.Tsaplin. In *V Vsesoyuznoe Soveshchanie po Detonatsii*. (The Vth All- Union Detonation Meeting). Vol. 2. (Chernogolovka: MP IMTEKH, 1991). P. 237
13. A.N.Aleshaev, P.I.Zubkov, G.N.Kulipanov, L.A.Luk'yanchikov, N.Z.Lyakhov, S.I.Mishnev, K.A.Ten, V.M.Titov, B.P.Tolochko, M.G.Fedotov, M.A.Sheromov. *Combust. Explos. Shock Waves*, **37**, 585 (2001)
14. V.M.Titov, B.P.Tolochko, K.A.Ten, L.A.Lukyanchikov, E.R.Pruuel. *Diam. Relat. Mater.*, **16**, 2009 (2007)
15. A.I.Lyamkin. Doctoral Thesis in Physical and Mathematical Sciences, Krasnoyarsk State Technological University, Krasnoyarsk, 2004
16. V.V.Danilenko. *Combust. Explos. Shock Waves*, **41**, 460 (2005)
17. V.V.Danilenko. *Combust. Explos. Shock Waves*, **41**, 577 (2005)
18. V.Yu.Dolmatov, V.Myllymaki, A.Vehanen. *J. Superhard Mater.*, **35**, 143 (2013)
19. B.G.Loboiko, S.N.Lyubyatinsky. *Combust. Explos. Shock Waves*, **36**, 716 (2000)
20. G.M.Khrapkovskii, D.V.Chachkov, E.V.Nikolaeva, I.S.Gaisin, A.G.Shamov. *Internet-Conferentsiya 'Butlerovskie Chteniya'* (Internet Conference 'Butlerov Readings'); http://butlerov.com/readings/ (Last accessed 31.10.2020)
21. V.B.Nguen. Candidate Thesis in Chemical Sciences, KNITU, Kazan, 2014
22. J.Postler, M.M.Goulart, C.Matias, A.Mauracher, F.Ferreira da Silva, P.Scheier, P.Limão-Vieira, S.Denifl. *J. Am. Soc. Mass Spectrom.*, **24**, 744 (2013)
23. P.J.Linstrom. *NIST Chemistry WebBook*. (Eds P.J.Linstrom, W.G.Mallard). (Gaithersburg, MD: National Institute of Standards and Technology, 20899); http://webbook.nist.gov (Last accessed 01.10.2020)
24. V.Yu.Dolmatov. *J. Superhard Mater.*, **40**, 290 (2018) ]
25. Patent RU 2359902 (2007)
26. V.Yu.Dolmatov, A.Vehanen, V.Myllymäki, A.S.Kozlov, T.T.B.Nguyen. *Russ. J. Appl. Chem.*, **91**, 225 (2018)
27. V.Yu.Dolmatov, A.A.Malygin, A.O.Dorokhov, A.S.Kozlov, V.A.Marchukov, V.G.Suschev, V.Myllymäki, A.Vehanen. *J. Superhard Mater.*, **42**, 17 (2020)
28. A.O.Dorokhov, V.Yu.Dolmatov, A.A.Malygin, A.S.Kozlov, V.A.Marchukov. *Russ. J. Appl. Chem.*, **93**, 1083 (2020)
29. A.M.Panich, A.I.Shames, D.Mogilyansky, S.D.Goren, V.Yu.Dolmatov. *Diam. Rel. Mater.*, **108**, 107918 (2020)
30. E.A.Petrov. In *Doklady Mezhdunarodnoi Nauchno-Tekhnicheskoi i Metodicheskoi Konferentsii*. (Proceedings of the International Scientific, Technical and Methodological Conference). (Kazan: KNITU, 2004). P. 881
31. A.M.Staver, A.I.Lyamkin. In *Ultradispersnye Materialy. Poluchenie i Svoistva. (Mezhvuzovskii Sbornik)*. [Ul'tradispersed Materials. Obtaining and Properties. (Interuniversity Collection)]. Krasnoyarsk: Krasnoyarsk Polytechnic Institute, 1990). P. 3.
32. V.M.Titov, V.F.Anisichkin, I.Yu.Mal'kov. *Fiz. Goreniya i Vzryva*, **25** (3), 117 (1989)
33. V.Yu.Dolmatov. *J. Superhard Mater.*, **38**, 373 (2016)
34. V.Yu.Dolmatov. In *Materialy i Struktury Sovremennoi Elektroniki: Materialy VIII Mezhdunarodnoi Nauchnoi Konferentsii*. (Materials and Structures of Modern Electronics: Proceedings of the VIIIth International Scientific Conference). (Minsk: Belorussian State University, 2018). P. 205
35. V.Yu.Dolmatov, V.Myllymäki, A.Vehanen, A.O.Dorokhov, M.N.Kiselev. *J. Superhard Mater.*, **41** (5), 355 (2019)
36. *Khimiya i Tekhnologiya Brizantnykh Vzryvchatykh Veshchestv*. (Chemistry and Technology of Blasting Explosives) (Ed. E.Yu.Orlova). (Leningrad: Khimiya, 1973)
37. A.N.Dremin, K.K.Shvedov. *Prikladnaya Mekhanika i Tekhnicheskay Fizika*, (2), 154 (1964)

38. *Kratkii Entsiklopedicheskii Slovar'. Energeticheskie Kondensirovannye Sistemy*. (Concise Encyclopedic Dictionary. Energetic Condensed Systems). (Ed. B.P.Zhukov). (Moscow: Yanus K., 2000)
39. V.Yu.Dolmatov. *J. Superhard Mater.*, **40** (2), 143 (2018)
40. A.P.Voznyakovskii, A.V.Smirnov, B.A.Fedorov, A.Kh.Khoreva, F.A.Shumilov. *J. Superhard Mater.*, **37**, 357 (2015)
41. V.Yu.Dolmatov. *Ul'tradispersnye Almazy Detonatsionnogo Sinteza*. (Ultradispersed Diamonds of Detonation Synthesis). (Saint Petersburg: Saint Pitersburg State Polytechnic University, 2003)
42. Patent RU 2109683 (1996)
43. Patent BY 4321 (2002)
44. Patent RU 2599665 (2016)
45. D.S.Volkov. Candidate Thesis in Chemical Sciences, MSU, Moscow, 2015
46. *Detonation Nanodiamonds: Science and Applications*. (Eds A.Vul', O.Shenderova). (Boca Raton, FL: Pan Stanford Publishing, 2014)
47. I.I.Kulakova. *Phys. Solid State*, **46**, 636 (2004)
48. R.Yu.Yakovlev, N.N.Dogadkin, I.I.Kulakova, G.V.Lisichkin, V.P.Leonidov, V.P.Kolotov. *Diamond Relat. Mater.*, **55**, 77 (2015)
49. D.S.Volkov, M.A.Proskurnin, M.V.Korobov. *Carbon*, **74**, 1 (2014)
50. D.S.Volkov, M.A.Proskurnin, M.V.Korobov. *Diamond Relat. Mater.*, **50**, 60 (2014)
51. I.I.Kulakova, V.V.Koral'kov, R.Yu.Yakovlev, G.V.Lisichkin. *Ross. Nanotekhnol.*, **5** (7 – 8), 66 (2010)
52. V.Yu.Dolmatov. *Sverkhtverd. Mater.*, (1), 28 (2005)
53. V.V.Korol'kov. Candidate Thesis in Chemical Sciences, MSU, Moscow, 2008
54. A.Yu.Koshkarov, E.R.Pruuel, K.A.Ten, P.I.Zubkov. *Mikroskopiya Detonatsionnogo Ugleroda. Al;bom Fotografii*. (Microscopy of Detonation Carbon. Photo Album, 2016); http://ancient.hydro.nsc.ru/srexpl/detcarbon/detonation_carbon_album_short.pdf
55. V.Yu.Dolmatov, G.S.Yur'ev, V.Myllymaki, K.M.Korolev. *J. Superhard Mater.*, **35**, 77 (2013)
56. R.Y.Yakovlev, A.S.Solomatin, N.B.Leonidov, A.S.Osipova, I.I.Kulakova, G.P.Murav'eva, G.V.Lisichkin. *Russ. J. Gen. Chem.*, **85**, 1565 (2015)
57. M.V.Korobov, D.S.Volkov, N.V.Avramenko, L.A.Belyaeva, P.I.Semenyuk, M.A.Proskurnin. *Nanoscale*, **5**, 1529 (2013)
58. A.S.Barnard. *J. Mater. Chem.*, **17**, 4811 (2007)
59. L.Lai, A.S.Barnard. *Nanoscale*, **3**, 958 (2011)
60. A.Alekswnskii, E.Eydelman, A.Vul'. *Nanosci. Nanotechnol. Lett.*, **3**, 68 (2011)
61. A.Pentecost, S.Gour, V.Mochalin, I.Knoke, Yu.Gogotsi. *ACS Appl. Mater. Int.*, **2**, 3289 (2010)
62. V.I.Zhornik, A.F.Il'yushchtnko, V.T.Senyut', A.I.Komarov, A.P.Korzhenevskii, A.V.Ivakhnik. *Nanoalmazy Detanatsionnogo Sinteza: Poluchenie i Primenenie*. (*Nanodiamonds of Detonation Synthesis: Obtaining and Applications* (Ed. P.A.Vityaz'). (Minsk: Belarus. Navuka, 2013)
63. B.V.Spitsyn, J.L.Davidson, M.N.Gradoboev, T.B.Galushko, N.V.Serebryakova, T.A.Karpukhina, I.I.Kulakova. *Diamond Relat. Mater.*, **15**, 296 (2006)
64. G.V.Lisichkin, I.I.Kulakova, Yu.A.Gerasimov, A.V.Karpukhin, R.Yu.Yakovlev. *Mendeleev Commun.*, **19**, 309 (2009)
65. O.A.Soboleva, G.A.Khamenov, V.Yu.Dolmatov, V.G.Sergeev. *Colloid J.*, **79**, 126 (2017)
66. V.Yu.Dolmatov, I.I.Kulakova, V.Myllymäki, A.Vehanen, A.N.Panova, A.A.Voznyakovskii. *J. Superhard Mater.*, **36**, 344 (2014)
67. Yu.Buchatskaya, A.Romanchuk, R.Yakovlev, A.Shiryaev, I.Kulakova, S.Kalmykov. *Radiochim. Acta*, **103**, 205 (2015)
68. I.I.Vlasov, O.Shenderova, S.Turner, O.I.Lebedev, A.A.Basov, I.Sildos, M.Rähn, A.A.Shiryaev, G.VanTendeloo. *Small*, **6**, 687 (2010)
69. D.Lin-Vien, N.B.Colthup, W.G.Fateley, J.G.Grasselli. *The Handbook of Infrared and Raman Characteristic Frequencies of Organic Molecules*. (San Diego, CA: Academic Press, 1991)
70. C.Bradac, T.Gaebel, N. Naidoo, M.J. Sellars, J.Twamley, L.J.Brown, A.S.Barnard, T.Plakhotnik, A.V.Zvyagin, J.R.Rabeau. *Nat. Nanotechnol.*, **5**, 345 (2010)
71. P.G.Baranov, A.A.Soltamova, D.O.Tolmachev, N.G.Romanov, R.A.Babunts, F.M.Shakhov, S.V.Kidalov, A.Y.Vul', G.V.Mamin, S.B.Orlinskii, N.I.Silkin. *Small*, **7**, 1533 (2011)
72. Y.S.Haiduk, A.A.Khort, N.M.Lapchuk, A.A.Savitsky. *Solid State Chem.*, **273**, 25 (2019)
73. N.E.Boboriko, I.A.Bobrikov, N.M.Lapchuk, D.V.Sviridov. *Solid State Chem.*, **275**, 181 (2019)
74. D.Terada, T.F.Segawa, A.I.Shames, S.Onoda, T.Ohshima, E.Osawa, R.Igarashi, M.Shirakawa. *ACS Nano*, **13**, 6461 (2019)
75. N.A.Poklonskii, T.M.Lapchuk, N.I.Gorbachuk, V.A.Nikolaenko, I.V.Bachuchin. *Semiconductors*, **39**, 894 (2005)
76. A.V.Khomich, V.P.Varnin, I.G.Teremetskaya, N.A.Poklonskii, N.M.Lapchuk. *Inorg. Mater.*, **41**, 812 (2005)
77. N.A.Poklonski, N.M.Lapchuk, A.V.Khomich, L.Fan-Xiu, T.Wei-Zhong. *Chin. Phys. Lett.*, **24**, 2088 (2007)
78. G.E.Remnev, V.V.Uglov, V.I.Shymanski, P.Konarski, M.P.Samtsov, N.M.Lapchuk. *J. Vacuum*, **89**, 118 (2013)
79. A.I.Shames, V.Yu.Osipov, A.E.Aleksenskiy, E.Ōsawa, A.Ya.Vul'. *Diamond Relat. Mater.*, **20**, 318 (2011)
80. A.V.Fionov, A.Lund, W.M.Chen, N.N.Rozhkova, I.A.Buyanova, G.I.Emel'yanova, L.E.Gorlenko, E.V.Golubina, E.S.Lokteva, E.Ōsawa, V.V.Lunin. *Chem. Phys. Lett.*, **493**, 319 (2010)
81. J.A.Weil, J.R.Bolton. *Electron Paramagnetic Resonance: Elementary Theory and Practical Applications*. (2nd Edn). (Hoboken: Wiley, 2007)
82. G.Burkard. *Nature (London)*, **442**, 749 (2006)
83. I.Žutić, J.Fabian, S.Das Sarma. *Rev. Mod. Phys.*, **76**, 323 (2004)
84. F.Gildas, Ya.Dan. *J. Nanophoton.*, **13**, 020901 (2019); http://doi.org/10.1117/1.JNP.13.020901
85. F.Jelezko, J.Wrachtrup. *Phys. Status Solidi A*, **203**, 3207 (2006)
86. A.N.Oleshkevich, T.T.B.Nguyen, V.Yu.Dolmatov, S.P.Sernov, A.V.Kolesnikov, T.M.Lapchuk, N.M.Lapchuk. In *Sbornik Nauchnykh Trudov. Priborostroenie — 2019: Materialy 12 Mezhdunarodnoi Nauchno-Tekhnicheskoi Konferentsii*. (Collection of Scientific Works. Instrumentation — 2019: Materials of the 12th International Scientific and Technical Conference). (Ed. O.K.Gusev). (Minsk: BNTU, 2019). P. 468
87. A.A.Shiryaev, A.V.Fisenko, I.I.Vlasov, L.F.Semjonova, S.Schuppler. *Geochim. Cosmochim. Acta*, **75**, 3155 (2011)
88. H.Nakano, A.Kouchi, M.Arakawa, Y.Kimura, C.Kaito, H.Ohno, T.Hondoh. *Proc. Jpn. Acad., Ser. B*, **78**, 277 (2002)
89. S.K.Simakov. *J. Mater. Res.*, **25**, 2336 (2010)
90. T.T.B.Nguyen, V.Yu.Dolmatov, N.M.Lapchuk, V.I.Shimanski. *J. Appl. Spectrosc.*, **84**, 780 (2017)
91. V.Yu.Dolmatov, N.M.Lapchuk, T.M.Lapchuk, B.T.T.Nguyen, V.Myllymäki, A.Vehanen, R.Yu.Yakovlev. *J. Superhard Mater.*, **38**, 219 (2016)
92. V.Yu.Dolmatov, T.T.B.Nguyen, T.M.Lapchuk, A.S.Kozlov, V.A.Ostrovskii. In *Sbornik Nauchnykh Trudov VII Mezhdunarodnoi Nauchnoi Konferentsii 'Materialy i Struktury Sovremennoi Elektroniki'*. (Collection of Scientific Works of the VIIth International Conference: Materials and Structures Modern Electronics). (Ed. Odzhaev). (Minsk: BSU, 2016). P. 234

93. A.N.Oleshkevich, V.Yu.Dolmatov, T.T.B.Nguyen, S.Munkhtsetseg, G. Shilagardi, N.M.Lapchuk, T.M.Lapchuk. In *Sbornik Nauchnykh Trudov VIII Mezhdunarodnoi Nauchnoi Konferentsii 'Materialy i Struktury Sovremennoi Elektroniki'*. (Collection of Scientific Works of the VIIIth International Conference: Materials and Structures Modern Electronics). (Ed. Odzhaev). (Minsk: BGU, 2016). P. 271
94. O.N.Poklonskaya. *Vestn. BGU*, **1** (2), 60 (2013)
95. T.T.B.Nguyen, N.M.Lapchuk, A.N.Oleshkevich, T.M.Lapchuk, V.Yu.Dolmatov. In *Priborostroenie — 2015: Materialy 8-i Mezhdunarodnoi Nauchno-Tekhnicheskoi Konferentsii*. (Instrumentation — 2015: Materials of the 12th International Scientific and Technical Conference. Vol. 1). (Ed. O.K.Gusev). (Minsk: BNTU, 2015). P. 262
96. V.V.Filippov, E.V.Ivakin, N.M.Lapchuk, A.S.Rubanov, S.P.Firsov. *Opt. Cryst.*, **4358**, 148 (2001); https://www.spiedigitallibrary.org/conference-proceedings-of-spie/4358/1/Long-lived-laser-induced-gratings-in-diamond-crystals/10.1117/12.418847.short
97. V.Yu.Dolmatov, A.N.Panova, A.A.Bochechka, M.V.Veretennikova, V.Myllymaki, S.A. Dushenok, E.V.Nikitin, G.G.Tsapyuk, E.V.Ishchenko. In *Porodorazrushayushchii i Metalloobrabatyvayushchii Instrument — Tekhnika i Tekhnologiya Ego Izgotovleniya i Primeneniya. Sbornik Nauchnykh Trudov*. (Rock-cutting and Metalworking Tools — Technique and Technology of its Production and Use. Collection of Scientific Works) No. 17. (Kiev: ISM, 2014). P. 213
98. A.N.Panova, V.Y.Dolmatov, E.V.Ishchenko, G.G.Tsapyuk, A.A.Bochechka, M.V.Veretennikova, V.Myllymäki, E.V.Nikitin. *J. Superhard Mater.*, **37**, 202 (2015)
99. V.Yu.Dolmatov, I.I.Kulakova, V.Myllymäki, A.Vehanen, A.A.Bochechka, A.N.Panova, B.T.T.Nguyen. *J. Superhard Mater.*, **38**, 58 (2016)
100. I.V.Shugalei, M.A.Ilyushin, A.M.Sudarikov. *Russ. J. Gen. Chem.*, **84**, 2539 (2014)
101. I.V.Shugalei, A.P.Voznyakovskii, A.V.Garabadzhiu, I.V.Tselinskii, A.M.Sudarikov, M.A.Ilyushin. *Russ. J. Gen. Chem.*, **83**, 851 (2013)
102. R.Yu.Yakovlev, A.S.Solomatin, N.B.Leonidov, I.I.Kulakova, G.V.Lisichkin. *Russ. J. Gen. Chem.*, **84**, 379 (2014)
103. E.Brun, H.A.Girard, J.-C.Arnault, M.Mermoux, C.Sicard-Roselli. *Carbon*, **162**, 510 (2020)
104. G.A.Badun, M.G.Chernysheva, R.Yu.Yakovlev, N.B.Leonidov, M.N.Semenenko, G.V.Lisichkin. *Radiochim. Acta*, **102**, 941 (2014)
105. R.Yu.Yakovlev, G.A.Badun, M.G.Chernysheva, N.B.Leonidov, G.V.Lisichkin. In *Proceedings of International Conference Diamond and Carbon Materials*. (Riva del Garda, Italy, 2013). 1.096
106. Patent RU 2538862 (2015)
107. O.A.Shenderova, G.E.McGuire. *Biointerphases*, **10**, 030802 (2015)
108. R.Yu.Yakovlev. Candidate Thesis in Chemical Sciences, MSU, Moscow, 2016
109. S.A.Denisov. Candidate Thesis in Chemical Sciences, MSU, Moscow, 2013
110. V.N.Khabashesku, J.L.Margrave, E.V.Barrera. *Diamond Relat. Mater.*, **14**, 859 (2005)
111. Y.Lu, Z.Gu, J.L.Margrave, V.N.Khabashesku. *Chem. Mater.*, **16**, 3924 (2004)
112. I.I.Kulakova, A.Yu.Pereyaslavtsev, G.V.Lisichkin. *Vestn. Mosk. Univ. Ser. 2, Khimiya,* **60**, 325 (2019)
113. *Nanodiamond*. (Ed. O.A.Williams). (London: The Royal Society of Chemistry, 2014)
114. *Carbon Nanoparticles and Nanostructures*. (Eds N.Yang, X.Jiang, D.W Pang). (Basel: Springer International Publishing, 2016)
115. V.Nesvizhevsky, U.Koster, M.Dubois, N.Batisse, L.Frezet, A.Bosak, L.Gines, O.Williams. *Carbon*, **130**, 799 (2018)
116. V.Yu.Dolmatov, E.K.Gorbunov, M.V.Veretennikova, K.A.Rudometkin, A.Vehanen, V.Myllymäki. *J. Superhard Mater.*, **35**, 251 (2013)
117. J.I.Chao, E.Perevedentseva, C.C.Chang, C.Y.Cheng, K.K.Liu, P.H.Chung, J.S.Tu, C.D.Chu, S.J.Cai, C.L.Cheng. In *Nanodiamonds: Applications in Biology and Nanoscale Medicine*. (Ed. D.Ho). (New York: Springer, 2010). P. 286
118. A.A.Vozniakovskii, T.S.Kol'tsova, A.P.Voznyakovskii, A.L.Kumskov, S.V.Kidalov. *J. Colloid Interface Sci.*, **565**, 305 (2020)
119. G.S.Aleksandrova, G.K.Burkat, E.V.Gmyzin, V.Yu.Dolmatov. *Vestn. Mosk. Univ. Ser. 2, Khimiya*, **93** (1), 15 (2016)
120. G.K.Burkat, V.Yu.Dolmatov, K.A.Svir' A.O.Dorokhov, D.V.Rudenko. In *Book of Abstracts of the 14th International Conference 'Advanced Carbon NanoStructures'*. (Saint Petersburg, 2019). P. 121
121. V.Yu.Dolmatov, G.K.Burkat, D.V.Rudenko, I.A.Dyakov. *J. Superhard Mater.*, **41**, 43 (2019)
122. G.K.Burkat, V.Yu.Dolmatov. *Phys. Solid State*, **46**, 703 (2004)
123. G.K.Burkat, T.Fujimura, V.Yu.Dolmatov, E.A.Orlova, M.V.Veretennikova. *Diamond Relat. Mater.*, **14**, 1761 (2005)
124. Patent RU 2631374 (2017)
125. G.K.Burkat, V.Yu.Dolmatov, I.V.Safronova, A.A.Malygin, V.Myllymäki, A.Vehanen, T.T.B.Nguyen. *J. Superhard Mater.*, **39**, 319 (2017)
126. Patent RU 2599473 (2016)
127. Patent RU 2599471 (2016)
128. Patent RU 2191227 (2002)
129. V.Yu.Dolmatov, D.V.Rudenko, G. K.Burkat, A.S.Aleksandrova, A.Ya.Vul', A.E.Aleksenskii, A.S.Kozlov, V.Myllymäki, A.Vehanen, I.A.D'yakov, A.O.Dorokhov, M.N.Kiselev. *J. Superhard Mater.*, **41**, 169 (2019)
130. Patent RU 2384524 (2008)
131. A.Krüger, F.Kataoka, M.Ozawa, T.Fujino, Y.Suzuki, A.E.Aleksenskii, A.Yu.Vul', E.Ōsawa. *Carbon*, **43**, 1722 (2005)
132. Patent RU 2446097 (2012)
133. G.K.Burkat, V.Yu.Dolmatov, G.S.Aleksandrova, E.D.Osmanova, V.Myllymäki, A.Vehanen. *J. Superhard Mater.*, **39**, 221 (2017)
134. V.A.Popov. Doctoral Thesis in Technical Sciences, MISIS, Moscow, 2017
135. Patent RU 2544219 (2015)
136. O.Elomaa, T.H.Hakala, V.Myllymäki, J.Oksanen, H.Ronkainen, V.K.Singh, J.Koskinen. *Diamond Relat. Mater.*, **34**, 89 (2013)
137. V.N.Mochalin, Y.Gogotsi. *Diamond Relat. Mater.*, **58**, 161 (2015)
138. Y.H.Zhang, K.Y.Rhee, D.Hui, S.J.Park. *Composites, Part B*, **143**, 19 (2018)
139. A.V.Shvidchenko, E.D.Eidelman, A.Ya.Vul', N.M.Kuznetsov, D.Yu.Stolyarova, S.I.Belousov, S.N.Chvalun. *Adv. Colloid Interfaces*, **268**, 64 (2019)
140. P.Karami, S.S.Khasraghi, M.Hashemi, S.Rabiei, A.Shojaei. *Adv. Colloid Interfaces*, **269**, 122 (2019)
141. J.T.Paci, H.B.Man, B.Saha, D.Ho, G.C.Schatz. *J. Phys. Chem. C*, **117**, 17256 (2013)
142. A.M.Panich. *Diamond Relat. Mater.*, **79**, 21 (2017)
143. T.Petit, L.Puskar. *Diamond Relat. Mater.*, **89**, 52 (2018)
144. H.Tinwala, S.Wairkar. *Mater. Sci. Eng. C*, **97**, 913 (2019)
145. S.A.Rakha, N.Ali, Y.A.Haleem, F.Alam, A.A.Khurram, A.Munir. *J. Mater. Sci. Technol.*, **30**, 753 (2014)
146. Y.A.Haleem, D.B.Liu, W.X.Chen, C.D.Wang, C.H.Hong, Z.He, J.W.Liu, P.Song, S.H.Yu, L.Song. *Composites, Part B*, **78**, 480 (2015)

147. A.Aris, A.Shojaei, R.Bagheri. *Ind. Eng. Chem. Res.*, **54**, 8954 (2015)
148. E.P.Tikunova, T.S.Kurkin, A.N.Ozerin, Yu.V.Kostina, M.Yu.Yablokova. *Polym. Sci., Ser. B*, **57**, 39 (2015)
149. A.Shakun, J.Vuorinen, M.Hoikkanen, M.Poikelispaa, A.Das. *Composites, Part A*, **64**, 49 (2014)
150. F.Hajiali, A.Shojaei. *Compos. Sci. Technol.*, **142**, 227 (2017)
151. S.Morimune, M.Kotera, T.Nishino, K.Goto, K.Hata. *Macromolecules*, **44**, 4415 (2011)
152. P.Karami, A. Shojaei. *Polym. Int.*, **66**, 557 (2017)
153. T.S.Kurkin, E.P.Tikunova, M.Yu.Yablokova, A.S.Kechek'yan, M.A.Beshenko, V.Yu.Dolmatov, A.N.Ozerin. *Dokl. Chem.*, **457**, 118 (2014)
154. T.S.Kurkin, A.N.Ozerin, E.P.Tikunova, A.S.Kechek'yan, E.K.Golubev, A.K.Berkovich, V.Yu.Dolmatov. *Nanotechnol. Russ.*, **10**, 878 (2015)
155. I.Neitzel, V.Mochalin, J.A.Bares, R.W.Carpick, A.Erdemir, Y.Gogotsi. *Tribol. Lett.*, **47**, 195 (2012)
156. A.N.Ozerin, T.S.Kurkin, G.G.Alkhanishvili, A.S.Kechek'yan, O.T.Gritsenko, N.S.Perov, L.A.Ozerina, M.A.Beshenko, V.Yu.Dolmatov. *Nanotechnol. Russ.*, **4**, 480 (2009)
157. W.Zhai, N.Srikanth, L.B.Kong, K.Zhou. *Carbon*, **119**, 150 (2017)
158. M.R.Ayatollahi, E.Alishahi, S.Doagou-R, S.Shadlou. *Composites, Part B*, **43**, 3425 (2012)
159. A.Golchin, A.Villain, N.Emami. *Tribol. Int.*, **110**, 195 (2017)
160. P.Karami, A.Shojaei. *Tribol. Int.*, **115**, 370 (2017)
161. R.Zhang, Z.X.Shi, Y.Liu, J.Yin. *J. Appl. Polym. Sci.*, **125**, 3191 (2012)
162. B.T.Branson, P.S.Beauchamp, J.C.Beam, C.M.Lukehart, J.L.Davidson. *ACS Nano*, **7**, 3183 (2013)
163. M.Bhadra, S.Roy, S.Mitra. *Desalination*, **341**, 115 (2014)
164. A.M.Schrand, L.Dai, J.J.Schlager, S.M.Hussain, E.Ōsawa. *Diamond Relat. Mater.*, **16**, 2118 (2007)
165. F.Ostadhossein, N.Mahmoudi, G.Morales-Cid, E.Tamjid, F.J.Navas-Martos, B.Soriano-Cuadrado, J.M.L.Paniza, A.Simchi. *Materials*, **8**, 6401 (2015)
166. Z.Delavar, A.Shojaei. *Carbohydron Polym.*, **167**, 219 (2017)
167. M.Angjellari, E.Tamburri, L.Montaina, M.Natali, D.Passeri, M.Rossi, M.L.Terranova. *Mater. Des.*, **119**, 12 (2017)
168. A.A.Shepelevskii, A.V.Esina, A.P.Voznyakovskii, Yu.A.Fadin. *Zh. Tekhn. Fiz.*, **87**, 1654 (2017)
169. D.M.Ivanov. Candidate Thesis in Technical Sciences, UPI, Ekaterenburg, 2006
170. E.A.Veretennikov, I.V.Tselinskii, V.Yu.Dolmatov, M.V.Veretennikova. *Vestn. Kazan. Tekhnolog. Univ.*, **20** (2), 13 (2017)
171. N.N.Vershinin, O.N.Efimov, V.A.Bakaev, A.E.Aleksenskii, M.V.Baidakova, A.A.Sitnikova, A.Ya.Vul'. *Fullerenes Nanotubes Carbon Nanostruct.*, **19** (1), 63 (2010)
172. O.V.Turova, E.V.Starodubtseva, M.G.Vinogradov, V.I.Sokolov, N.V.Abramova, A.Ya.Vul', A.E.Alexenskiy. *Catal. Commun.*, **12**, 577 (2011)
173. E.E.Lin, S.A.Novikov, A.B.Glushak. In *Fizikokhimiya Ul'tradispersnykh Sistem. Sbornik Nauchnykh Trud Vserossiiskoi Konferentsii*. (Physicochemistry of Ul'tradispersed Systems. Collection of Scientific Works of the IV All-Russian Conference). (Moscow: MEPhI, 1998). P. 262
174. O.O.Bochechka, I.A.Sveshnikov, S.M.Nazarchuk, S.D.Zabolotskii, V.S.Gavrilova, V.V.Bozhenok, E.M.Lutsak, L.O.Romanko, G.D.Il'nits'ka, S.V.Smekalenkov *Instrumental'nyi Svit*, **1** – **2**, 50 (2011)
175. V.T.Golovchan. *J. Superhard Mater.*, **42**, 6 (2000)
176. O.O.Bochechka. In *Porodorazrushayushchii i Metalloobrabatyvayushchii Instrument — Tekhnika i Tekhnologiya Ego Izgotovleniya i Primeneniya. Sbornik Nauchnykh Trudov*. (Rock-cutting and Metalworking Tools — Technique and Technology of its Production and Use. Collection of Scientific Works). No. 20. (Kiev: ISM, 2017). P. 177
177. S.N.Nazarchuk, A.A.Bochechka, V.S.Gavrilova, L.A.Romanko, N.N.Belyavina, L.I.Aleksandrova, V.N.Tkach, E.F.Kuz'menko, S.D.Zabolotnyi. *J. Superhard Mater.*, **33**, 1 (2011)
178. V.Ya.Zabuga, O.O.Bochechka, G.G.Tsapyuk, T.O.Kurylyak, O.S.Fedorchuk. *J. Superhard Mater.*, **38**, 8 (2016)
179. T.O.Kurylyak, O.O.Bochechka, O.M.Kutsay. In *Book of Scientific Works of 16th Internftional Young Scientists Conference Optics and High Technology Material Science (SPO 2015)*. (Kyiv, 2015). AP 18, 68
180. N.V.Novikov, O.O.Bochechka, S.N.Nazarchuk. In *Porodorazrushayushchii i Metalloobrabatyvayushchii Instrument — Tekhnika i Tekhnologiya Ego Izgotovleniya i Primeneniya. Sbornik Nauchnykh Trudov*. (Rock-cutting and Metalworking Tools — Technique and Technology of its Production and Use. Collection of Scientific Works) No. 15. (Kiev: ISM, 2012). P. 2012. P. 232
181. *Shlifporoshki Sinteticheskikh AlmazovTermostiiki*. (Heat-resistant Synthetic Diamond Grinding Powders) TU U 28.5-05417377-075 – 2003. [Current type 2003-12-23]. (Kiev: Ukrmetrteststandart, 2003)
182. O.O.Bochechka, A.E.Perekos, S.N.Nazarchuk, A.D.Rud', V.S.gavrilova, I.M.Kir'yan. In *Tezisy Dokladov III Mezhdunarodnoi Samsonovskoi Konferentsii 'Materialovedenie Tugoplavkikh Soedinenii'*. (Abstracts of Reports of the IIIrd International Samsonov Conference 'Materials Science of Refractory Compounds'). (Kiev, 2012). P. 196
183. N.E.Stakhniv, L.N.Devin, O.O.Bochechka, S.N.Nazarchuk. In *Porodorazrushayushchii i Metalloobrabatyvayushchii Instrument — Tekhnika i Tekhnologiya Ego Izgotovleniya i Primeneniya. Sbornik Nauchnykh Trudov*. (Rock-cutting and Metalworking Tools — Technique and Technology of its Production and Use. Collection of Scientific Works) No. 20. (Kiev: ISM, 2017). P. 428
184. N.E.Stakhniv, L.N.Devin, O.O.Bochechka, A.A.Osadchii, S.N.Nazarchuk, S.V.Rychev. *J. Superhard Mater.*, **40**, 197 (2018)
185. A.A.Osadchii, S.N.Nazarchuk, O.O.Bochechka, L.N.Devin, T.A.Garbuz. In *Sbornik Trudov VI Mezhdunarodnoi Samsonovskoi Konferentsii 'Materialovedenie Tugoplavkikh Soedinenii'*. (Proceedings of the VIth International Samsonov Conference 'Materials Science of Refractory Compounds'). (Kiev, 2018). P. 164
186. A.V.Valueva, R.Yu.Yakovlev, E.V.Rodina, I.I.Kulakova, G.V.Lisichkin, N.B.Leonidov. In *Proceeding of IVth International Science Conference 'Fullerenes and Nanostructures in Condensed Matter'*. (Minsk, 2014). P. 146
187. R.Yu.Yakovlev, I.I.Kulakov, G.A.Badun, G.V.Lisichkin, A.V.Valueva, N.G.seleznev, N.B.Leonidov. *Razrabotka i Registratsiya Lekarstvennykh Sredstv*, **3** (16), 36 (2016)
188. Patent EP 2687207 (2015)
189. Patent EP 2662080 (2015)
190. Patent US 9254340 (2016)
191. Patent RU 2519755 (2014)
192. Patent RU 2508098 (2014)
193. Patent RU 2506075 (2014)
194. Patent RU 2519760 (2014)
195. Patent RU 2519759 (2014)
196. Patent RU 2519761 (2014)
197. Patent RU 2521404 (2014)
198. A.S.Barnard. *Analyst*, **134**, 1751 (2009)
199. O.Faklaris, D.Garrot, V.Joshi, J. P.Boudou, T.Sauvage, P.A.Curmi, F.Treussart. *J. Eur. Opt. Soc.: Rapid Publ.*, **4**, 09035 (2009)
200. R.Martin, M.Alvaro, J.R.Herance, H.Garcia. *ACS Nano*, **4**, 65 (2010)
201. E.Neu, M.Agio, C.Becher. *Opt. Express*, **20**, 19956 (2012)

202. I.I.Vlasov, A.A.Shiryaev, T.Rendler, S.Steinert, S.-Y.Lee, D.Antonov, M.Voros, F.Jelezko, A.V.Fisenko, L.F.Semjonova, J.Biskupek, U.Kaiser, O.I.Lebedev, I.Sildos, P.R.Hemmer, V.I.Konov, A.Gali, J.Wrachtrup. *Nat. Nanotechnol.*, **9**, 54 (2014)
203. W.Baaziz, G.Melinte, O.Ersen, C.Pham-Huu, I.Janowska. *Phys. Chem.*, **59**, 15988 (2014)
204. L.M.Manus, D.J.Mastarone, F.A.Waters, X.-Q.Zhang, E.A.Schultz-Sikma, K.W.MacRenaris, D.Ho, T.J.Meade. *Nano Lett.*, **10**, 484 (2010)
205. T.Nakanmwura, V.Ohana, H.Yabuno, R.Kasai, T.Suzuki, T.Hasebe. *Appl. Phys. Express*, **6**, 015001 (2013)
206. L.Zhao, A.Shiino, H.Qin, T.Kimura, N.Komatsu. *J. Nanosci. Nanotechnol.*, **15**, 1076 (2015)
207. H.A.Girard, A.El-Kharbachi, S.Garcia-Argote, T.Petit, P.Bergonzo, B.Rousseau, J.C.Arnault. *Chem. Commun.*, **50**, 2916 (2014)
208. V.Vaijayanthimala, D.K.Lee, S.V.Kim, A.Yen, N.Tsai, D.Ho, H.-C.Chang, O.Shenderova. *Exp. Opin. Drug Deliv.*, **12**, 735 (2015)
209. H.-J.Kim, K.Zhang, L.Moore, D.Ho. *ACS Nano*, **8**, 2998 (2014)
210. L.Zhao, Y.-H.Xu, T.Akasaka, S.Abe, N.Komatsu, F.Watari, X.Chen. *Biomaterials*, **35**, 5393 (2014)
211. L.Moore, M.Gatica, H.Kim, E.Osawa, D.Ho. *J. Dent. Res.*, **92**, 976 (2013)
212. E.Haartman, H.Jiang, A.A.Khomich, J.Zhang, S.A.Burikov, T.A.Delenko, J.Ruckolainen, H.Gu, O.A.Shenderova, I.I.Vlasov, J.M.Rosenholm. *J. Mater. Chem. B*, **1**, 2358 (2013)
213. E.V.Rodina, A.V.Valueva, R.Yu.Yakovlev, N.N.Vorobyeva, I.I.Kulakova, G.V.Lisichkin, N.B.Leonidov. *Biointerphases*, **10**, 041005-1 (2015)
214. R.Yu.Yakovlev, I.I.Kulakov, N.B.Leonidov, G.V.Lisichkin. In *Nanostruktury v Kondensirovannykh Sredakh. Sbornik Nauchnykh Statei.* (Nanostructures in Condensed Media Collection of Scientific Papers). (Minsk: ITMO NAN Belarus, 2016). P. 84